



**L'INFLUENCE DE L'ENVIRONNEMENT PHYSIQUE SUR LES
FLORAISONS DU PHYTOPLANCTON AUX HAUTES LATITUDES:
UNE PERSPECTIVE SATELLITAIRE**

Thèse présentée

dans le cadre du programme de doctorat en sciences de l'environnement
en vue de l'obtention du grade de Philosophiae Doctor (Ph.D.)

PAR

©CHRISTIAN MARCHESI

Mars 2018

Composition du jury :

Christian Nozais, président du jury, Université du Québec à Rimouski

Simon Bélanger, directeur de recherche, Université du Québec à Rimouski

Jean-Éric Tremblay, codirecteur de recherche, Université Laval

Michel Gosselin, examinateur interne, Institut des Sciences de la Mer

Paty Matrai, examinateur externe, Bigelow Laboratory of Ocean Sciences

Dépôt initial le 23 Octobre 2017

Dépôt final le 09 Mars 2018

UNIVERSITÉ DU QUÉBEC À RIMOUSKI

Service de la bibliothèque

Avertissement

La diffusion de ce mémoire ou de cette thèse se fait dans le respect des droits de son auteur, qui a signé le formulaire « *Autorisation de reproduire et de diffuser un rapport, un mémoire ou une thèse* ». En signant ce formulaire, l'auteur concède à l'Université du Québec à Rimouski une licence non exclusive d'utilisation et de publication de la totalité ou d'une partie importante de son travail de recherche pour des fins pédagogiques et non commerciales. Plus précisément, l'auteur autorise l'Université du Québec à Rimouski à reproduire, diffuser, prêter, distribuer ou vendre des copies de son travail de recherche à des fins non commerciales sur quelque support que ce soit, y compris l'Internet. Cette licence et cette autorisation n'entraînent pas une renonciation de la part de l'auteur à ses droits moraux ni à ses droits de propriété intellectuelle. Sauf entente contraire, l'auteur conserve la liberté de diffuser et de commercialiser ou non ce travail dont il possède un exemplaire.

A mio padre, che ha sempre
creduto in me.

REMERCIEMENTS

Aller jusqu'au bout d'un parcours est toujours un défi. Le réussir loin de sa terre d'attache est sans aucun doute plus difficile encore. Le défi prend dès lors la forme d'une aventure, qu'on acceptera ou refusera de vivre. Après six ans, je peux dire que ce parcours aura été pour moi une expérience de vie qui va bien au-delà de l'acquisition d'un titre universitaire : j'ai appris une nouvelle langue, connu un nouveau pays et de belles personnes dont je conserverai toujours un vibrant souvenir.

Je voudrais tout d'abord témoigner ma reconnaissance à mon directeur de recherche, Simon Bélanger, qui m'a donné la possibilité de faire un doctorat, qui m'a fait confiance, soutenu à plusieurs titres et toujours permis de travailler librement à mon projet.

Je remercie également mon codirecteur de recherche, Jean-Éric Tremblay, pour son expérience et ses commentaires constructifs à l'égard de mon travail.

Je salue par ailleurs la précieuse contribution des membres du jury d'évaluation qui ont lu et commenté ma thèse.

Merci à Camille Albouy pour l'aide concrète et indispensable qu'il m'a accordée au bon moment, et pour être aussi devenu mon ami au gré de ce parcours de recherche.

Je suis également reconnaissant à Laurent Oziel, dont l'enthousiasme et les encouragements m'ont amené à finaliser le travail et à atteindre le terme de ma thèse. Je le remercie de son amitié, et notamment de m'avoir fait découvrir la série italienne *Gomorra*.

Je voudrais par ailleurs remercier mes coauteur·es, dont Laura Castro de la Guardia et Igor Yashayaev, qui, grâce à leurs connaissances et à leur soutien technique, m'ont permis d'avancer en m'apportant beaucoup sur le plan du travail. Merci aussi à mes collègues étudiant·es du laboratoire Aquatel de l'Université du Québec à Rimouski

pour leur humour, leur complicité et leur accompagnement.

Je remercie également toutes les personnes que j'ai rencontrées à Rimouski ou ailleurs au Québec, dont le mot gentil ou le sourire m'a encouragé à persévérer jusqu'à la fin de mon doctorat.

Un merci tout particulier va à Sylvie Dubé pour sa générosité, son énergie positive, son hospitalité, son amitié inconditionnelle, et aussi pour m'avoir fait apprivoiser le Bas-Saint-Laurent.

Un grand merci à Marco Alberio pour tous ces moments de franche rigolade en italien qui ont allégé mon séjour à Rimouski.

Je voudrais aussi profiter de cette occasion pour témoigner mon affection à Claudie Gagné. Sa présence rassurante, au fil du temps et des différents passages de la vie, est demeurée vraie et sentie.

Enfin, je remercie mes parents, Enzo et Marisa, de même que ma compagne Barbara de m'avoir laissé libre de rêver, de m'avoir toujours appuyé dans mes choix et d'avoir cru en moi.

RÉSUMÉ

Des observations satellitaires et des modèles climatiques récents font valoir que l'augmentation du réchauffement de la surface de la mer, la réduction de la glace marine et le forçage atmosphérique sont à l'origine de modifications écologiques à grande échelle dans les régions marines. Par exemple, les modifications de la durée et de la magnitude de l'efflorescence phytoplanctonique saisonnière peuvent entraîner de lourdes conséquences pour le fonctionnement du réseau trophique et la dynamique du carbone. Nous avons investigué la réponse du phytoplancton océanique aux changements qui s'opèrent à la subsurface du milieu physique de deux régions arctiques et subarctiques reconnues comme des points névralgiques marins. Un ensemble de données satellitaires, d'observations in situ et de sorties de modèle ont conduit à la définition d'indices utiles pour chiffrer la phénologie du phytoplancton et évaluer si sa variabilité est attribuable à des changements de forçage physique. Les méthodes phénologiques proposées dans cette étude ont dressé le portrait de l'étendue régionale des efflorescences grâce à l'identification des modèles de variabilité et des différences déterminantes en matière de période, de magnitude et de durée. Or les observations suggèrent qu'une combinaison de modifications des variables environnementales est souvent à l'origine d'une forte modulation de la phénologie de l'efflorescence phytoplanctonique. Toutefois, les interactions de la dynamique du phytoplancton et de l'environnement physique peuvent considérablement varier à l'échelle subrégionale selon les caractéristiques intrinsèques d'une région marine donnée et le mécanisme de forçage qui y prédomine. Le seuil biotique peut alors différer, voire sembler inattendu là où des transformations locales donnent lieu à un environnement de grande variabilité. Dans leur ensemble, les résultats indiquent que la dynamique du phytoplancton varie sur des distances relativement courtes et qu'elle exige un examen qui s'appuie sur de fines échelles spatiotemporelles. Enfin, notre étude réaffirme le rôle du phytoplancton à titre d'élément biotique clé dans l'évaluation de la réponse des écosystèmes marins de haute altitude au changement climatique.

Mots clés : écosystèmes pélagiques, phénologie du phytoplancton, forçage physique, Arctique, Atlantique Nord subpolaire

ABSTRACT

Recent climate models and satellite observations highlight how increasing sea-surface warming, sea-ice reduction and atmospheric forcing are triggering extensive ecological modifications in marine regions. Alterations in the timing and magnitude of the seasonal phytoplankton bloom may lead to important consequences on food web functioning and carbon dynamics. We investigated the response of oceanic phytoplankton to changes in the near-surface physical environment in two Arctic and subarctic regions recognized as marine biological hotspots. Satellite datasets, together with in situ observations and model outputs, were used to define a suite of indices useful to quantifying phytoplankton phenology and to test whether its variability is likely to be attributable to shifts in physical forcing. The phenological methods proposed in this study provided a picture of the regional extent of the blooms by identifying variability patterns and determining differences in timing, magnitude and duration. Observations suggest that often it is a combination of environmental variable changes that strongly modulate phytoplankton bloom phenology. However, interactions among phytoplankton dynamics and the physical environment may vary significantly across sub-regional spatial scales, depending on the intrinsic characteristics of the marine region and the dominant forcing mechanism. The biotic response might be different or even unexpected where local processes create a highly variable environment. As a whole, results stress the view that phytoplankton dynamics can vary over relatively short distances and require detailed examinations at adequate temporal and spatial scales. Finally, this study reinforces the role of phytoplankton as a key biotic element for evaluating the response of high-latitude marine ecosystems to climate change.

Keywords : pelagic ecosystems, phytoplankton phenology, physical forcing, Arctic, sub-polar North Atlantic

TABLE DES MATIÈRES

REMERCIEMENTS	vi
RÉSUMÉ	viii
ABSTRACT	ix
TABLE DES MATIÈRES	x
LISTE DES TABLEAUX	xiv
LISTE DES FIGURES	xv
LISTE DES ABRÉVIATIONS	xxi
INTRODUCTION GÉNÉRALE	1
Marine phytoplankton blooms and their importance	1
High-latitude sea-ice cover and primary production in a changing climate : a brief overview	2
Phytoplankton phenology in the Northern Hemisphere : a bottom-up synthesis	8
Thesis objectives and study areas	13
CHAPITRE 1	
BIODIVERSITY HOTSPOTS: A SHORTCUT FOR A MORE COMPLICATED CONCEPT	16
1.1 Résumé	17
1.2 Abstract	18
1.3 Introduction	19
1.4 Biodiversity hotspots	22
1.4.1 The biodiversity hotspots concept	22
1.4.2 Criticism of biodiversity hotspots	24
1.5 Hotspots identification	26
1.5.1 Species-based metrics	26
1.5.2 Phylogenetic diversity	28
1.5.3 Which metric?	29

1.6	Marine hotspots	31
1.6.1	Pelagic hotspots	31
1.6.2	Deep-water hotspots	34
1.7	Biodiversity conservation and priorities	36
1.8	Conclusion	39

CHAPITRE 2

CHANGES IN PHYTOPLANKTON BLOOM PHENOLOGY OVER THE NORTH WATER (NOW) POLYNYA: A RESPONSE TO CHANGING ENVIRONMENTAL CONDITIONS

2.1	Résumé	43
2.2	Abstract	45
2.3	Introduction	46
2.4	Material and methods	49
2.4.1	Cloud-free satellite chlorophyll-a time series	49
2.4.2	Models and estimation of phenological metrics	52
2.4.3	Environmental parameters	55
2.4.3.1	Sea-ice concentration	55
2.4.3.2	Sea-surface temperature	56
2.4.3.3	Cloud fraction	56
2.4.3.4	Surface wind data	57
2.4.4	Statistical analyses	58
2.5	Results	58
2.5.1	Spatiotemporal variability of satellite chlorophyll-a	58
2.5.2	Bloom phenology features and environmental parameters	60
2.5.2.1	Bloom start	60
2.5.2.2	Bloom duration	64
2.5.2.3	Bloom amplitude	65
2.6	Discussion	66
2.6.1	Phytoplankton bloom dynamics and phenology	66

2.6.2	Limitation of the data	72
2.7	Conclusions	73
CHAPITRE 3		
REGIONAL DIFFERENCES AND INTER-ANNUAL VARIABILITY IN THE		
TIMING OF SURFACE PHYTOPLANKTON BLOOMS IN THE LABRADOR		
SEA 76		
3.1	Résumé	77
3.2	Abstract	79
3.3	Introduction	80
3.4	Material and methods	84
3.4.1	Satellite chlorophyll-a time series	84
3.4.2	Clustering K-means analysis	85
3.4.3	Mixed-layer depth from ARGO data	85
3.4.4	Simulated mixed-layer depth and heat fluxes	86
3.4.5	Surface bloom onset and physical timing metrics	88
3.5	Results and Discussion	89
3.5.1	Bioregionalization and phytoplankton seasonal cycles differences	89
3.5.2	The southern bioregion	91
3.5.3	The northern bioregion	97
3.5.4	Limitation	101
3.6	Conclusion	103
CHAPITRE 4		
ANOMALOUS MESOSCALE ACTIVITY LEADS TO MASSIVE PHYTOPLANK-		
TON SPRING BLOOM IN THE LABRADOR SEA 106		
4.1	Résumé	107
4.2	Abstract	108
4.3	Introduction	109
4.4	Material and Methods	111
4.4.1	Satellite-derived data and eddy kinetic energy	111
4.4.2	Large-scale climate indices	113

4.5 Results and Discussion	114
CONCLUSION GÉNÉRALE	125
In a nutshell : context and originality	125
Overview : main findings, limitations and future directions	126
ANNEXE I	
CHAPITRE 2 : MATÉRIEL SUPPLÉMENTAIRE	133
ANNEXE II	
CHAPITRE 3 : MATÉRIEL SUPPLÉMENTAIRE	139
ANNEXE III	
CHAPITRE 4 : MATÉRIEL SUPPLÉMENTAIRE	144
RÉFÉRENCES	147

LISTE DES TABLEAUX

1	Biodiversity hotspots from 1988 to present (modified from Mittermeier et al. 2011)	21
2	The proactive, reactive and representative approaches used for the selection of biodiversity conservation priority areas at global scale. All the approaches are based on a combination of the ecological criteria of vulnerability and irreplaceability (Modified from Schmitt 2011)	37
3	Gaussian-models for the different types of seasonal phytoplankton cycles	54
4	Main bloom phenology parameters extracted for each year at each pixel	54
5	Summary of the annual average values (and standard deviation, SD) of the regional phenological parameters obtained from the Gaussian fits. R^2 is the coefficient of determination of the Gaussian fits. The percentage of valid fits within the study region is also reported.	59
6	Description of physical metrics	89

LISTE DES FIGURES

1	The figure shows the temperature anomaly trends from different international science institutions. All show rapid warming in the past few decades and that the last decade has been the warmest on record (Source : https://climate.nasa.gov)	3
2	Arctic sea-ice volume is plotted for each day of the year, moving clockwise around the graph and taking one full year to complete a circuit. The volume of sea-ice on a particular day is represented by that plot's distance from the center of the graph. Less sea-ice volume places the plot closer to the center (0%). Thin gray lines represent past years, while decadal averages and the current year (2018 in red) are thicker and color-coded as detailed in the legend	4
3	The figure shows (a) the North Water (NOW) polynya located in northern Baffin Bay (>75°N) and southernmost (b) the Labrador Sea, a sub-polar sea that connects the North Atlantic with the Arctic Ocean. The Arctic Circle is also indicated (yellow line). The color gradient, from blue (low values) to red (high values), is given by the chlorophyll-a climatology derived from GlobColour (http://www.globcolour.info) images from 1998 to 2015.	12
4	The world's biodiversity hotspots (see also Table 1 for hotspots names). Figure licensed under the Creative Commons Attribution-Share Alike 4.0 International license (Author: Conservation International).	23
5	North Water polynya is situated in northern Baffin Bay between Canada and Greenland. Smith Sound, the Arctic sea passage between Greenland and Ellesmere Island, links Baffin Bay with Kane Basin. Nares Strait (not indicated in the map) is the waterway between Ellesmere Island and Greenland that includes, from south to north, Smith Sound, and Kane Basin, respectively (a); monthly climatology of merged satellite chlorophyll-a data from April 1998 to September 2014 at 25 km of resolution within the NOW polynya: 74°N-81°N, 82°W-63°W (b); time series of 8-day composite images of chlorophyll-a, averaged for the NOW polynya from April 1998 to September 2014 (c)	51
6	Workflow describing the multi-step tasks to obtain (a) 8-day composite cloud-free chlorophyll-a images and (b) multiple-Gaussian models approach to increase the number of fits.	52

- 7 Climatology (1998-2014) maps of a) bloom start, b) bloom duration, c) bloom amplitude, d) sea surface temperature, e) wind stress, and f) sea-ice concentration 61
- 8 Time series analysis of the main bloom phenology characteristics (bloom start, bloom duration, and bloom amplitude) and environmental parameters (SST, wind stress, and SIC) averaged for the NOW polynya area. The black line is the mean \pm standard deviation (shaded grey area). The red line represents linear trend (days year⁻¹) for the 17-year time series. Coefficient of determination (r^2) and probability levels (p) is shown for each figure in the upper right box. 62
- 9 Spearman's rank correlation (ρ) matrix (a) between phytoplankton phenological parameters: BS (bloom start), BD (bloom duration), BA (bloom amplitude), and abiotic factors: SST (sea surface temperature), WS (wind stress), CF (cloud fraction), SIC (sea-ice concentration), SIE (sea-ice extent), IRT (ice-retreat timing), OWP (open-water period), and D (frequency of wind-driven entrainment). The red color indicates a significant ($p < 0.05$) negative correlation, while the blue color indicates a significant ($p < 0.05$) positive correlation. The color gradient (from red to blue) indicates the magnitude of the correlation. The color white means that the correlation between indicators is not significant ($p > 0.05$) according to the Spearman correlation statistical test. Principal component analysis biplot (b) of: variables (red arrows; see text above for abbreviations) and years (1998-2014) represented by dots. 63
- 10 (a) Spatial distribution of the clusters obtained from the K-means analysis and (b) the mean biomass (chlorophyll-a) annual cycles in each cluster ± 1 standard deviation (light grey area). The spatial distribution of each cluster constitutes a specific bioregion representative of a characteristic seasonal cycle. (c) Time (day of the year) of the maximum chlorophyll-a amplitude (i.e., the date at which the chlorophyll-a reaches its maximum value) for each bioregion. 90

- 11 Time series (2002-2014) of chlorophyll-a (green solid line), heat fluxes (the shaded areas show negative values in winter) and simulated mixed layer depth (green area) over the southern bioregion. The heat fluxes annual cycle is made up by negative values (cooling) in winter (grey shaded areas), which favors convective mixing and by positive values in spring-summer (period between grey shaded areas). The vertical (black dotted) lines represent the date (for each year) on which the heat fluxes became positive for a minimum of 20 consecutive days (note one time-step is 10-days). The mixed layer is still deep when chlorophyll-a starts growing at the end of winter and the heat fluxes change sign (black dotted lines). 93
- 12 (a) Net surface growth rate increase averaged over the southern bioregion (green solid line ± 1 standard deviation) as a function of the days since the net heat fluxes turns positive. The average net surface growth rate is much larger closer to the date when the heat fluxes turns positive (i.e., day zero). (b) The mixed layer depth (from 2002 to 2014) at the time when the air-sea heat flux turned positive over the southern bioregion. Green bars represent the modeled mixed layer depth, while the black two-dashed line with successive segments represents the ARGO mixed layer depth (note that for the year 2002 no ARGO data were available at the time when the air-sea heat flux turned positive). In both cases, when heat fluxes first exceed zero the depth of the mixed layer is often deeper than 100 m. (c) The stratification index for both bioregions (see different colors) at the time when the HFs change sign over the southern bioregion (green bars). In 8 out of 13 years ($\sim 62\%$) the stratification is stronger (i.e., larger N^2) in the northern bioregion (yellow bars). 94
- 13 Time series (2002-2014) of chlorophyll-a (yellow solid line), stratification (grey areas), and simulated mixed layer depth (yellow area) over the northern bioregion. As the MLD shoals the stratification within the upper 25 m of the ocean increases. The vertical (black dotted) lines represent the date (for each year) of maximum mixed layer shoaling (i.e., the steepest gradient that occurs between its maximum and minimum). The vertical (red dashed) lines represent the date (for each year) on which the heat fluxes became positive. The cooling-to-heating shift in air-sea heat flux (red dashed lines) occurs, on average 1.9 ± 1.4 time-steps (with a range spanning from a minimum of 0 to a maximum of 5; note that one time-step is 10-days) after the shoaling of the MLD (black dotted lines). 99

- 14 Phytoplankton growth rates values at the time of the cooling-to-heating shift in air-sea heat flux over the northern bioregion. The red dashed line represents the average value, while the light grey area is ± 1 standard deviation from the mean. Growth rates are near-zero or already negative (i.e., declining biomass). (b) Net surface growth rate increase averaged over the northern bioregion (yellow solid line ± 1 standard deviation) as a function of the days since the mixed layer depth reaches the steepest gradient (i.e., becoming shallower) that occurs between its maximum and minimum. The average net surface growth rate is larger closer to the date on which the mixed layer depth became shallower (i.e., day zero). (b) The stratification index for both bioregions (see different colors) at the time when the mixed layer depth reaches the steepest gradient in the northern bioregion. In 9 out of 13 years, the upper ocean stratification is much stronger over the northern bioregion. 100
- 15 Temporal and spatial characterization of remotely sensed surface, chlorophyll-a concentration over the Labrador Sea. (a) Time-series (1998-2015) obtained from the mean of all chlorophyll-a values (in mg m^{-3}) available from eight-day composites of the Labrador Sea area between March 1998 and September 2015. Chlorophyll-a values (red dots) that were obtained from less than 30% of all pixels contained in the Labrador Sea area are also indicated. Maps showing (b) climatological (1998-2015) monthly mean of chlorophyll-a concentration for May; (c) monthly anomaly of chlorophyll-a for May 2011; and (d) monthly anomaly of chlorophyll-a for May 2015. In (d) the area of deepest mixing is indicated by the dashed black line. 114
- 16 (a) Time-series of the winter (December to March average) of the NAO index. (b) Correlation between the NAO and the convection depths. (c) Correlation between the depths of the winter convection and the surface chlorophyll-a (area-averaged from May to June) over the period 1998-2015. (d) Correlation between the Sub-Polar Gyre Index (SPG-I) and the area-averaged surface chlorophyll-a between 1998 and 2015. 117
- 17 Temporal and spatial characterization of altimetry-derived surface EKE (Eddy Kinetic Energy) and absolute geostrophic velocities over the Labrador Sea. (a) Time-series of altimetry-derived EKE in the Labrador Sea averaged between April and May (spring), for the period 1998-2015. Maps showing (b) the climatological (1998-2015) mean distribution of surface EKE in the Labrador Sea; (c) monthly anomaly of EKE in spring 2011; (d) monthly anomaly of EKE in spring 2015; (e) absolute geostrophic velocities average (May 1st; 1993-2015); (f) absolute geostrophic velocities on May 1st 2015 and (g) 2011. 119

- 18 Eddy Kinetic Energy (EKE) seasonal cycle in the Labrador Sea for the years 2015 (green), 2011 (red) and the mean period (blue). The dark gray area indicates the period of deepest convection (February-April). The pale gray area indicates the bloom period (from late April to the end of May) over the year 2015. The 2015 spring bloom seems to coincide with a phase of increased eddy activity. 121
- 19 High-resolution images of chlorophyll-a (Chl-a) and Sea Surface Temperature (SST) the 17th of May 2015. On both sides, small boxes (from a to f) of Chl-a and SST show more in details some of the small cyclonic eddies within the bloom area. 123
- 20 An example of fit. CHL_B (0.38 mg/m^3) corresponds to the background chlorophyll-a determined by the fitted function (red line). CHL_1 (1.91 mg/m^3) correspond to the peak amplitude, ω_1 is the standard deviation of the Gaussian curve and define the temporal width of the bloom, and tp_1 (day 90 of year) define the peak timing, i.e. the day of the year at which the maximum of bloom occurs. The bloom start is determined using a relative threshold : it is the date (day of the year) at which the fitted function reaches the threshold of 20% (blue line) of its maximum amplitude. The same criterion was used to define the bloom end in the downslope of the Gaussian curve. The time interval, represented in figure by the blue lines, gives the bloom duration (the difference between bloom end and bloom start). 134
- 21 Bloom start phenology : inter-annual differences for selected years (1998-2000, 2002, 2003, 2005, 2007, 2009, 2012, 2014) over the study region. White areas represent pixels with low variability or persistent periods of missing data. Highest values are represented by the red color and lowest values by the blue color. 135
- 22 Bloom duration phenology : inter-annual differences for selected years (1998-2000, 2002, 2003, 2005, 2007, 2009, 2012, 2014) over the study region. White areas represent pixels with low variability or persistent periods of missing data. Highest values are represented by the red color and lowest values by the blue color. 136
- 23 Bloom amplitude phenology : inter-annual differences for selected years (1998-2000, 2002, 2003, 2005, 2007, 2009, 2012, 2014) over the study region. White areas represent pixels with low variability or persistent periods of missing data. Highest values are represented by the red color and lowest values by the blue color 137

- 24 Plot of the proportion of variances (y-axis) explained by the components (x-axis) of annual change in phytoplankton phenology and physical parameters across the years (1998-2014). Based on this figure, we decided to retain 4 principal components and to focus only on the two most important that represent more than 70% of the proportion of variances (Axe 1 = 57.4%; Axe 2 = 15.7%) 138
- 25 The Calinski-Harabazs index used to estimate the optimal number of cluster to bio-regionalize the Labrador Sea. The index measures the ratio between the dispersion of the observations (i.e., chlorophyll-a data) within a cluster and the dispersion between the clusters. The optimal clustering is the one with the highest value for the pseudo F-statistic. 140
- 26 Hovmöller diagram used to plot the latitudinal evolution of the 10-days climatological (2002-2014) chlorophyll-a mean as function of the time over the Labrador Sea. Compared to the North Atlantic where blooms tend to follow the general south-to-north progression, the reversed pattern within the Labrador Sea represents a distinctive feature. 141
- 27 Salinity values are from the surface layer (0-50 m) and were extracted from the World Ocean Database 2009 (<https://www.nodc.noaa.gov>). In the top panel, dots indicate individual original measurements (n = 45768). 142
- 28 Scatter plot comparing the time-series of mean MLD computed with the ANHA4 configuration and ARGO-floats using the density criteria. The mean from ARGO-floats was computed when there were more than five floats available after outliers were removed. Outliers were defined as values being more than two standard deviations from the mean. The model represents relatively well the shallower MLD (<200 m) with biases of only 8 meters (small panel on the right). 143
- 29 Standardized monthly anomalies maps of surface chlorophyll-a for the month of May over the period 1998-2015. Satellite data indicates elevated phytoplankton biomass in the Labrador Sea during May 2015 when compared to data for the eighteen-year period (1998-2015). 145
- 30 Depth-averaged (0-25 m) chlorophyll-a concentration in the central Labrador Sea derived from Biogeochemical-Argo (BGC-Argo) float measurements in May 2013 and 2015. The box in the upper left shows the free-drifting profiling floats position taken into account. 146

LISTE DES ABRÉVIATIONS

BS	Bloom Start
BD	Bloom Duration
BA	Bloom Amplitude
CF	Cloud Fraction
CHL-A	Chlorophyll-a
D	Frequency of wind-driven entrainment
EKE	Eddy Kinetic Energy
HF_s	Heat Fluxes
IRT	Ice-Retreat Timing
MLD	Mixed-Layer Depth
NAO	North Atlantic Oscillation Index
OWP	Open-Water Period
SIC	Sea-Ice Concentration
SIE	Sea-Ice Extent
SPG-I	Sub-Polar Gyre Index
WS	Wind Stress

INTRODUCTION GÉNÉRALE

Marine phytoplankton blooms and their importance

Phytoplankton are mostly microscopic photosynthetic (single-celled and colonies) organisms that float freely in the uppermost sunlit layer of marine and freshwater ecosystems. Similar to terrestrial plants, phytoplankton contain chlorophyll to capture sunlight and use photosynthesis to turn it into chemical energy. Marine phytoplankton fuel the oceanic food web and through the photosynthetic carbon fixation (i.e., primary production) mitigate the oceanic and atmospheric carbon dioxide (CO₂) levels (Sanders et al., 2014). The Earth's cycle of carbon and, to a large extent, its climate depend on these photosynthetic organisms that strongly influence ocean-atmosphere gas exchanges (Sanders et al., 2014).

Phytoplankton blooms (i.e., a condition of elevated phytoplankton concentration) are ubiquitous and recurrent phenomena that contribute significantly to annual primary production and to biogeochemical processes, such as the biological carbon pump, which transfer the organic carbon from the sunlit surface waters to the ocean interior (Diehl et al., 2015; Sanders et al., 2014; Tremblay et al., 2015). Phytoplankton blooms vary in timing, magnitude, and duration both spatially and inter-annually as a consequence of annual fluctuations in light and nutrient regime, water column stability (i.e., stratification) and grazing activity (Winder and Sommer, 2012; Waniek, 2003). In particular, a phytoplankton bloom occurs when seasonal light limitation lapses due to the shoaling of the mixed layer above a critical-depth, where the loss terms (i.e., respiration, grazing, sinking and natural mortality) are largely compensated by photosynthetic production (the so-called "critical depth hypothesis" ; Sverdrup 1953).

However, although the "critical-depth hypothesis" formulated by Sverdrup (1953) remains the most cited and widely accepted theory, new physical and biological me-

chanisms have been suggested to drive phytoplankton blooms, especially in subarctic Atlantic. In recent years, different studies have agreed (Mahadevan et al., 2012), challenged (Behrenfeld, 2010; Boss and Behrenfeld, 2010) or merely refined Sverdrup’s model by testing the hypothesis that the shutdown of winter convective mixing could serve as a better indicator for the onset of the spring bloom than the mixed-layer depth (Taylor and Ferrari, 2011). Recently observations (Lacour et al., 2017) showed evidence for widespread winter (January-March) phytoplankton blooms in a large part of the North Atlantic sub-polar gyre triggered by a combination of eddy-driven restratification and prolonged periods of calm (i.e., relaxation of atmospheric forcing). All these works highlight the complex interplay between abiotic and biotic factors in triggering the phytoplankton bloom dynamics. Probably, there is not a single dominant physical mechanism that best predicts the inter-annual variability of the bloom onset (Ferreira et al., 2015). In this connection, to move beyond the “single mechanism” point of view, an integrated conceptual model of the physical and biological controls initiating the onset of the phytoplankton spring bloom has been proposed (Lindemann and St John, 2014). Finally, it is becoming increasingly clear that the cells’ ability (i.e., adaptive qualities) to modify physiological rates in response to changes in the external environment may also play an important role in the onset of phytoplankton spring bloom (Lindemann et al., 2015). For instance, restratification during the winter period may cause a phytoplankton community shift from small phytoplankton cells (i.e., pico- and nano-) to micro-phytoplankton cells such as diatoms (Lacour et al., 2017). Overall, factors controlling the phytoplankton seasonal cycle dynamics still remain controversial.

High-latitude sea-ice cover and primary production in a changing climate : a brief overview

There is no doubt that global climate is changing. A considerable number of studies published in peer-reviewed scientific journals shows that $\sim 97\%$ of actively publishing

climate scientists agree that climate-warming trends (Figure 1) over the past century are most likely due to human activities (Cook et al., 2016, 2013).

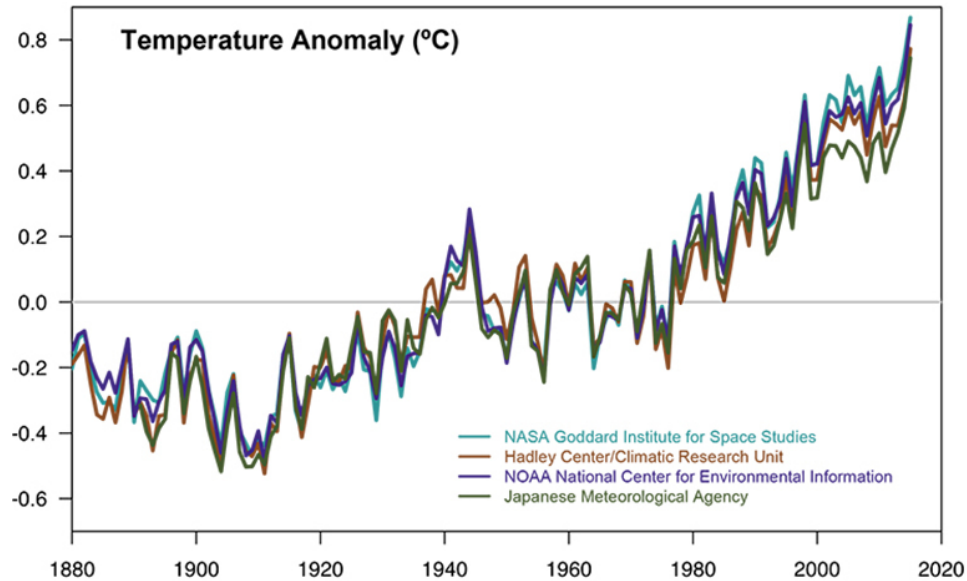


Figure 1: The figure shows the temperature anomaly trends from different international science institutions. All show rapid warming in the past few decades and that the last decade has been the warmest on record (Source : <https://climate.nasa.gov>).

The impacts of climate warming are now increasingly visible in northern high-latitude ocean areas. In particular, the Arctic and subarctic marine ecosystems are experiencing a rapid sea-ice habitat loss and fragmentation that challenges the adaptive capacity of sea-ice dependent marine mammals (Moore and Huntington, 2008; Laidre et al., 2015) and under-ice fauna (Kohlbach et al., 2016). Changes in the sympagic biota (i.e., organisms that live in, on or associated with the ice, ranging from microbial communities to the charismatic mega-fauna, including seals, walrus and polar bears) are now more than evident.

The sea-ice extent, one of the largest biomes on Earth, has significantly decreased in recent decades (Comiso et al., 2008), hitting its lowest in 2012 (Parkinson and Comiso,

2013). More precisely, in September 2012 the average Arctic sea-ice extent (Figure 2) was the lowest in the satellite record. Other record lows occurred in September 2007 and recently in September 2016 (Figure 2). Based on estimates produced by the National Snow and Ice Data Center (NSIDC) Sea Ice Index (Fetterer et al., 2002) the September 2016 seaice minimum extent was 33% lower than the 1981-2010 average sea-ice minimum extent and tied with 2007 for the second lowest value in the satellite record (1979-2016). These recent observations strengthen even more the idea that the sea-ice cover is becoming more sensitive to ocean warming.

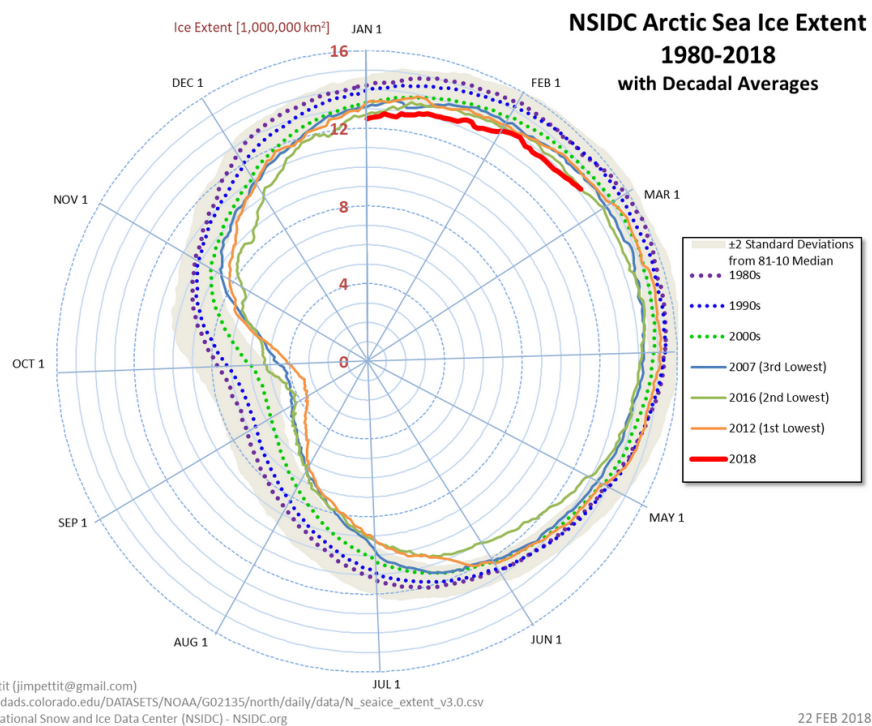


Figure 2: Arctic sea-ice volume is plotted for each day of the year, moving clockwise around the graph and taking one full year to complete a circuit. The volume of sea-ice on a particular day is represented by that plot's distance from the center of the graph. Less sea-ice volume places the plot closer to the center (0%). Thin gray lines represent past years, while decadal averages and the current year (2018 in red) are thicker and color-coded as detailed in the legend

As temperatures have increased, much of the multiyear sea-ice has disappeared and been replaced by a markedly thinner first-year ice that melts earlier in spring (Maslanik et al., 2011; Ricker et al., 2017). As a result, the earlier melt has allowed an ever-increasing fraction of the sea surface to absorb more solar radiation, thus delaying the sea-ice freeze-up timing in the fall throughout most of the Arctic (Stroeve et al., 2014). A later freeze-up timing implies that the sea-ice has less time to thicken before the start of the next melt season, therefore resulting in its being more prone to melt. Basically, the heat gained by the ocean mixed-layer during summer feeds a loop that causes temperatures to rise : regions with especially higher than average temperatures correspond to regions with lower sea-ice extent (Stroeve et al., 2014). Moreover, intensification of the hydrological cycle is also predicted to occur due to increasing precipitation (Kopeck et al., 2016), rivers discharge (Bring et al., 2017) and melting of glaciers and ice-sheets on land (Luo et al., 2016).

Although the ongoing changes in the physical domain are well documented, the response of the marine ecosystem to these major external disturbances is still uncertain. For instance, changes in sea-ice phenology (i.e., break-up, freeze-up and length of the open-water season) have regionally dependent and significant impacts on pelagic primary production (Wassmann and Reigstad, 2011). Sea-ice plays an important role in promoting active biological and chemical processes and in regulating interactions between the upper ocean and the atmosphere (Budikova, 2009; Vancoppenolle et al., 2013). In particular, the sea-ice coverage directly influences the pelagic system by regulating the amount of solar radiation reaching the water column and thus limiting the length of the productive season (Arrigo and van Dijken, 2011). Historically, regions underneath a full sea-ice cover (i.e., optically thick with a high reflection) have usually been considered incapable of supporting phytoplankton production. However, in the present-day Arctic the undergoing shift from multi-year ice to first-year ice caused the thinner summertime sea-ice to be increasingly covered by melt ponds, which efficiently transmit light to the underlying ocean (Frey et al., 2011; Palmer et al., 2014). Recent observations indicate that massive

phytoplankton blooms start beneath the sea-ice when under-ice light conditions are favorable (Arrigo et al., 2012). The presence of melt ponds may therefore stimulate the light-limited biological productivity. According to a recent study (Horvat et al., 2017), at the present day nearly 30% of the ice-covered Arctic Ocean between June and July permits sub-ice blooms. However, even under favorable light conditions, nutrient availability can limit biological productions in sea-ice melt ponds (Arrigo et al., 2014; Sørensen et al., 2017).

Connected with the sea-ice dynamics are sea-ice edge phytoplankton blooms, which occur when sea-ice retreats (Perrette et al., 2011). The sea-ice edge blooms can be favored by a shallow mixed-layer (i.e., due to warm and fresher water that minimizes vertical mixing), increasing light and by the release from melted ice of material (i.e., nutrients and metals) into the water column (Vancoppenolle et al., 2013). However, quantifying the contribution of primary production of the ice-associated blooms remains a challenge because of the lack of observational data (Perrette et al., 2011).

Both *in situ* and satellite observations are used to estimate the biological productivity (Matrai et al., 2013; Tremblay et al., 2015). *In situ* measurements directly estimate primary production throughout the water column (i.e., from surface to subsurface) but they are usually restricted to very small areas. Satellite ocean colour observations provide more extensive spatial and temporal coverage but are limited to the surface and affected by data gaps (Perrette et al., 2011). Overall, the increase in phytoplankton biomass and productivity over the Arctic Ocean has been based mainly on open-water measurements. For instance, satellite observations over a 12-year (1998-2009) period reported a 20% overall increase in primary production, mostly due to an increase in open-water extent (+27%) and duration (+45 days) of the open-water season (Arrigo and van Dijken, 2011). A new study (Arrigo and van Dijken, 2015) incorporating a more recent reprocessing version of the ocean color data suggests that primary production in the Arctic Ocean continues to increase rapidly. Other remote sensing studies (Petrenko

et al., 2013) and model simulation (Slagstad et al., 2015) suggest an increase, although unevenly, in primary production. However, although these estimates currently lack the ice-associated production, the observed enhancement in primary production has to be carefully considered. In high-latitude ocean areas, numerical models still lack validation with *in situ* time series (Babin et al., 2015). Furthermore, satellite-derived ocean-color models are still subject to large uncertainties (Lee et al., 2015) due to different methodological approaches and/or high concentrations of colored dissolved organic matter that impede clear-cut estimates of chlorophyll-a (Matsuoka et al., 2011; Matrai et al., 2013) a key diagnostic marker of phytoplankton (Huot et al., 2007). Another source of uncertainty is the presence of a subsurface chlorophyll-a maximum (Ardyna et al., 2013), which can become more important on a regional scale and critical for the pelagic-benthic coupling system and higher-trophic-levels organisms (Wassmann and Reigstad, 2011). Finally, the role of increasing cloudiness on the light intensity reaching the water column and its effect on primary production has recently been debated (Bélanger et al., 2013a). The latter analysis suggests that although the duration of the open-water period may further increase, the phytoplankton photosynthetic activity might not follow a similar positive trend because it is light-limited (Bélanger et al., 2013a).

Against this background, it follows that one of the key issues is whether or not the ongoing changes will translate into enhanced phytoplankton production. Results suggest that the decrease in sea-ice cover should cause an increase in primary production by lengthening the growth season and allowing more sunlight to enter the sea-surface layer. However, as previously discussed, cloudiness may influence the length of the productive season by controlling the photosynthetic light requirement (Bélanger et al., 2013a). Moreover, the nutrient availability and distribution over the entire productive period is also of fundamental importance. Both factors (i.e., light and nutrient availability) have been found to limit primary production in the Arctic and subarctic seas (Tremblay et al., 2015). A recent study based on *in situ* measurements showed that the freshwater variability in the Chukchi Sea has a strong influence on primary production by lowering

the nutrient inventory in the euphotic zone (Yun et al., 2016). These results are consistent with those of previous studies (e.g., McLaughlin and Carmack, 2010) that indicate that an increase in stratification may strongly limit the availability of nutrients and therefore negatively impact productivity. Some authors (e.g., Coupel et al., 2015) argued that despite higher light penetration, a further increase in freshening might lead the Arctic deep basins to become more oligotrophic because of a weaker nutrient entrainment into the seasonal mixed layer. Basically, the freshwater accumulation could lead to a decline in biological production because it restricts mixing of deep nutrients to the ocean surface. The greatest decrease in primary production is expected in those marine regions characterized by stratification-induced nutrient limitation (Slagstad et al., 2015). Due to the heterogeneity of Arctic and subarctic marine regions, the idea that strongly emerges is that photosynthetic production is expected to vary regionally (or even locally) on the basis of different environmental factors controlling phytoplankton blooms (Wassmann and Reigstad, 2011). For instance, a recent study suggests that the increase in phytoplankton biomass and productivity in southwest Greenland waters is likely triggered by a greater nutrient supply associated with glacial meltwater (Arrigo et al., 2017). The nutrients released can be transported long distances and potentially fertilize surrounding areas (Arrigo et al., 2017). Besides, the nutrient load supplied by rivers seems to have a greater contribution at local scale but so far it does not appear to fuel a major portion of the overall pan-Arctic primary production (Tremblay et al., 2015). Certainly, these processes could become much more important in years to come.

Phytoplankton phenology in the Northern Hemisphere : a bottom-up synthesis

Most of the above-mentioned studies focus mainly on estimates of primary production. However, obtaining annual (seasonal) estimates of pelagic primary production should not obscure the importance of closely monitoring the phytoplankton seasonal

cycle dynamics (i.e., phenology : changes in timing, amplitude and duration). In marine ecology, phenological studies are increasingly used to inspect pelagic ecosystems' response to changing climatic conditions. Phytoplankton phenology is a sensitive indicator useful in assessing the response of the pelagic ecosystems ([Platt and Sathyendranath, 2008](#)) to major external disturbances such as changes in water temperature and ice coverage. In particular, in northern high-latitude pelagic ecosystems, phytoplankton phenology requires special consideration for several reasons :

1. The strong seasonality in environmental conditions such as light, temperature, nutrients, snow and sea-ice cover heavily characterize this remote environment ;
2. The organism's reproductive strategies are adapted to both the harsh conditions and the narrow time window defined by the strong seasonality. For instance, phytoplankton blooms seasonality is strongly coupled with the light regime, which is influenced by the seasonal and latitudinal controls and by the presence of snow and sea-ice cover. The latter both attenuates and reflects light and is thus an important contributor to the phytoplankton growth cycle ([Ji et al., 2010](#)) ;
3. Even a small timing mismatch ([Søreide et al., 2010](#)) between the organism's life strategy and the physical environment could have a substantial consequence for the entire food web. In particular, changes in bloom timing may affect the energy flow throughout the whole food web, which in turn may impact higher trophic level productivity ([Malick et al., 2015](#)) ;
4. Climate warming through mechanisms that influence water column conditions is predicted to lead marked and unexpected changes in Arctic and subarctic marine ecosystems ([Wassmann et al., 2011](#)). Continued climate warming can modify not only the bloom timing but also species composition and size structure, favouring species traits best adapted to changing conditions ([Winder and Sommer, 2012](#)).

Recent studies revealed that dramatic changes in bloom characteristics and phenology have occurred in the Arctic and subarctic marine regions. According to [Li et al.](#)

(2009), the phytoplankton community composition has changed under the warming, freshening and stratifying condition in the Canada Basin. The authors revealed a shift toward a dominance of small phytoplankton cells. These findings are consistent with recent field observations (Blais et al., 2017) showing a drastic modification of the phytoplankton community structure (from large to small cells) and a drop in phytoplankton biomass between 1999 and 2011 in the north of Baffin Bay. Changes in phytoplankton community composition have also been reported in the Chukchi Sea and correlated with the sea-ice retreat timing (Fujiwara et al., 2014). Using satellite data, Kahru et al. (2011) reported significant trends (from 1997 to 2009) towards earlier (up 3-5 days per year) phytoplankton blooms in Arctic Ocean and peripheral seas. Particular regions experiencing earlier blooms include e.g., the Hudson Bay, Baffin Sea, off the coasts of Greenland and Kara Sea, which are also areas roughly coincident with trends toward earlier summer ice break-up (Kahru et al., 2011). Model outputs together with satellite data also suggest that changes in ice-retreat timing have a strong impact on the timing variability in pelagic phytoplankton and ice-algae peaks (Ji et al., 2013). As an example, in the Barents Sea, phytoplankton blooms are triggered by different stratification mechanisms : heating of the surface layers in ice-free waters and melting of the sea-ice along the ice edge (Oziel et al., 2017). Another study (Zhai et al., 2012) also detected earlier blooms north of the Iceland-Faroe area (Arctic waters) due to early stratification and a later bloom in the southern area (Atlantic waters) characterized by a weakly stratified water-column. In Greenland, Iceland and Norwegian seas, results from a biophysical model showed that earlier phytoplankton blooms lead to an earlier and more severe nutrient drawdown (Zhang et al., 2010). Further south, in the Baltic Sea, satellite observation (from 2000 to 2014) indicates that while bloom timing and duration co-vary with meteorological conditions, the bloom magnitude is mainly determined by winter nutrient concentration (Groetsch et al., 2016). In the Labrador Sea, the positive relationship between deep winter (convective) mixing and nutrients concentration creates favorable conditions for phytoplankton growth in spring and summer (Harrison et al.,

2013). Recent increases in Arctic freshwater flux may weak convective mixing (Yang et al., 2016) and thereby potentially lead to a significant reduction in phytoplankton production. However, a progressive deepening of winter convection in the Labrador Sea was observed since 2012 (Yashayaev and Loder, 2017).

On the above basis, it seems clear that in northern high-latitude oceans the seasonality of the phytoplankton bloom is controlled primarily by sea-ice dynamics, light and nutrient availability. In this context, the interplay between stratification and mixing plays a fundamental role in shaping the biological production. Stratification causes the retention of phytoplankton within the euphotic layer, making light more available but limiting access to inorganic nutrients. Light levels and the availability of nutrients can therefore vary according to the intensity of the vertical stratification. The latter in turn depends upon the temperature and salinity gradients as well as vertical mixing processes (Drinkwater et al., 2010). It follows that changes in physical forcing result in a modification of the balance between stratification and mixing. For instance, although freshwater strengthens the stratification, a reduced sea-ice cover exposes an ever-increasing fraction of the water column to wind-induced mixing processes. Periodic vertical mixing, driven by wind events enhancing the nutrient replenishment, can therefore burst and sustain the biological production, eventually throughout the growing season (Tremblay et al., 2011, 2015). Recently, Ardyna et al. (2014) using satellite data, documented a fundamental shift from a polar to a temperate mode. The development of a second bloom in several regions of the Arctic and sub-arctic oceans seems to coincide with the delayed freeze-up and the increased exposure of sea surface to wind stress.

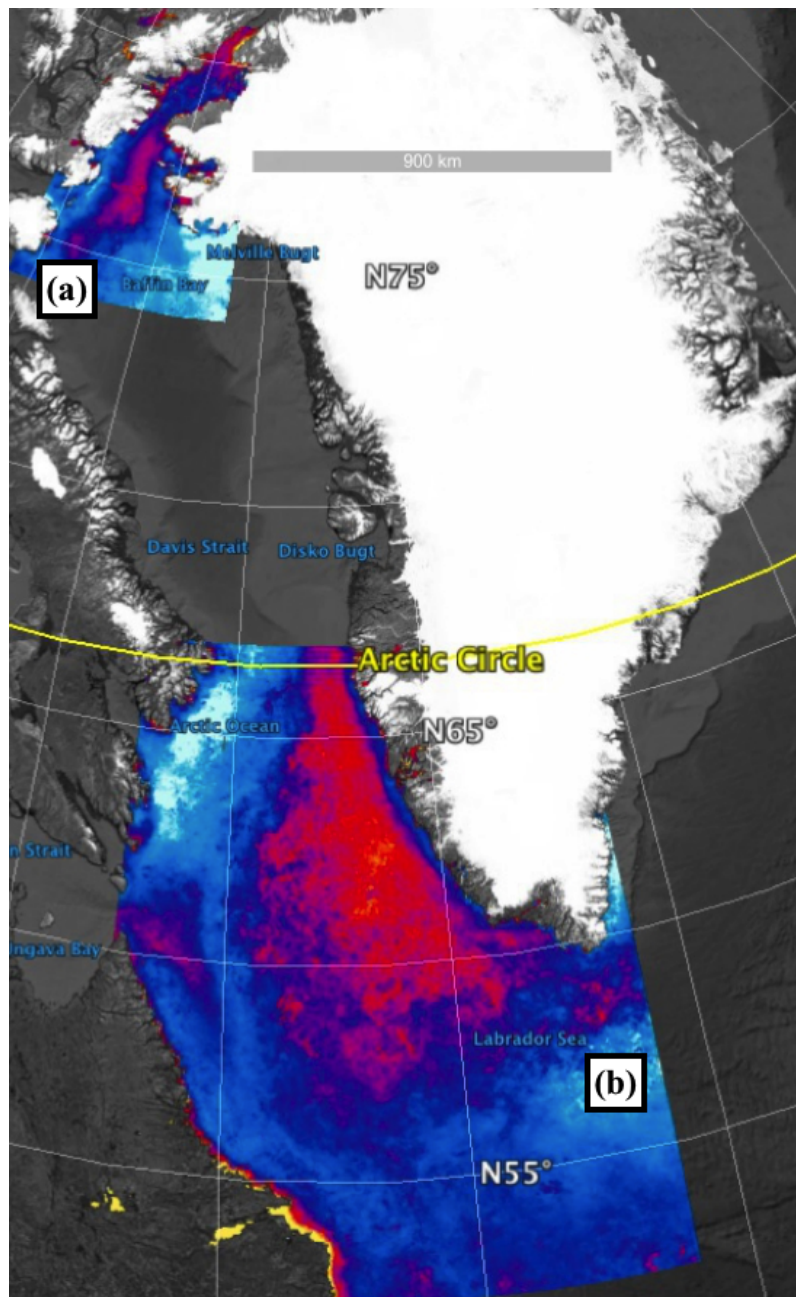


Figure 3: The figure shows (a) the North Water (NOW) polynya located in northern Baffin Bay ($>75^{\circ}\text{N}$) and southernmost (b) the Labrador Sea, a sub-polar sea that connects the North Atlantic with the Arctic Ocean. The Arctic Circle is also indicated (yellow line). The color gradient, from blue (low values) to red (high values), is given by the chlorophyll-a climatology derived from GlobColour (<http://www.globcolour.info>) images from 1998 to 2015.

Thesis objectives and study areas

The large seasonality in light, temperature, and sea-ice extent is an integral aspect of the Arctic and subarctic marine regions. However, the continuous Arctic-wide decrease in sea-ice cover and its amplifying effect on the warming are modifying abiotic (e.g., balance between stratification and mixing) and biotic (e.g., grazing) mechanisms (Winder and Sommer, 2012). In present-day climate conditions, monitoring the extent of the shifts in timing together with the spatial distribution of phytoplankton blooms is relevant because of their influence on biogeochemical cycles and marine ecosystem structure and functioning. A better understanding of the phytoplankton response to these ongoing environmental alterations may therefore provide a sensitive indicator of climate change.

Therefore, given the central role of phytoplankton in marine ecosystems, the main objectives of this thesis are (1) to detect and quantify changes in timing, magnitude, duration and spatial distribution of phytoplankton blooms in Arctic and subarctic regions recognized as marine biological hotspots; and (2) to relate these changes with variability in oceanic and meteorological forcing mechanisms.

To accomplish these goals we used a remote sensing approach supplemented by *in situ* measurements and models outputs. While essential knowledge on marine ecosystem structure and functioning will continue to be derived from specific *in situ* observations, the estimation of biological parameters (such as chlorophyll-a) through satellite remote sensing provides a powerful tool to characterize phytoplankton phenology at local, regional and global scales. Although satellite observations are limited to the ocean surface, the possibility of periodically mapping areas at relatively high temporal frequency provide compensating benefits.

The study was conducted at regional (and sub-regional scale) in two marine areas (Figure 3) sensitive to the effects of ongoing climate changes and considered as hotspots because of their biological and physical importance :

1. **The North Water (NOW) polynya**, located between Greenland and Ellesmere Island in northern Baffin Bay is the largest and one of the most biologically productive marine areas of the Arctic Ocean. The NOW serves as an important winter and summer habitat for marine birds and mammals and is considered an oceanographic “window” through which it is possible to evaluate the state of the Arctic marine ecosystem ;
2. **The Labrador Sea**, a sub-polar sea that connects the North Atlantic with the Arctic Ocean, represents a major focal point for ocean feedback to the climate system. It is a region characterized by a pronounced seasonality in biological production. The northern part of Labrador Sea host one of the largest phytoplankton spring bloom of the whole North Atlantic Ocean, with surface area that can reach as much as 700 000 km². In addition, deep convection and biology processes work together making the Labrador Sea one of the principle oceanic “sinks” for atmospheric carbon dioxide of the World Ocean.

This thesis includes a review (Chapter 1) of the current literature on the general concept of hotspots, three research articles (Chapters 2-4) and a general conclusion. Specifically, the chapters of this thesis addressed the following topics :

Chapter 1 provides a comprehensive review to introduce the approach that lies behind the concept of biodiversity hotspots. The main criticisms and controversies concerning this approach are also discussed. Next, links between biodiversity hotspots, marine pelagic ecosystem processes and the deep-sea realm are taken into consideration. Finally, some challenges in assigning global conservation priorities are briefly discussed. This chapter was done as part of the Ph.D. program and specifically in relation to the course *Synthèse Environnementale*. This chapter was published in *Global Ecology and Conservation* ([Marchese, 2015](#)).

Chapter 2 begins the research part of this thesis. The specific objective of this study is to investigate how contrasting effects of environmental factors may modulate

the phytoplankton bloom response over the North Water (NOW) polynya. A novel framework that combines an improved interpolation scheme to fill data gaps together with Gaussian-models is used to increase accuracy when phenology metrics were applied. This chapter was published in Polar Biology ([Marchese et al., 2017](#)).

Chapter 3 focuses on the bloom onset variability over the whole Labrador Sea. A biogeographic analysis is used to partition the Labrador Sea into regions with similar phytoplankton variability. Finally, the relationships between the spring bloom onset and physical forcing are investigated using satellite-derived ocean color observations and simulated data from a state-of-the-art ocean global circulation model (CGM). This chapter is at an advanced preparation stage and will be submitted to an high-impact and high-quality peer-reviewed journal at the earliest possible date.

Chapter 4 provides evidence for the occurrence of an anomalous springtime phytoplankton bloom that occurred in the Labrador Sea in 2015. The study, by using a combination of satellite and *in situ* observations, attempts to elucidate the mechanisms behind the extensive 2015 spring bloom. This chapter requires a little bit more work before being sent as a research letter to a scientific peer-reviewed journal.

The general conclusion reviews the main findings, highlights some possible limitations of the present study and presents a brief discussion on future research directions.

CHAPITRE 1

BIODIVERSITY HOTSPOTS: A SHORTCUT FOR A MORE COMPLICATED CONCEPT

Global Ecology and Conservation 2015, 3, 297-309

Christian Marchese¹

¹Université du Québec à Rimouski, Département de biologie, chimie et géographie, 300 allée des Ursulines, Rimouski (Québec), G5L 3A1 Canada

1.1 Résumé

Dans une ère caractérisée par l'activité humaine, les changements de l'environnement planétaire, la perte d'habitat et la disparition des espèces, les stratégies de conservation marquent une avancée décisive pour réduire la perte de biodiversité. C'est le cas notamment de l'acidification des océans et du changement d'affectation des terres qui s'intensifient en plusieurs endroits, et dont les conséquences sont souvent irréversibles pour la biodiversité. Bien que critiqués, les points névralgiques de la biodiversité sont devenus des éléments clés pour élaborer les priorités de conservation et jouent un rôle important dans les décisions et stratégies économiques en matière de préservation de la biodiversité des écosystèmes terrestres, et marins, par extension. Cette action locale, applicable à toute échelle géographique, est tenue pour l'une des meilleures approches pour maintenir une large part de la diversité biologique mondiale. En revanche, la délimitation des points névralgiques repose à la fois sur des critères quantitatifs et des considérations subjectives, d'où le risque de négliger certaines zones, comme les points froids, dont la valeur de conservation pourrait sembler moindre. Or il est largement reconnu de nos jours que la biodiversité va bien au-delà du nombre d'espèces dans une région donnée et qu'une stratégie de conservation ne saurait simplement se baser sur le nombre de taxa dans un écosystème. L'idée qui s'impose de plus en plus, par conséquent, est la nécessité de revoir les priorités de conservation sur la base d'une approche interdisciplinaire qui en passe par la mise en place de partenariats politiques et scientifiques.

Mots clés : changement climatique, points froids, richesse spécifique, diversité phylogénétique, services écosystémiques

1.2 Abstract

In an era of human activities, global environmental changes, habitat loss and species extinction, conservation strategies are a crucial step toward minimizing biodiversity loss. For instance, oceans acidification and land use are intensifying in many places with negative and often irreversible consequences for biodiversity. Biodiversity hotspots, despite some criticism, have become a tool for setting conservation priorities and play an important role in decision-making for cost-effective strategies to preserve biodiversity in terrestrial and, to some extent, marine ecosystems. This area-based approach can be applied to any geographical scale and it is considered to be one of the best approaches for maintaining a large proportion of the world's biological diversity. However, delineating hotspots includes quantitative criteria along with subjective considerations and the risk is to neglect areas, such as coldspots, with other types of conservation value. Nowadays, it is widely acknowledged that biodiversity is much more than just the number of species in a region and a conservation strategy cannot be based merely on the number of taxa present in an ecosystem. Therefore, the idea that strongly emerges is the need to reconsider conservation priorities and to go toward an interdisciplinary approach through the creation of science-policy partnerships.

Keywords: climate change, Coldspots, Species richness, Phylogenetic diversity, Ecosystem services

1.3 Introduction

As demonstrated by several researches, maintaining biodiversity is essential to the supply of ecosystem services and not less important to support their health and resilience (Pereira et al., 2013). However, despite there being an international interest to sustain and protect biodiversity, its loss does not seem to slow down (Butchart et al., 2010). Although there has been an extension of protected areas (Pimm et al., 2014), these provide a still low species coverage (Venter et al., 2014) and do not appear to optimally protect biodiversity (Pimm et al., 2014). For instance, a recent analysis for conservation priorities in marine environments by combining spatial distribution data for nearly 12,500 species with human impacts information, identified new areas of high conservation value that are located in Arctic and Antarctic Oceans and beyond national jurisdictions (Selig et al., 2014).

Overall, habitat change and their over-exploitation, pollution, invasive species and in particular climate change are the major causes for biodiversity loss. The combined effect of these anthropogenic pressures may have already started a critical transition toward a tipping point (Barnosky et al., 2012). In particular, climate is modifying rapidly forcing biodiversity to adapt either through the change of habitat and life cycles or the development of new physical traits (Bertheaux et al., 2010). For instance, rising temperatures can lead to potential biodiversity increases in northern regions (i.e., northern biodiversity paradox) where low temperatures usually are a limiting factor for the establishment of many species (Bertheaux et al., 2010). Given the importance that biodiversity plays, the understanding of the main threats to biodiversity is today than ever before a central objective in conservation biology. Nowadays there is serious concern about the effectiveness of existing strategies for biodiversity protection. A central issue in conservation is to identify biodiversity-rich areas to which conservation resources should be directed. Based on the observation that some parts of the world have far more species than others, the area-based approaches are widely advocated for species

conservation planning. Areas with high concentrations of endemic species (species that are found nowhere else on Earth) and with high habitat loss are often referred to as "hotspots" (Myers, 1988). The hotspot approach can be applied at any geographical scale and both in terrestrial and marine environments. However, hotspots represent conservation priorities in terrestrial ecosystems but remain largely unexplored in marine habitats (Worm et al., 2003) where the amount of data is still poor (Mittermeier et al., 2011).

Despite this lack of homogeneity in data between terrestrial and aquatic ecosystems, the recent concerns over loss of biodiversity have led to calls for the preservation of hotspots as a priority. As reported by Myers (2003) at the end of his article, "Edward O. Wilson, one of the leading authorities on conservation, described the hotspot approach as "the most important contribution to conservation biology of the last century". Closely linked to the concept of biodiversity, the hotspot concept is used with increasing frequency in biology and conservation literature and often with different meanings. While in a strict sense, the meaning is based on an estimate of endemic species and habitat loss, in a broad sense it refers to any area or region with exceptionally high biodiversity at the ecosystem, species and genetic levels.

The aim of this work is to review the current literature on the general concept of hotspots. We first introduce the approach that lies behind the concept of hotspots, in both terrestrial and marine ecosystems. Next we discuss the main criticisms and controversies concerning this approach and we present the possibility of using different alternative metrics to identify hotspots. Then we bring to light the links between biodiversity hotspots and marine pelagic ecosystem processes and we briefly introduce the deep-sea, a realm for the most part unknown for which several key questions are still waiting for an answer. Finally, we briefly discuss additional approaches and criteria, such as costs, in order to highlight some challenges in assigning global conservation priorities.

Table 1: Biodiversity hotspots from 1988 to present (modified from [Mittermeier et al. 2011](#))

Myers (1988)	Myers(1990)	Myers et al. (2000)	Mittermeier et al. (2004)	2011 Revision
Uplands of Western Amazonia	Uplands of Western Amazonia	Tropical Andes (a)	Tropical Andes	Tropical Andes
Western Ecuador	Western Ecuador			
Colombian Choco	Colombian Choco	Choco/Darien/western Ecuador (b)	Tumbes-Choco-Magdalena	Tumbes-Choco-Magdalena
Atlantic Coast Brazil	Atlantic Coast Brazil	Atlantic Coast Brazil	Atlantic Forest	Atlantic Forest
		Brazilian Cerrado	Cerrado	Cerrado
	Central Chile	Central Chile (a)	Chilean Winter Rainfall and Valdivian Forest	Chilean Winter Rainfall and Valdivian Forest
		Mesoamerica	Mesoamerica	Mesoamerica
		Caribbean	Madrean Pine-Oak Woodlands	Madrean Pine-Oak Woodlands
	California Floristic Province	California Floristic Province	Caribbean Islands	Caribbean Islands
	Ivory Coast	Guinean Forest of West Africa (a)	California Floristic Province	California Floristic Province
	Cape Floristic Region	Cape Floristic Province	Guinean Forest of West Africa	Guinean Forest of West Africa
		Succulent Karoo	Cape Floristic Region	Cape Floristic Region
			Succulent Karoo	Succulent Karoo
			Maputaland-Podoland-Albany	Maputaland-Podoland-Albany
	Tanzania	Eastern Arc and Coastal Forest of Tanzania/Kenya (c)	Eastern Afromontane (d)	Eastern Afromontane
			Coastal Forests of Eastern Africa (d)	Coastal Forests of Eastern Africa
			Horn of Africa	Horn of Africa
Eastern Madagascar	Eastern Madagascar	Madagascar and Indian Ocean Islands	Madagascar and Indian Ocean Islands	Madagascar and Indian Ocean Islands
		Mediterranean Basin	Mediterranean Basin	Mediterranean Basin
		Caucasus	Caucasus	Caucasus
			Irano-Anatolian	Irano-Anatolian
			Mountains of Central Asia	Mountains of Central Asia
	Western Ghats in India			
	Southwestern Sri Lanka	Western Ghats and Sri Lanka (b)	Western Ghats and Sri Lanka	Western Ghats and Sri Lanka
		Mountains of South-Central China	Mountains of South-Central China	Mountains of South-Central China
			Indo-Burma	Indo-Burma
Eastern Himalayas	Eastern Himalayas	Indo-Burma (e)	Himalaya (f)	Himalaya
Peninsular Malaysia	Peninsular Malaysia			
Northern Borneo	Northern Borneo	Sundaland(b)	Sundaland	Sundaland
		Wallacea	Wallacea	Wallacea
	Philippines	Philippines	Philippines	Philippines
			Japan	Japan
	Southwest Australia	Southwest Australia (a)	Southwest Australia	Southwest Australia
				Forests of East Australia (g)
			East Melanesian Islands	East Melanesian Islands
		New Zealand	New Zealand	New Zealand
New Caledonia	New Caledonia	New Caledonia	New Caledonia	New Caledonia
		Polynesia-Micronesia	Polynesia-Micronesia	Polynesia-Micronesia

(a) Expanded.

(b) Merged and/or expanded.

(c) Expanded to include Coastal Forests of Tanzania and parts of Kenya.

(d) The Eastern Arc and Coastal Forests of Tanzania/Kenya hotspots was split into the Eastern Afromontane hotspot (the Eastern Arc Mountains and Southern Rift, the Albertine Rift, and the Ethiopian Highlands) and Coastal Forests of EasternAfrica (southern Somalia south through Kenya, Tanzania and Mozambique).

(e) Eastern Himalayas was divided into Mountains of South-Central China and Indo-Burma, the latter of which was expanded.

(f) The Indo-Burma hotspot was redefined, and the Himalayan chain was separated as a new Himalayan hotspot, which was expanded.

(g) The Forests of Eastern Australia the 35th biodiversity hotspot.

1.4 Biodiversity hotspots

1.4.1 The biodiversity hotspots concept

The British ecologist Norman Myers first published the biodiversity hotspot thesis in 1988. Myers, although without quantitative criteria but relying solely on the high levels of habitat loss and the presence of an extraordinary number of plant endemism, identified ten tropical forest "hotspots" (Mittermeier et al., 2011). A subsequent analysis (Myers, 1990) added a further eight hotspots, including four in Mediterranean regions. Conservation International (CI: <http://www.conservation.org>) adopted Myers' hotspots as its institutional blueprint in 1989, and afterwards worked with him in a first systematic update of the global hotspots. Myers, Conservation International, and collaborators later revised estimates of remaining primary habitat and defined the hotspots formally as biogeographic regions with >1500 endemic vascular plant species and $\leq 30\%$ of original primary habitat (Myers et al., 2000). This collaboration, which led to an extensive global review (Mittermeier et al., 1999) and a scientific publication (Myers et al., 2000) saw the hotspots expand in area as well as in number, on the basis of both the better-defined criteria and new data. A second major revision and update in 2004 (Mittermeier et al., 2005) did not change the criteria but by redefining several hotspots boundaries, and by adding new ones that were suspected hotspots for which sufficient data either did not exist or were not easily accessible, brought the total to 34 biodiversity hotspots (Mittermeier et al., 2011). Recently, a 35th hotspot was added (Williams et al., 2011), the Forests of East Australia. The 35-biodiversity hotspots (Table 1; Figure 4) that cover only 17.3% of the Earth's land surface are characterized by both exceptional biodiversity and considerable habitat loss (Myers et al., 2000). More precisely, hotspots maintain 77% of all endemic plant species, 43% of vertebrates (including 60% of threatened mammals and birds), and 80% of all threatened amphibians (Mittermeier et al., 2011; Williams et al., 2011).

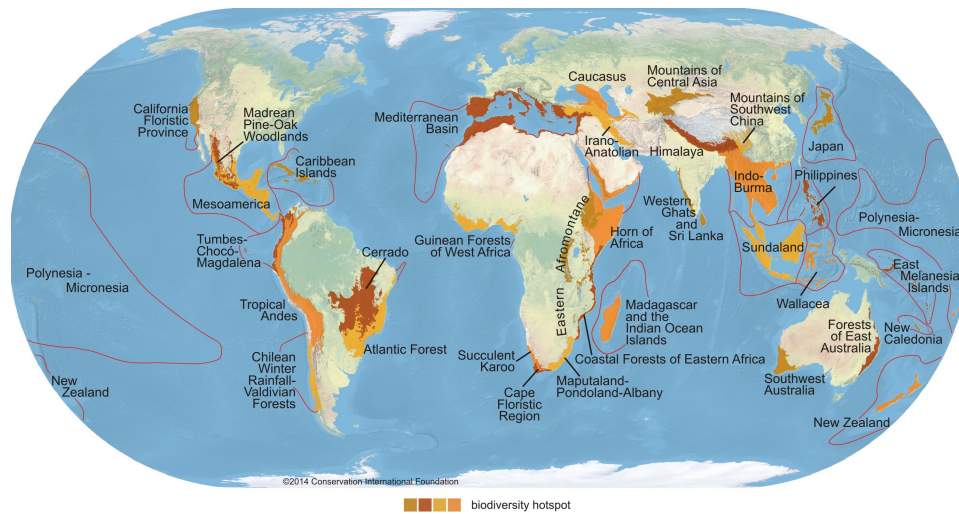


Figure 4: The world's biodiversity hotspots (see also Table 1 for hotspots names). Figure licensed under the Creative Commons Attribution-Share Alike 4.0 International license (Author: Conservation International).

Biodiversity is important in the oceans as on land. Myers and colleagues, however, excluded the oceans from their analysis. In particular, coral reefs are one of the most biologically diverse ecosystems in the ocean and provide important structures and habitat in tropical and sub-tropical coastal waters (Bellwood et al., 2004). In these areas, where the explanation for the high number of species is still debated (Bowen et al., 2013; Cowman and Bellwood, 2013), ocean acidification and changes in sea surface temperature (Ateweberhan et al., 2013) are likely to cause major coral reef losses and changes in the distribution and relative abundances of marine organisms. Moreover, apart from the intrinsic biodiversity value, there are economic arguments for the protection of marine biodiversity (Balmford et al., 2002). This makes the maintenance of marine biodiversity a valuable environmental management goal. Roberts et al. (2002), through the publication of one of the most comprehensive studies of hotspots on global coral reefs, have brought much-needed attention to marine hotspots, extending the hotspot concept to coral reefs and arguing that biodiversity hotspots are major centers of endemism in the sea as well as on land. Overall, the analysis revealed the 18 richest multi- taxon

centers of endemism, of which 10 were considered to be marine biodiversity hotspots. Furthermore, 8 of 10 marine biodiversity hotspots and 14 of 18 centers of endemism were found to be adjacent to terrestrial biodiversity hotspots, suggesting a possible integration among terrestrial and marine conservation ([Roberts et al., 2002](#)).

1.4.2 Criticism of biodiversity hotspots

Since its introduction, the concept of hotspots was used as a key strategy for global conservation action. For this reason, it has become the principal global conservation-prioritization approach, attracting over \$1 billion in conservation investment ([Sloan et al., 2014](#)). The approach is thus partly economic and it is based on the fact that it is not possible to protect the full range of biodiversity since it would certainly not be a realistic target. Basically, biodiversity conservation requires prioritization to be effective, if only because funds are limited and must be allocated carefully ([Myers, 2003](#)). Therefore, among many others, entities like Conservation International, have explicitly adopted the hotspot concept as a central conservation-investment strategy ([Sloan et al., 2014](#)).

In a 2003 essay entitled "Conserving Biodiversity Coldspots", conservation biologists Peter Kareiva and Michelle Marvier argued that non-governmental organizations, foundations and international agencies have been seduced by the simplicity of the hotspot idea, and significant financial resources ([Dalton, 2000](#)) have been directed toward them. In particular, the two conservation biologists argued that coldspots, despite being poorer for number of species, play an important ecological role. By investing exclusively in hotspots and ignoring coldspots the risk is to lose large, natural and ecologically important areas that contribute to many ecosystem services ([Kareiva and Marvier, 2003](#)). On the same wavelength, [Jepson and Canney \(2001\)](#) have warned that the biodiversity hotspots approach provides only a partial response for the conservation. The authors agree that promoting biodiversity hotspots, as a "silver bullet" strategy for conserving

the most species for the least cost is a risk in complex areas of international policy, such as biodiversity conservation, because decision makers may view it as a cure-all. As a result, they conclude that spatial priorities and public policy cannot be determined on the basis of simple species counts, which is the foundation of the biodiversity hotspot approach. Furthermore, as pointed out by [Smith et al. \(2001\)](#) biodiversity hotspots entirely ignore regions of ecological transition. Hence, the authors promote a more comprehensive approach to include regions important to the generation and maintenance of biodiversity, regardless of whether they are "species-rich". Recently, [Stork and Habel \(2014\)](#) have emphasized the lack of consideration for the role of invertebrates (e.g., herbivorous insects, herbivorous fungi and nematodes) in decision-making about global biodiversity hotspots, suggesting a more detailed analysis of the role of plants as umbrella species for these herbivorous organisms.

Furthermore, since data on species distributions are usually scarce the conservation of an entire global hotspot may be difficult and unsustainable. In this regard, [Cañadas et al. \(2014\)](#) pointed out the need to focus strategies on small areas that represent maximum diversity and/or endemism. Finally, for some of the same reasons that fueled disputes for terrestrial ecosystems, hotspots on coral reefs ([Roberts et al., 2002](#)) have also been the subject of controversy ([Baird et al., 2002](#); [Hughes et al., 2002](#)). In this respect, [Parravicini et al. \(2014\)](#) have recently identified tropical reef areas that are critical for preventing the loss of fish taxonomic and functional biodiversity. These areas, such as the Western Indian Ocean, differ in important ways from the fish richness hotspots previously identified close to the Indo-Australian Archipelago.

These criticisms highlight the problems associated with the idea of biodiversity hotspots, even though [Myers \(2003\)](#) (whose criteria include endemism and species richness) points out that other criteria are not ruled out by the theory itself. Essentially, the author affirms that the hotspot approach does not exclude other areas that need conservation, but nevertheless claims that a conservation strategy will always need

a measure to determine priorities. In conclusion, although not completely free from criticism, the hotspot approach has become a key tool to guide conservation efforts and presently plays a leading role in decision-making regarding conservation cost-effective strategies (O'Donnell et al., 2012).

1.5 Hotspots identification

Biodiversity hotspots are particular areas where extraordinary concentrations of biodiversity exist. Although hotspots have also been identified through different ways (Hoekstra et al., 2005), these areas are usually defined by one or more species-based metrics (number of species - species richness; number of species restricted to a particular area - endemic species richness; and number of rare or threatened species) or focusing on phylogenetic and functional diversity in order to protect species that support unique and irreplaceable roles within the ecosystem.

1.5.1 Species-based metrics

A central issue in conservation today is to identify biodiversity-rich areas. Species richness (SR) has been the main focus of conservation studies and is still widely used, mainly because it is easy to quantify and interpret data (Davies and Cadotte, 2011). In particular, conservation planning has traditionally used richness information combined with different irreplaceability measures (e.g., endemism or rarity) to prioritize some regions over others (e.g., biodiversity hotspots). In the methodology proposed by Myers et al. (2000), the key factors considered for the analysis were: (1) numbers of endemics and endemic species/area ratios for both plants and vertebrates, and (2) habitat loss. More precisely, vascular plants were chosen as the metric for endemism because fairly well known and essential to all forms of animal life, while vertebrates (four groups: mammals, birds, reptiles and amphibians) were mainly used to determine congruence

and to facilitate other comparisons among the hotspots. However, the analysis omitted invertebrates because they are not yet well documented and fish, because of lack of good data. Finally, the boundaries of the hotspots were determined by examining biological commonalities with each of the areas featuring a separate biota or community of species that fits together as a biogeographic unit. Therefore, selecting biodiversity hotspots requires data on species distributions together with the definition of a threshold useful to define the boundaries between hotspots and non-hotspots (Cañadas et al., 2014).

Increasing evidence, both in marine and terrestrial environments, shows that hotspots of total species richness are not always concordant with hotspots of endemism or threat. Concentrations of threatened species or local endemics may also occur in areas of lower richness (Hughes et al., 2002). Orme et al. (2005), using a global database to map the geographical distribution of birds, found an alarming lack of congruence between hotspots defined with the criterion of species endemism and areas of high species richness and concentrated threat. Furthermore, species richness for one taxon may not match perfectly with hotspots in the richness of another (Davies and Cadotte, 2011). For example, while Lamoreux et al. (2006) have found high congruence between conservation priorities for terrestrial vertebrate species, Grenyer et al. (2006) reported low congruence between conservation priorities for mammals, birds, and amphibians. Recently, a new assessment of global conservation priorities (Jenkins et al., 2013) mapped global priority areas using the latest data on mammals, amphibians, and birds at a scale 100 times finer than previous assessments (Ceballos and Ehrlich, 2006; Grenyer et al., 2006; Lamoreux et al., 2006). This analysis has identified areas in the world that are currently ignored by biodiversity hotspots but critical for preventing vertebrate extinctions. Finally, focusing on small areas Cañadas et al. (2014) showed that even in areas that are noted to be hotspots, the endemic-plant richness is not uniformly distributed, but rather depends largely on environmental conditions. Specifically, according to the authors, it is possible to identify hotspots within hotspots that can be organized in a hierarchy helping to focus conservation efforts at different scales within a given hotspot.

1.5.2 Phylogenetic diversity

The use of species-based metrics remains the primary method for characterizing and mapping the distribution of biological diversity and thus to identify areas as biodiversity hotspots. However, because diversity, or evolutionary history, is distributed unequally between taxa as well as between areas, taking into consideration only traditional species diversity may not be sufficient to fully capture differences among species (Chao et al., 2015). Therefore, to quantify biodiversity the focus shifted from pure species counting to a more integrative approach that quantifies the evolutionary information represented within groups of taxa (i.e., phylogenetic diversity, PD) along with the diversity of ecological traits (i.e., functional diversity, FD). The loss of FD or PD per unit of habitat loss may be a better indicator of ecosystem vulnerability, providing a more comprehensive measure than those based exclusively on the loss of single species. Recently, D'agata et al. (2014) showed that despite a minimal loss of fish richness that can occur along a human pressure gradient, many functions and phylogenetic lineages might be lost. PD might thus be more useful than species richness in maintaining ecosystem services (Cadotte and Jonathan Davies, 2010). Its use redefines the identification of species of conservation interest by taking into consideration the evolutionary information represented within groups of taxa, providing additional information to guide conservation decision-making. Phylogenetic information is increasingly being used in ecological studies (Cadotte et al., 2010) in parallel with an increasing number of new and sophisticated metrics that incorporate different community attributes such as abundance information and geographical rarity (Cadotte and Jonathan Davies, 2010; Cadotte et al., 2010). Probably, the increasing availability of molecular data and the recent advances in software and phylogenetic methods (Roquet et al., 2013) will enhance even more the use of phylogenetic information to better characterize and describe biodiversity patterns and ecosystem functioning.

1.5.3 Which metric?

A limiting factor in conservation assessments is the availability of appropriate and quality data on spatial information upon which the effectiveness of conservation planning depends. For example, assessing endemism in the western Amazon (one of the world's last high-biodiversity wilderness areas) continues to be a major challenge and vast areas have yet to be surveyed by scientists, and in consequence many species distributions are poorly known (Bass et al., 2010). Moreover, biodiversity is not an easy concept to measure and the choice of metrics to define hotspots is thus an important and sensitive issue that may lead to different conclusions regarding the future positioning of hotspots (Possingham and Wilson, 2005). For instance, a recent study by integrating abundance and functional traits revealed new global hotspots of fish diversity and identified unrecognized biodiversity value in some temperate and southern hemisphere marine regions (Stuart-Smith et al., 2013).

Species richness has been a convenient criterion to identify hotspots (Cadotte and Jonathan Davies, 2010). However, as noted above, biodiversity metrics might better reflect spatial diversity patterns for biogeography and conservation planning by considering evolutionary history and functional diversity. Although measures of species richness assume all species have equal weights, a common criticism of the alternative diversity metrics is that they are sensitive to the calculations and the weighting scheme used to construct them (Tucker et al., 2012). As evidenced by Cadotte and Jonathan Davies (2010), the reliability of these metrics is closely linked with the quality of the underlying phylogenetic and distributional data. The choice of a particular metric can, therefore, significantly alter conservation priority. Recently, understanding if there is a broad agreement between the results obtained from the use of different metrics has become of common interest to correctly detect biodiversity distribution patterns and identify diversity hotspots. For instance, Mazel et al. (2014) have found that SR, PD and FD are not necessarily good surrogates for each other. Furthermore, the effect

of considering PD metrics in existing conservation planning is still debated (Rosauer and Mooers, 2013; Winter et al., 2013). Recently, Zupan et al. (2014) investigated patterns of PD in relation to species diversity across three European taxonomic groups (birds, mammals and amphibians) to evaluate their congruence and to emphasize areas of particular evolutionary history. Results indicated that phylogenetic diversity patterns strongly mismatch in space between groups and demonstrated that the diversity of one taxonomic group is not representative of the diversity of other groups. Very likely, the increasing availability of phylogenetic data and advances in informatics tools may continue to facilitate a rapid expansion of studies that apply PD metrics and methods to community ecology (Cavender-Bares et al., 2009). Finally, the development of ever more sophisticated metrics (Rosauer et al., 2009; Cadotte et al., 2010) may help to provide new and significant information into the mechanisms that underlie the current patterns of biological diversity across different spatial scales.

Focusing our attention once again on species-based metrics, it is possible to consider the conservation status, which indicates the probability that a given species is vulnerable, at risk or close to extinction. For example, the IUCN Red List of Threatened Species (<http://www.iucnredlist.org/>) was conceived for this purpose becoming through time the most used system for assigning species' threat status (Keith et al., 2014). Nowadays the IUCN Red List may be used to aid effective conservation strategies by incorporating genetic data (Rivers et al., 2014), in conjunction with models to detect extinction risk from climate change (Keith et al., 2014) and to identify species at extinction risk using global models of anthropogenic impact (Peters et al., 2015).

Finally, terrestrial biodiversity can be modeled at different scales using remote sensing. Remote sensing is a useful tool to orient fieldwork, predict spatial patterns and to improve species richness models (Camathias et al., 2013). Especially, remote sensing can greatly aid conservation decisions, which are often made with relatively sparse information (Pressey, 2004) providing high-resolution spatial data and continuously

updated information on habitat status (area and degradation), alterations in species diversity and distribution, and trends in pressures and threats. As summarized in a recent review ([Nagendra et al., 2013](#)), different studies have used remote sensing tools and satellite imagery to quantifying terrestrial biodiversity (e.g., [Hernández-Stefanoni et al., 2012](#); [Mazor et al., 2013](#)). Remote sensing shows thus great promise for monitoring, managing protected areas and protecting biodiversity (see also [Pettorelli et al. 2014](#) for an up-to-date review). Basically, at this point, the improvement of existing technologies together with a better availability of global data quality on species ecologies and geographies represent an opportunity to improve our understanding on biodiversity patterns and to make a difference in environmental management.

1.6 Marine hotspots

Oceanic ecosystems sustain the human well being by providing major services like jobs and food supply. Due to climate change, physical and chemical conditions marine ecosystems are changing with time ([Doney et al., 2012](#)). In particular, ocean acidification represents a major threat to biodiversity ([Sunday et al., 2014](#)) whose maintenance promotes ocean health and service provision ([Worm et al., 2006](#)). Overall, the marine environment comprises two distinct and interconnected realms. The entire area of the open water is the pelagic realm and the pelagic organisms are those that live in the open sea away from the bottom. This is in contrast to the benthic realm, which is a general term referring to organisms and zones of the sea bottom. Oceanic waters and the deep-sea are here defined as waters and sea-floor areas over 200 m of depth.

1.6.1 Pelagic hotspots

The identification and monitoring of pelagic hotspots in marine ecosystems could constitute an effective approach to ocean conservation and resource management. How-

ever, the hotspot concept that fits well to more "static" marine habitats such as coral reefs (Roberts et al., 2002) is more difficult to apply in pelagic ecosystems (oceanic waters) where both boundaries and features are in constant movement due to the presence of highly dynamic physical processes (Hazen et al., 2013). For instance, this aspect is particularly evident in Arctic Ocean where oceanic fronts, polynyas or marginal ice zone, act as local hotspots of both productivity and biodiversity. In this dynamic context, it is thus important to examine biotic and abiotic environmental predictors (e.g., bathymetry, shelf-breaks, sea surface temperature, chlorophyll-a) of hotspots occurrence in order to explain their spatial distribution and persistence. As a consequence, the hotspot concept applied to marine ecosystems has received somewhat mixed definitions (e.g., Piatt et al., 2006; Worm et al., 2003; Sydeman et al., 2006). Overall, hotspots in the epipelagic zone have been described as areas where, relatively to the surrounding environment, particular and favorable physical condition promote high biological activity and thus the aggregation of primary and secondary consumers (Palacios et al., 2006). In these areas, upwelling, mesoscale eddies, and fronts may act in accordance with the local geomorphology to generate conditions that greatly promote the availability of prey for large fauna (Wingfield et al., 2011; Sigler et al., 2012). For example, seamounts are fixed locations but can act as biodiversity hotspots, attracting top pelagic predators and migratory species (Morato et al., 2010). Fundamentally, physical processes leading to hotspot formation and persistence are different and operate through different spatial and temporal scales. Mesoscale structure (10-1000 km; days to months) can determine the occurrence and persistence of marine hotspots and provide criteria for defining areas of high trophic transfer (Hazen et al., 2013). For example, cyclonic eddies enhancing nutrient inputs to the surface ocean are important sources of biological production that may contain high concentrations of biomass and probably affect the spatial and temporal variation in top predator hotspots (Santora and Veit, 2013).

Finally, given the dynamic nature of pelagic hotspots the integration of shipboard based studies with satellite remote sensing data may help to resolve possible spatiotem-

poral mismatches (Hazen et al., 2013). Although limited to surface conditions, due to their ability to sample local to global spatial scales over days to years, satellite-based observations of ocean conditions offer the greatest opportunity to quantify the persistence of many marine hotspots in space and time (Palacios et al., 2006). The primary biological indicator accessible remotely from space is the phytoplankton chlorophyll-a concentration, a good proxy of ocean productivity, which in turn has a significant effect on marine biodiversity (Corliss et al., 2009). For instance, Suryan et al. (2012) used a satellite-derived peak of surface chlorophyll-a as an index to identify seabird hotspots. Recently, a variety of bio-optical and ecological methods (Brewin et al., 2014) have been established to use satellite data to identify and differentiate between phytoplankton functional types (PFTs) that are relevant proxies of ecosystem functioning. The attempts to identify PFTs from space represent a new frontier, which no doubt has potential for further improvement. Remote sensing of ocean color, besides being an established tool to observe the global distribution of phytoplankton, may thus contain untapped potential for marine biodiversity studies. However, it is just as important to realize that remote sensing cannot provide all the answers. Recently, to provide support for the assessment of the state of the marine ecosystem, Racault et al. (2014a) proposed a suite of plankton indicators from different observing systems (e.g., mooring stations, ships, autonomous floats and remote sensing) and subsequently have classified them in an ecological framework that characterizes key attributes of the marine ecosystem. Finally, remote sensing analysis can be used in fisheries management (Chassot et al., 2011) and to characterize marine protected areas (Kachelriess et al., 2014) based on the dynamics of oceanographic boundaries (and thus in areas beyond national jurisdiction which remain vulnerable to uncontrolled exploitation) rather than on geographic boundaries employed by traditional marine protected areas. As long-term time series become available in the near future, remote sensing will offer opportunities to identify resilient pelagic marine hotspots.

1.6.2 Deep-water hotspots

Deep-sea ecosystems, which include the waters and sediments beneath approximately 200 m depth covering more than 65% of the Earth's (Danovaro et al., 2010) are going toward widespread changes in benthic ecosystems and the functions and services they provide (Jones et al., 2014). In particular, biodiversity hotspots such as seamounts, canyons, and cold-water coral reefs (Ramirez-Llodra et al., 2010), may be projected to experience changes in benthic food supply (Jones et al., 2014) with a significant impact on the distribution of species richness (Gambi et al., 2014). However, because of the vastness and remoteness of the habitats (the majority of which are found in international waters) the management and conservation of deep-sea ecosystems is not an easy task (Ramirez-Llodra et al., 2010) and several key questions are still waiting for an answer. Only recently deep-sea biodiversity was incorporated in the analysis of global biodiversity through international monitoring programs (Weaver et al., 2004; Brandt et al., 2014), the outcomes of which might contradict the assumptions and paradigms advanced in the past (Danovaro et al., 2014). For instance, recent results showed the existence of an exponential relationship between ecosystem functioning and deep benthic biodiversity (Danovaro et al., 2008). These new observations suggest that (1) open continental slope systems and deep basins are characterized by positive functional interactions between different seafloor organisms and (2) indicate that a considerable biodiversity loss in deep-sea ecosystems might lead to a drastic abatement of the key ecosystem processes (Danovaro et al., 2008, 2009). However, the two major trends in deep-sea biodiversity, the latitudinal and bathymetric gradients, are still strongly debated.

Preliminary results based on a large dataset collected during a collaborative project have provided new insights into latitudinal patterns (Danovaro et al., 2009) but their existence in deep-sea habitats remains still debated (Berke et al., 2014). For instance, while findings suggest that deep-sea diversity in the Southern Ocean presents high levels of biodiversity (Brandt et al., 2014) in the Northern Hemisphere studies with larger and

more robust datasets are required to fill data gaps. In the Arctic, apart from works that have investigated the distribution and diversity of benthic fauna in specific areas of the Arctic sea ([Meyer et al., 2014](#)), not many studies have been carried out to explicitly investigate the relationship between biodiversity and ecosystem functions ([Link et al., 2013](#)). However, a recent review that has achieved an inventory of benthic diversity of pan-Arctic shelves ([Piepenburg et al., 2011](#)), seems to confute the common paradigm of low Arctic diversity, providing evidence that Arctic shelves are not particularly impoverished.

About the bathymetric gradient, qualitative and quantitative sampling studies indicated a relationship between diversity and depth with a peak at mid-slope depths ([Ramirez-Llodra et al., 2010](#)). However, although some hypotheses together with biological and environmental factors have been proposed to explain why species diversity changes as a function of depth, the mechanisms that potentially control bathymetric patterns have not yet been fully understood ([Danovaro et al., 2009](#)). For instance, some abyssal regions (e.g., the Equatorial Pacific and Southern Ocean) are characterized by very high diversity ([Ramirez-Llodra et al., 2010](#)). The rate, nature and spatial variability of food supply can play a key role in modulating ecosystem structure and function ([Smith et al., 2008](#)). Recently, a long time series data was used to document the importance of large episodic pulses of particulate organic carbon (POC) as vital food supply for abyssal communities ([Smith Jr et al., 2014](#)). The analysis of time series reveals that in the past few years these pulses have increased in magnitude. Such increases in food supply that appears to change the structure and functioning of deep-sea communities seem to be connected with changes in surface ocean conditions ([Smith et al., 2013](#)). These outcomes suggest that different taxa may display different spatial patterns with increasing depth and thus, as evidenced by other authors ([Ramirez-Llodra et al., 2010](#)), the hump shaped curve ([Weaver et al., 2004](#)) does not represent the general rule. Certainly, topographic and geological features may also play a key role in shaping the biodiversity spatial patterns ([Danovaro et al., 2009](#)). For instance, seamounts can

act as biodiversity hotspots, attracting top pelagic predators and migratory species, such as whales, sharks, tuna or rays (Morato et al., 2010), as well as hosting a seafloor fauna with a large number of endemic species (Stocks and Hart, 2007). Considering the particularity and importance of these particular areas (Clark et al., 2010) a new method that uses seamounts has been recently proposed (Clark et al., 2014) for the selection of candidate "Ecologically or Biologically Significant Marine Areas" (EBSAs). Certainly, the development of new methods, international monitoring programs and new technologies can promote, as advocated by some organizations such as Convention on Biological Diversity (CBD), the conservation of open-ocean and deep-sea ecosystems.

1.7 Biodiversity conservation and priorities

Biodiversity conservation, for several reasons (e.g., climate change), cannot be considered an easy task and the establishment of priorities therein is complex. Given this intrinsic difficulty, developing a global biodiversity observation system might look something insurmountable (Pereira et al., 2013). However, a growing number of environmental organizations together with the scientific community are working on a number of different approaches (Table 2) to identify biodiversity patterns, threats and locations for future acquisition or management (Schmitt, 2011). These approaches, which prioritize globally important areas for biodiversity conservation, are based on two key ecological selection criteria (vulnerability and irreplaceability) and can be grouped into three main categories: proactive, reactive and representative (Schmitt, 2011). Like the hotspot approach, these efforts usually depend on species as the relevant unit of biodiversity, some important biodiversity dimensions, such as genetic diversity is often lacking (Pereira et al., 2013) and none of these approaches directly incorporate economic costs (Brooks et al., 2006). However, although their importance is still debated (Duke et al., 2013), economic costs could represent an important step in conservation planning. For instance, a recent study (Venter et al., 2014) clearly demonstrates that considerable

increase in global protected area coverage of species could be achieved at minimal additional cost with a consequent improvement in biodiversity trends ([Butchart et al., 2012](#)).

Table 2: The proactive, reactive and representative approaches used for the selection of biodiversity conservation priority areas at global scale. All the approaches are based on a combination of the ecological criteria of vulnerability and irreplaceability (Modified from [Schmitt 2011](#))

Approach	Organization	Vulnerability	Irreplaceability
<i>Proactive approaches</i>			
Frontier forests	World Resources Institute	Low	Low
Last intact forest landscapes	Greenpeace	Low	Low
Last of the wild	Wildlife Conservation Society	Low	Low
Wilderness areas	Conservation International	Low	Low
High biodiversity wilderness	Conservation International	Low	High
<i>Reactive approaches</i>			
Biodiversity hotspots	Conservation International	High	High
Alliance for Zero Extinction (AZE)*	52 Conservation organizations	High	High
Key biodiversity areas (KBAs)*	Conservation International	High	High
	Birdlife International		
	Plantlife International		
Important Bird Areas (IBAs)*	Birdlife International	High	High
<i>Representative approaches</i>			
Centers of plant diversity	WWF/IUCN		High
Endemic Bird Areas (EBAs)	Birdlife International		High
Global 200	WWF		High
Megadiversity countries	Conservation International		High

*Site-specific approaches

Incorporating information on costs and biodiversity benefit could thus provide a more cost-efficient allocation of limited conservation resources. In this respect, results from a recent study ([Waldron et al., 2013](#)) showed that funding for conservation measures

is scarce despite the high levels of threatened biodiversity. Finally, as evidenced by [Duffy et al. \(2013\)](#), there is not a proactive marine biodiversity observation network for monitoring and evaluating global ocean biodiversity.

Another issue is the loss of habitat structure that generally leads to a decline in species richness and biomass. The combined impacts of climate change and land use are expected to drive unprecedented rates of environmental change and biodiversity loss ([Riordan and Rundel, 2014](#)). In particular, climate change is likely to have a large impact on biodiversity, from organisms to biomes (see [Bellard et al. 2012](#) for an exhaustive review). In this respect, recent studies ([Bellard et al., 2014a,b](#)) examined the potential effects of global changes on hotspots. Results showed that 19% of the insular biodiversity hotspots might be entirely submerged by the global sea level rise while, by a combined effects of global changes, hotspots might experience an average loss of 31% of their area, with some hotspots more affected than others (e.g., Polynesia–Micronesia). Approaches that integrate climate change adaptation into conservation planning (see [Watson et al. 2012](#) for a review) are vital to monitor biodiversity responses and thus to maintaining the resilience of hotspots ([Bellard et al., 2014b](#)).

Finally, other dimensions of the problem, such as ecosystem services, need to be considered as well. Basically, changes in biodiversity can influence ecosystem processes and an alteration of these can influence ecosystem services ([Díaz et al., 2006](#)). Although there is still disagreement in the scientific community ([Reyers et al., 2012](#); [Schröter et al., 2014](#)), ecosystem services-based strategies could be used for specific conservation actions ([Bhagabati et al., 2014](#)) and for protected areas designation ([Potts et al., 2014](#)). Anyhow, the exploration of possible congruencies between the targets of protecting ecosystem services and conserving biodiversity ([Turner et al., 2007](#)) is still difficult. The absence of credible, reproducible and sustainable frameworks makes the integration of ecosystem services into decision making still debated ([Daily et al., 2009](#)).

1.8 Conclusion

In 1988, Norman Myers published the first of a series of high-impact articles on global biodiversity hotspots that opened the way for a new strategy of nature conservation. Although not entirely free from criticism, the hotspot approach has played an important role in conservation prioritization. Since it is not possible to conserve all biodiversity due to lack of resources, international conservation agencies have used it as the most effective approach to minimize species extinctions on a global scale. However, focusing all the conservation attention on biodiversity hotspots could create a disproportionate impact on the maintenance of biodiversity in other biomes. For instance, although desert ecosystems cover 17% of the world's landmass and harbor surprisingly high biodiversity, they have not received substantial financial support for conservation actions ([Durant et al., 2014](#)). An optimal conservation network would then include both areas with high levels of diversity, as well as larger coldspots that are home to rare species ([Kareiva and Marvier, 2003](#)). Not surprisingly, recent results emphasize the importance of rare species conservation and a more detailed understanding of the role of rarity and functional vulnerability in ecosystem functioning ([Mouillot et al., 2013](#)). Basically, coldspots could be as good as hotspots for directing conservation strategies since they might provide important ecosystem services. As pointed out by [Bøhn and Amundsen \(2004\)](#), an interesting study ([Price, 2002](#)) showed that stressful marine environments with low species richness could unexpectedly be both hotspots and coldspots of biodiversity. This may seem unusual, but as mentioned by the authors it represents a lack of focus on the ecological processes and interaction between organisms. Essentially, with the loss of the diversity of interactions and processes within and between organisms, the major risk is to irreversibly disrupt the integrity of the ecosystems and consequently the possibility to preserve functions and evolutionary processes indispensable to the maintenance and creation of new life ([Bøhn and Amundsen, 2004](#)).

Furthermore, another dimension of the problem, such as the incongruence among

diversity metrics, needs to be considered as well. The identification of biodiversity hotspots frequently relies on the basis of partial knowledge and is commonly based on an assumption that areas significant for well-known species are also important for other species. This implies that measures of diversity in different groups of organisms are highly correlated, but as we have seen, it may not always be necessarily true. Nonetheless, as previously reported, the development of new metrics that consider multiple aspects of biodiversity could help to provide new insights into the mechanisms that underlie the current patterns of biological diversity. Nowadays, an increasing number of studies (e.g., [Daru et al., 2015](#)) reinforce the need to adopt more integrative strategies, which considering evolutionary components and geographical distribution data, can better identify areas of high conservation priority.

Finally, it is becoming clear that the biodiversity hotspots approach represents a shortcut for a more complicated concept that is part of a bigger picture that includes consideration of ecosystem services, policies, costs, social preferences, and other factors, such as human activities and climate change. As mentioned by several authors, we need to go toward a common, modern and broader vision of biodiversity conservation. Scientific community, together with decision-makers in agencies, governments and non-governmental organizations, should thus carefully reconsider conservation priorities and, possibly, in order to avoid duplicating efforts ([Mace et al., 2000](#)), establish close partnerships ([Berteaux et al., 2010](#); [Maury et al., 2013](#)) to develop successful conservation strategies for biodiversity management ([Heller and Zavaleta, 2009](#)). Because of the complexity of the topic and the unpredictability brought by climate change, there is no single definitive praxis to effective conservation, but rather an interdisciplinary approach ([Pohl and Hadorn, 2008](#)) that is necessary today as never before.

Acknowledgements

I thank J. Ferron, S. Bélanger, J.-É. Tremblay, F. D'Ortenzio and D. Dumont for their constructive comments on an earlier draft of this manuscript. I am also grateful to an anonymous reviewer for his suggestions and useful criticisms, which significantly improved the paper.

CHAPITRE 2

CHANGES IN PHYTOPLANKTON BLOOM PHENOLOGY OVER THE NORTH WATER (NOW) POLYNYA: A RESPONSE TO CHANGING ENVIRONMENTAL CONDITIONS

Polar Biology 2017, 40 (9), 1721-1737

Christian Marchese¹, Camille Albouy^{1,2,3}, Jean-Éric Tremblay⁴, Dany Dumont⁵, Fabrizio D'Ortenzio⁶, Steve Vissault¹, Simon Bélanger¹

¹Université du Québec à Rimouski, Département de biologie, chimie et géographie, 300 allée des Ursulines, Rimouski (Québec), G5L 3A1 Canada

²Landscape Ecology, Institute of Terrestrial Ecosystems, ETH Zürich, Zurich, Switzerland

³Swiss Federal Research Institute WSL, 8903 Birmensdorf, Switzerland

⁴Québec-Océan et Takuvik, Département de biologie, Université Laval, Pavillon Alexandre-Vachon, 1045 av. de la Médecine, Québec, G1V 0A6 Canada

⁵Institut des sciences de la mer de Rimouski, Université du Québec à Rimouski, 310 allée des ursulines, Rimouski (Québec), G5L 3A1 Canada

⁶Laboratoire d'Océanographie de Villefranche (LOV), Université Pierre et Marie Curie and CNRS, UMR 7093, Villefranche-sur-Mer, France

2.1 Résumé

Certains indicateurs écologiques marins permettent de mesurer l'état des écosystèmes pélagiques. C'est le cas de l'apparition de l'efflorescence, qui nous prévient des possibles changements dans les interactions trophiques et les processus biochimiques. Cependant, représenter la phénologie de l'efflorescence du phytoplancton en de hautes latitudes où des observations à long terme sont rares ou non disponibles n'est pas une mince tâche. Un algorithme à fonction orthogonale empirique d'interpolation de données a été appliqué aux images satellitaires quotidiennes de chlorophylle pour produire des données à long terme (1998-2014) et sans nuages de la polynie des eaux du Nord. L'efflorescence saisonnière a été modélisée à partir d'une approche multigaussienne grâce à laquelle on a pu extraire une base de caractéristiques phénologiques. Ensuite, une analyse de corrélation met en évidence l'influence des facteurs environnementaux, dont la température de surface de l'océan, la fraction nuageuse, la tension du vent et la concentration de la glace marine, par la modulation de la date de début de l'efflorescence, sa durée et son amplitude. La variabilité annuelle de l'apparition de l'efflorescence semble tributaire d'un fragile équilibre entre les conditions océanographiques et météorologiques. Ainsi, l'efflorescence durera plus longtemps les années caractérisées par une plus longue période d'eaux libres et moins longtemps celles où la couverture de glace de mer sera plus étendue. Un déclin remarquable de l'amplitude de l'efflorescence du phytoplancton a été observé au cours de la période de dix-sept ans étudiée. Ces résultats croisés désignent les eaux du Nord comme un secteur sensible au climat, où l'écosystème pélagique marin semble mener à la baisse des concentrations en chlorophylle. Les séries temporelles par satellite demeurent encore trop courtes, cependant, pour qu'on soit en mesure de distinguer entre la variabilité d'une année ou d'une décennie à l'autre et un signe de changement climatique. Mais si ces changements devaient persister, les eaux du Nord pourraient ne plus représenter encore longtemps ce productif oasis régional qui abrite de prospères populations de zooplancton et de superprédateurs.

Mots clés: phénologie, phytoplancton, polynie des eaux du Nord, modèle gaussien, télédétection, forçage physique

2.2 Abstract

Marine ecological indicators can be used to assess the condition of the pelagic ecosystems. The bloom onset provides a warning bell for possible changes in trophic interactions and biogeochemical processes. However, depicting the phenology of phytoplankton blooms at high latitudes, where long-term observations are sparse or unavailable, is not a straightforward task. A data-interpolating empirical orthogonal function algorithm was applied to daily satellite-retrieved chlorophyll-a images to produce a long-term (1998-2014) and cloud-free data set over the North Water (NOW) polynya. The seasonal bloom was modeled using a multi-Gaussian approach from which a baseline of phenological characteristics was extracted. The correlation analysis highlights the influence of environmental factors, such as sea surface temperature, cloud fraction, wind stress, and sea-ice concentration, in modulating the bloom start date, its duration, and amplitude. The year-to-year variability in bloom onset appears to be controlled by a delicate balance between oceanographic and meteorological conditions. Blooms last longer during years characterized by a longer open-water period and are shorter during those characterized by greater sea-ice coverage. Noteworthy is the decrease in phytoplankton bloom amplitude over the 17 years examined. Collectively, these outcomes depict the NOW as a climate-sensitive region in which the pelagic marine ecosystem seems to be going toward a decline in chlorophyll-a concentrations. Satellite time series are still too short to differentiate between inter-annual variability, inter-decadal variability, and climate change signal. Should these changes persist; however, the NOW may no longer act as a productive regional oasis supporting thriving populations of zooplankton and top predators.

Keywords: phenology, phytoplankton, NOW polynya, Gaussian model, remote-sensing, physical forcing

2.3 Introduction

The Northern Hemisphere continues to experience profound environmental modifications in response to anthropogenic pressures (Gillett et al., 2008). One of the most evident changes is the decline of the Arctic sea-ice cover, which plays a crucial role in regulating light for phytoplankton primary production and the exchange of heat and moisture between the upper ocean and the atmosphere. Recent models and satellite observations show changes in the age of sea ice through a shift from multiyear to first-year types (Maslanik et al., 2011), drastic reductions in their extent and thickness (Stroeve et al., 2012), and an increasing of the melt season length (Stroeve et al., 2014). These remotely observed changes in the Arctic sea-ice cover were recently corroborated using a time series (2003-2012) constructed from direct observations (Renner et al., 2014). Profound alterations of the seasonal cycle of the Arctic seaice cover may lead to unexpected changes in Arctic marine ecosystem (Wassmann et al., 2011). Recent declines in minimum Arctic sea-ice extent and increasing cloudiness have affected, although unevenly, primary production over the Arctic Ocean (Petrenko et al., 2013; Bélanger et al., 2013a; Arrigo and van Dijken, 2015). For instance, the timing of sea-ice retreat has had a strong influence on the timing of the pelagic phytoplankton bloom (e.g., Ji et al., 2013; Kahru et al., 2011), leading to changes in phytoplankton community structure (Li et al., 2009; Fujiwara et al., 2014). Furthermore, these changes may consequently cause a temporal mismatch between primary producers, arctic grazers, and apex predators (Søreide et al., 2010). Finally, the delayed formation of sea ice and a longer exposure of the ocean surface to the wind force are probably enhancing momentum transfer to the upper Arctic ocean in summer and in fall (Rainville et al., 2011), with an increase in the occurrence of secondary blooms resulting from upward nutrient supply (Ardyna et al., 2014).

Closely linked to sea-ice conditions, polynyas (large areas of persistent open water surrounded by sea ice) are known as unique marine polar environments with peculiar

physical features. Polynya areas provide favorable conditions for primary producers by exposing surface water to solar radiation much earlier than adjacent ice-covered waters (Tremblay et al., 2002b). They also constitute key habitats for Arctic upper trophic predators, such as seabirds and marine mammals (Karnovsky and Hunt Jr, 2002; Heide-Jørgensen et al., 2013), serving as hotspots of both productivity and biodiversity (Marchese, 2015). Consequently, polynyas are usually considered as oceanographic "windows" through which it is possible to assess and evaluate the state of the Arctic marine ecosystem (Smith Jr and Barber, 2007; Tremblay and Smith Jr, 2007). Because changes in sea-ice dynamics and warming sea surface temperature (SST) will affect the onset and the lifespan of polynyas, as well as carbon flux and food webs, monitoring these particular areas is, therefore, of crucial importance.

Among the different Arctic polynyas (which number approximately 61, Barber and Massom 2007), the North Water (NOW) polynya located between Greenland and Ellesmere Island in northern Baffin Bay (Figure 5a) is the largest ($\sim 85,000 \text{ km}^2$) and historically one of the most biologically productive marine areas of the Arctic Ocean (Klein et al., 2002; Odate et al., 2002). The NOW is usually considered as a latent heat polynya, whose recurrent formation is mostly due to the divergent flow of sea ice away from an ice arch (or ice bridge) forming at the southern end of Nares Strait (Dumont et al., 2009). The NOW starts to expand in late March or early April and usually reaches its greatest extent in late July when it eventually opens to the bay and stops being a polynya in the strict sense (Tremblay et al., 2002b). The ice bridge, which represents the northern extent of the polynya, is also essential for the maintenance of the polynya. It prevents sea ice from drifting southward into northern Baffin Bay and allows strong northerly winds and sensible heat flux over localized areas to promote open water conditions (Ingram et al., 2002; Tremblay et al., 2006b). Specifically, the supply of oceanic heat occurs along the Greenland side due to upwelling and vertical and tidal mixing of relatively warm Atlantic waters yielded by a branch of the West Greenland Current. Conversely, cold and silicate-rich Pacific-derived water joins the

NOW region from the North through Smith Sound ([Tremblay and Smith Jr, 2007](#)). Once the polynya has formed, the interplay of physical factors, such as light availability, density stratification, wind mixing, and advection of nutrient into the euphotic layer, combines to support high levels of productivity in this region ([Mei et al., 2002](#); [Tremblay et al., 2002b](#)).

Given its biological importance, the NOW has been the site of a conspicuous number of studies and oceanographic missions mostly from 1997 to 2000 via the International North Water Polynya Study and more recently the ArcticNet field program (2005-onward). Overall, these studies suggest that the NOW ecosystem is subject to large inter-annual variability in primary production and whether its productivity increases or decreases will be strongly dependent on physical environmental factors (i.e., the formation of the Smith Sound ice arch; [Kwok et al. 2010](#)). A recent analysis ([Bélanger et al., 2013a](#)), using a satellite-based model to assess primary production trends (1998-2010) in Arctic waters, showed a substantial decrease in annual primary production over the NOW, suggesting changes in phytoplankton phenology. Based on seasonal nutrient drawdown, [Bergeron and Tremblay \(2014\)](#) inferred a 65% decline in the net community production from 1997 to 2011, which was attributed to freshening and increasing stratification. Recently, a field-based study ([Blais et al., 2017](#)) has also emphasized a sharp decrease in phytoplankton biomass and diatom abundance probably due to changes in sea-ice dynamics and water column stratification.

In this context, the action of specific physical processes is thus of particular importance. For instance, the interplay between strong wind activity and calm periods may foster surface nutrient replenishment and a more productive and long-lived bloom ([Tremblay et al., 2002b](#)). Since the observed changes in northern Baffin Bay would affect the supply of nutrients in the surface layer, the biological response of the pelagic ecosystem should be detectable using remote-sensing data. Although several satellite studies have investigated phytoplankton phenology at the global scale and over large

oceanic areas (e.g., Henson et al., 2006; Frajka-Williams and Rhines, 2010; Sasaoka et al., 2011; D’Ortenzio et al., 2012; Racault et al., 2012; Sapiano et al., 2012), only a few studies (Kahru et al., 2011; Ji et al., 2013; Ardyna et al., 2014) on phytoplankton phenology have been carried out in Arctic waters, where extensive cloudiness may obscure the extent and magnitude of the bloom.

Given the lack of specific information about the phytoplankton phenology over the NOW, the specific objectives of this study were twofold:

1. To fully capture in NOW waters the variability in bloom characteristics through the development of a novel framework, which is based on the combined use of cloud-free chlorophyll-a concentration [Chl-a; a proxy of phytoplankton biomass (Huot et al., 2007)] images and Gaussian models;
2. To describe inter-annual changes in phytoplankton phenology and to determine the extent to which contrasting effects of environmental factors may modulate the initiation, amplitude, and duration of phytoplankton blooms in the NOW polynya.

2.4 Material and methods

2.4.1 Cloud-free satellite chlorophyll-a time series

The area lying between 81°N-74°N and 82°W-63°W was selected to study changes in phytoplankton phenology over the NOW polynya (Figure 5a). For the period April-September of 1998-2014, daily time series of satellite-derived (Case I water) Chl-a (mg m^{-3}) binned at 25 km of spatial resolution (to reduce the frequency of spatial data gaps), estimated using the Garver-Siegel-Maritorena (GSM) algorithm (Maritorena et al., 2002), were obtained from the GlobColour Project (<http://hermes.acri.fr>). The latter, combining (when possible) data from different sensors [SeaWiFS (1998-2010), MERIS (2002-2011), MODIS-Aqua (2002-), and VIIRS (2012-)], provided an

enhanced spatiotemporal coverage (Maritorena et al., 2010) useful to partially overcome the problem of data gaps, thus representing the best available data for phytoplankton phenology studies (Ferreira et al., 2014). However, in the Arctic Ocean, clouds and fog near the sea surface can affect ocean-color data availability and estimates (Cole et al., 2012; Ferreira et al., 2014): data can be so sparse that the full seasonal phytoplankton cycle may not be detected. One solution is to bin several years of ocean color data to minimize data gaps in the time series and increase the goodness of phenological fitting procedure (e.g., Ardyna et al., 2014; Lacour et al., 2015). However, such an approach may mask the inter-annual variability in physical forcing and biological response, which may be very large at high latitudes (e.g., Frajka-Williams and Rhines, 2010).

Given the presence of missing values in the data set used here, we applied the data interpolating empirical orthogonal functions method (DINEOF; Beckers and Rixen 2003) to produce high temporal and spatial resolution cloud free Chl-a time series. The iterative DINEOF technique, by identifying the dominant spatial and temporal patterns, allowed a more accurate reconstruction of missing data without any *a priori* statistical information of the analyzed field (Alvera-Azcárate et al., 2005). This method has been shown to be appropriate for missing data reconstruction and prediction (Taylor et al., 2013). It has been used both for physical and biological data, such as surface Chl-a (Mauri et al., 2007; Sirjacobs et al., 2011; Wang and Liu, 2014), and has recently been applied to phytoplankton phenology studies (Corredor-Acosta et al., 2015).

To meet the DINEOF requirements, we excluded each daily image (spatial dimension) holding less than 5% of the expected data. The same criterion was applied through the temporal dimension, excluding all pixels holding less than 5% of valid data during the course of the open water season. Finally, the remaining spatial domain (67% of the original data set) was log-transformed prior to interpolation. Once the DINEOF method was applied (Taylor, 2016), for each interpolated image, a daily sea ice-mask (based on a 15% threshold - see the "Sea ice concentration" subsection) was superimposed to

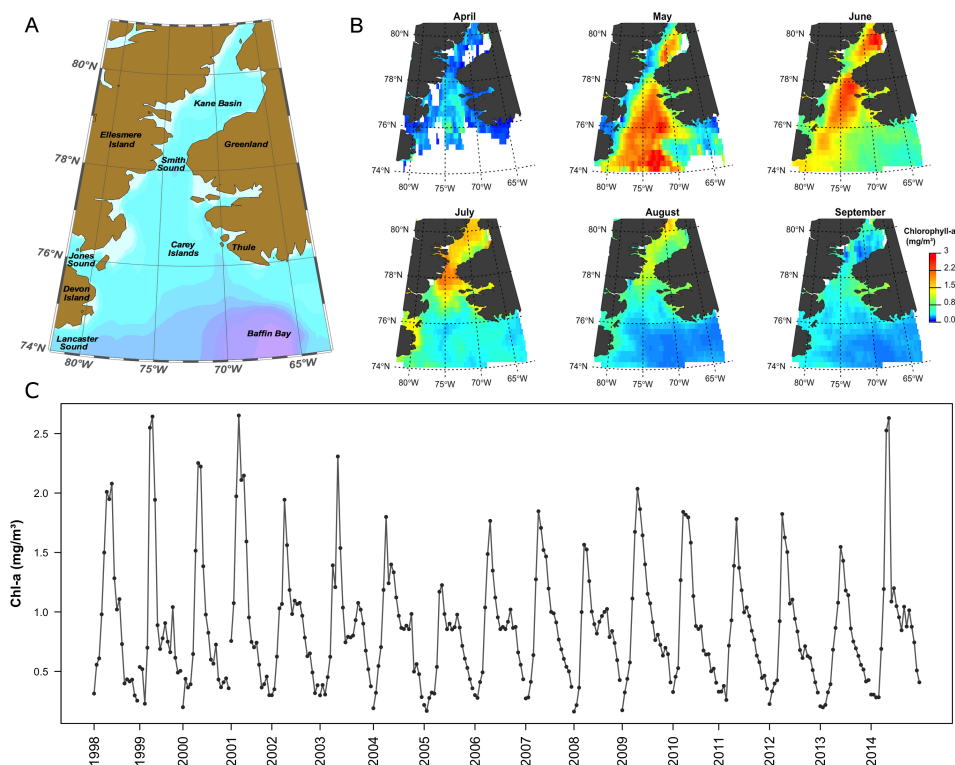


Figure 5: North Water polynya is situated in northern Baffin Bay between Canada and Greenland. Smith Sound, the Arctic sea passage between Greenland and Ellesmere Island, links Baffin Bay with Kane Basin. Nares Strait (not indicated in the map) is the waterway between Ellesmere Island and Greenland that includes, from south to north, Smith Sound, and Kane Basin, respectively (a); monthly climatology of merged satellite chlorophyll-a data from April 1998 to September 2014 at 25 km of resolution within the NOW polynya: 74°N-81°N, 82°W-63°W (b); time series of 8-day composite images of chlorophyll-a, averaged for the NOW polynya from April 1998 to September 2014 (c)

avoid interpolation over ice-covered areas. Finally, to reduce the effect of outliers and to have an appropriate temporal resolution to describe the bloom phenology, daily images were aggregated over time to create 8-day composite Chl-a using the interquartile mean (Land et al., 2014). The resulting data set had about 36% more data, showing a good agreement ($r^2 = 0.98$; $rmse = 0.107$) with the 8-day merged Chl-a composite directly processed by the GlobColour team. The procedure described above is schematically illustrated in Figure 6a.

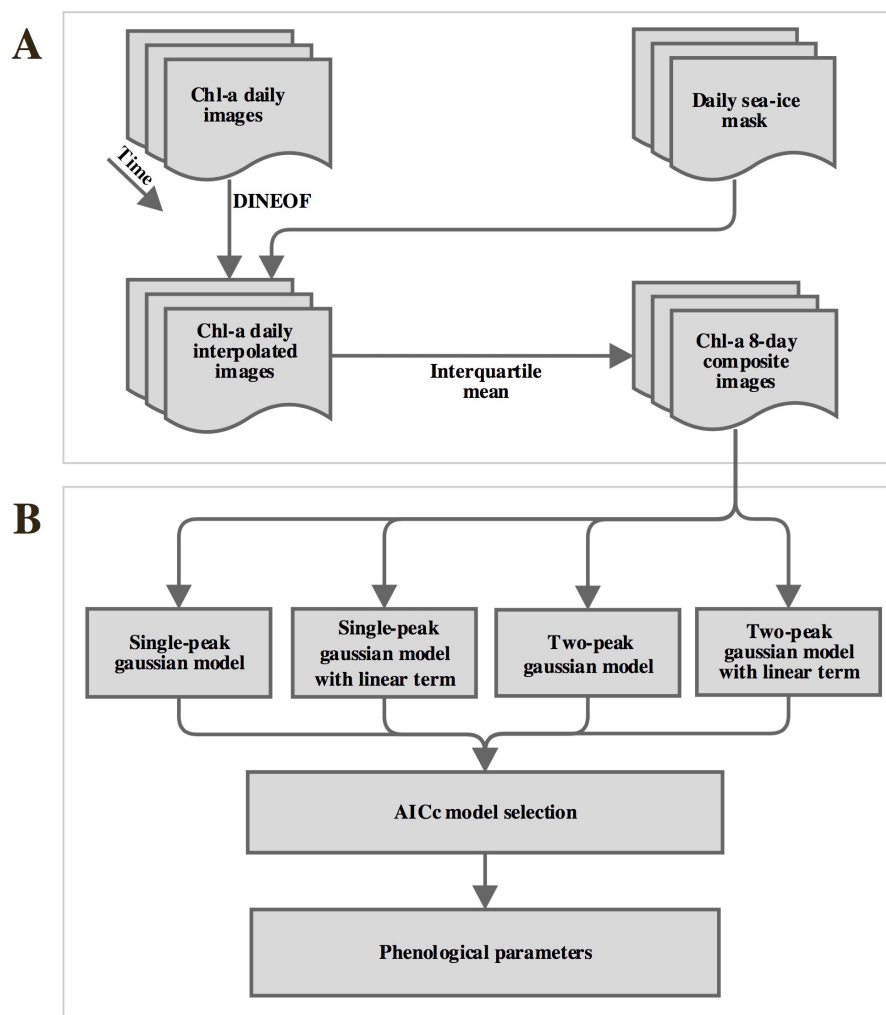


Figure 6: Workflow describing the multi-step tasks to obtain (a) 8-day composite cloud-free chlorophyll-a images and (b) multiple-Gaussian models approach to increase the number of fits.

2.4.2 Models and estimation of phenological metrics

To retain spatial patterns, four Gaussian models were fitted for each year on a pixel-by-pixel basis (Platt and Sathyendranath, 2008) to the cloud-free time-series of

8-day composite Chl-a images. The use of several Gaussian functions increased the number of fits and provided a better capture of the bloom variability. However, if the number of valid values for a pixel was less than the half of the time-series length (i.e., due to the continued presence of ice cover), the pixel was removed from the fitting. The most complex model (see Table 3 for all model equations) used to describe the characteristics of the annual bloom was a twopeak Gaussian (Zhai et al., 2012), which is expressed as follows:

$$Chl(t) = Chl_B + \beta t + Chl_1 \exp\left[-\frac{(t - tp_1)^2}{2\omega_1^2}\right] + Chl_2 \exp\left[-\frac{(t - tp_2)^2}{2\omega_2^2}\right] \quad (1)$$

where Chl_B (mg m^{-3}) is the background value of Chl-a concentration, βt ($\text{mg m}^{-3} \text{ day}^{-1}$) is a linear time trend, Chl_1 and Chl_2 (mg m^{-3}) correspond to the peak amplitudes, ω_1 and ω_2 (days) are the standard deviations of the Gaussian curve and define the temporal width of the bloom, and tp_1 and tp_2 (day of year) define the peak timing, the date at which the maximum bloom occurs. The optimal parameter values that provide the fit were determined using the Levenberg-Marquardt algorithm (LMA) for non-linear regression (Elzhov et al., 2016). Finally, for each time series the best-fit model was chosen by using the Akaike Information Criterion with a correction for finite sample sizes (AICc; Burnham et al. 2011): smaller AICc values indicate a better-fitting model. This procedure allowed the creation of phenological maps enabling the examination of seasonal and inter-annual variations in bloom patterns (see Figure 6b).

Table 3: Gaussian-models for the different types of seasonal phytoplankton cycles

Model name	Type of annual cycle	Fitted models
Single-peak Gaussian	Single bloom	$Chl(t) = Chl_B + Chl_1 \exp\left[-\frac{(t-tp_1)^2}{2\omega_1^2}\right]$
Single-peak Gaussian with linear term		$Chl(t) = Chl_B + \beta t + Chl_1 \exp\left[-\frac{(t-tp_1)^2}{2\omega_1^2}\right]$
Two-peak Gaussian	Double bloom	$Chl(t) = Chl_B + Chl_1 \exp\left[-\frac{(t-tp_1)^2}{2\omega_1^2}\right] + Chl_2 \exp\left[-\frac{(t-tp_2)^2}{2\omega_2^2}\right]$
Two-peak Gaussian with linear term		$Chl(t) = Chl_B + \beta t + Chl_1 \exp\left[-\frac{(t-tp_1)^2}{2\omega_1^2}\right] + Chl_2 \exp\left[-\frac{(t-tp_2)^2}{2\omega_2^2}\right]$

The phenological metrics obtained for each pixel, as illustrated in Figure 20 (annex I), are summarized in detail in Table 4. In particular, the bloom start was determined using a relative threshold: it is the date (day of year) at which the fitted function reached the threshold of 20% of its maximum amplitude. This criterion was previously proposed by [Platt et al. \(2009\)](#) and used by [Zhai et al. \(2012\)](#) to define the bloom initiation date in Arctic and subArctic waters. Nevertheless, different thresholds (i.e., 15 and 25%) were tested, but no significant differences in the results were detected (not shown).

Conversely, the bloom end is defined as the date at which the Chl-a decreased to 20% of the amplitude. The difference between bloom end and bloom start gives the bloom duration. The bloom amplitude is defined in correspondence of the peak timing, as the highest value of Chl-a during the bloom event.

Table 4: Main bloom phenology parameters extracted for each year at each pixel

Parameters (unit)	Description
1. Bloom start (day of year)	Date at which Chl-a concentration rises above the defined threshold*
2. Bloom end (day of year)	Date at which Chl-a concentration falls below the defined threshold*
3. Bloom duration (days)	Difference between 1 and 2
4. Peak time (day of year)	Date at which the Chl-a concentration reaches its maximum value
5. Bloom amplitude (mg m ⁻³)	The highest value of Chl-a concentration during the bloom event
6. Background Chl-a concentration (mg m ⁻³)	The baseline of Chl-a concentration determined by the fitted function

*See text for details

2.4.3 Environmental parameters

Over the NOW polynya, physical oceanographic and meteorological conditions may subject the start, the duration, and the amplitude of the bloom to inter-annual variability. For instance, the rate at which the sea-ice melts and forms within the polynya is of fundamental importance, since it determines ice concentration patterns and stabilizes the upper water column (Ingram et al., 2002). Another important physical parameter strictly interrelated with the sea-ice is the SST, which may directly affect process rates (i.e., phytoplankton growth rate) but also reflect patterns of sea-ice retreat and absorption of solar radiation into the upper water column. This latter process may be influenced in part by the presence of cloud cover. In the Arctic, the cloudiest months are in summer and fall when the sea ice starts to melt and a greater portion of water is exposed to the atmosphere (Chernokulsky and Mokhov, 2012). Finally, wind plays an important role in maintaining the upper ocean structure within the NOW polynya. In this region, winds are usually strongest in Smith Sound (see Figure 5a) due to the topographic structure (Ingram et al., 2002). The time series of the environmental parameters were retrieved from April to September for the years between 1998 and 2014. The environmental parameters used in this study are described in the following sections.

2.4.3.1 Sea-ice concentration

Daily satellite-derived sea-ice concentrations (SIC) with a spatial resolution of ~ 25 km \times 25 km from SSM/I (1998-2007) and SSMIS (2008-2014) sensors were obtained from the National Snow and Ice Data Center (NSIDC) and from their website at <http://nsidc.org> (Meier et al., 2013). SIC is defined as the percent of a pixel area covered by sea ice. The use of sea-ice data was twofold. First, to avoid Chl-a interpolation over an ice-covered area, the sea-ice data were used to create a daily sea ice-mask based on a 15% threshold. Second, we used daily sea-ice concentrations to compute the sea-ice

phenology: the day of the year when the ice concentration at each pixel dropped below the threshold of 35% and later reached the same threshold again, was used as a proxy for ice-retreat and freeze-up timing, respectively (similar to [Ji et al. 2013](#)). Consequently, for each pixel, the open-water period (days) is defined as the period between the ice-retreat and the freeze-up timing.

2.4.3.2 Sea-surface temperature

For the same period (1998-2014), the NOAA daily Optimum Interpolation (OI) SST v2 data were obtained from the NOAA Physical Sciences Division, Earth System Research Laboratory, from their website (<http://www.esrl.noaa.gov/psd/>). The data have a spatial grid resolution of 0.25° ($\sim 25 \text{ km} \times 25 \text{ km}$) and provide an interpolated estimate of the SST for each day of the year combining satellite SST retrievals and SST observations from ships and buoys. The OISST methodology includes a bias adjustment step of the satellite data to in situ data prior to interpolation. For Arctic waters and marginal ice zones, where in situ observations tend to be sparse, proxy SSTs are computed from sea-ice concentrations (from satellite) above 50% using an empirically derived linear regression equation with respect to SST observations. A description of the complete OI analysis procedure can be found in [Reynolds et al. \(2007\)](#).

2.4.3.3 Cloud fraction

For the period 1998-2014, 8-day composite cloud fraction (CF) images were obtained from the Globcolour project. The CF data are provided on the same 0.25° ($\sim 25 \text{ km} \times 25 \text{ km}$) resolution grid as the Chl-a estimates and obtained from different ocean color sensors, such as SeaWiFS, MERIS, MODIS, and VIIRS. The CF images are generated by a classification and statistical merging method (see also the Globcolour products user guide).

2.4.3.4 Surface wind data

For the period 2000-2014, daily sea surface wind stress (WS) from QuikSCAT and ASCAT with a spatial resolution of 0.25° ($\sim 25 \text{ km} \times 25 \text{ km}$) was obtained from the Centre ERS d'Archivage et de Traitement (CERSAT: <http://cersat.ifremer.fr>). In the CERSAT data set, the wind field accuracy is investigated through the comparisons with daily-averaged winds from moored buoys and the error associated with each parameter (i.e., wind speed and stress) is also provided. In Arctic regions, near-surface wind can be estimated through remote sensing only over ice-free areas. The data are, therefore, provided with a daily sea-ice mask that is used to remove wind values from all those pixels contaminated by sea ice. More details about data, method, and algorithm can be found in [Bentamy et al. \(2012\)](#). However, since in the CERSAT data set, the daily wind fields are calculated from October 1999, satellite wind data for the period 1998-1999 were instead obtained from NOAA's National Centers for Environmental Information (NCEI) at the same spatial resolution ([Zhang et al., 2006](#)). Periods of strong wind force may significantly contribute to the nutrient (i.e., nitrate) transport into the euphotic zone by destroying the pycnocline. To assess the likelihood of this mechanism, as in [Tremblay et al. \(2002b\)](#), we estimated the depth D of the wind entrainment as a function of the wind stress using the formulation of [Deardorff \(1983\)](#):

$$D = \frac{0.3u^*}{f} \quad (2)$$

where f is the Coriolis parameter and u^* is the friction velocity. Values of u^* are calculated as $\left(\frac{\tau}{\rho_{sw}}\right)^{\frac{1}{2}}$, where τ is the wind stress and ρ_{sw} is the seawater density which, for simplicity, was set as constant (1027 kg/m^3). The number of days for which a threshold D value of 35 m was exceeded was used as an index of the frequency of wind-driven entrainment of intermediate waters events (hereafter refer to as frequency D of wind-driven entrainment). The threshold value was based on [Tremblay et al. \(2002b\)](#)

who found that a value D of 34 m was deep enough to disrupt the pycnocline.

2.4.4 Statistical analyses

All statistical calculations and analyses were performed in the R programming language (R Team, 2016). Pearson's linear regressions (r) were used to determine temporal trend ($p < 0.05$ mean statistically significant). To identify and test the strength of a correlation among environmental variables and phytoplankton phenology parameters, a Spearman's rank correlation (ρ) matrix was computed ($p < 0.05$ mean statistically significant). In addition to the correlation analysis, to distinguish each year in a function of the abiotic and biotic factors, we performed a principal component analysis (PCA).

2.5 Results

2.5.1 Spatiotemporal variability of satellite chlorophyll-a

The climatological monthly Chl-a (1998-2014) for the whole study area ranged from a minimum of $\sim 0.05 \text{ mg m}^{-3}$ to values higher than 3 mg m^{-3} (Figure 5b). Overall, for the investigation period, a clear seasonal signal was observed in the mean Chl-a, with the lowest values in April and September and the highest from May to August. In April, except for an area close to the Greenland coast, where slightly higher concentrations were visible, the Chl-a was still low (around $< 0.5 \text{ mg m}^{-3}$). A sudden increase occurred later: the bloom clearly reached high Chl-a values in May and continued in June, encompassing the whole polynya (Figure 5b). Chl-a values remained high at a relatively constant level throughout these 2 months, with maximum concentrations ($> 2 \text{ mg m}^{-3}$) in the central part of the region. Later, in July and August, the intensity of the bloom declined gradually, except in Smith Sound and further north. In the south, however,

Chl-a concentrations became low, marking the end of the bloom. Finally, Chl-a returned to the lowest values in September ($<0.8 \text{ mg m}^{-3}$) except for a small and circumscribed area close to the Greenland coast (Figure 5b).

The regionally averaged time series of the annual Chl-a cycle (Figure 5c) showed that the NOW is characterized by a repetitive pattern with a single peak-bloom (i.e., maximum Chl-a reached) that is sometimes followed by a less pronounced secondary peak (e.g., 2003 and 2008). A maximum in late May, early June was observed with regularity. However, the bloom intensity and duration were highly variable between years (maximum ranging from an average value of $1.23 - 2.65 \text{ mg m}^{-3}$). Overall, the period 1998-2001 and the year 2014 showed the highest Chl-a peaks. Conversely, the period 2002-2013 was characterized by lower Chl-a values (see Figure 5c).

Table 5: Summary of the annual average values (and standard deviation, SD) of the regional phenological parameters obtained from the Gaussian fits. R^2 is the coefficient of determination of the Gaussian fits. The percentage of valid fits within the study region is also reported.

Year	R^2	Bloom start		Peak time		Bloom duration		Bloom amplitude		Background Chl-a		Number of fits
		day	SD	day	SD	days	SD	mg m^{-3}	SD	mg m^{-3}	SD	%
1998	0.95	144	± 25	174	± 18	60	± 26	2.35	± 1.32	0.46	± 0.57	66
1999	0.92	169	± 26	194	± 21	50	± 28	3.01	± 2.10	0.71	± 0.72	84
2000	0.95	148	± 22	175	± 18	55	± 23	2.44	± 2.52	0.44	± 0.35	85
2001	0.95	151	± 24	178	± 18	54	± 23	2.65	± 1.79	0.49	± 0.27	74
2002	0.97	140	± 25	175	± 20	67	± 24	1.52	± 0.67	0.42	± 0.28	88
2003	0.92	146	± 30	175	± 28	58	± 30	1.44	± 0.72	0.46	± 0.47	86
2004	0.94	145	± 27	177	± 23	63	± 26	1.41	± 1.19	0.40	± 0.28	84
2005	0.92	156	± 29	185	± 21	59	± 33	1.14	± 0.54	0.38	± 0.26	77
2006	0.91	141	± 24	172	± 25	63	± 26	1.24	± 0.59	0.39	± 0.29	82
2007	0.97	134	± 32	170	± 18	72	± 25	1.53	± 0.77	0.30	± 0.22	91
2008	0.92	145	± 18	174	± 30	58	± 28	1.27	± 0.86	0.57	± 0.44	83
2009	0.94	128	± 22	161	± 16	65	± 21	1.95	± 0.92	0.46	± 0.31	98
2010	0.95	140	± 22	170	± 16	61	± 26	1.86	± 2.45	0.44	± 0.25	89
2011	0.94	147	± 26	175	± 20	56	± 25	1.56	± 2.02	0.39	± 0.23	85
2012	0.96	127	± 24	163	± 20	72	± 24	1.48	± 0.68	0.34	± 0.23	82
2013	0.93	154	± 19	180	± 15	53	± 19	1.71	± 0.94	0.38	± 0.24	84
2014	0.92	150	± 31	183	± 26	65	± 36	1.65	± 0.88	0.53	± 0.35	78

2.5.2 Bloom phenology features and environmental parameters

Spatial patterns and inter-annual variability in bloom characteristics for the NOW were examined by fitting four Gaussian models to the time series of Chl-a between April and September for each year. For parsimony, we focused exclusively on three important bloom characteristics: the bloom start, its duration, and amplitude. The mean values and corresponding standard deviation for the phenological parameters for each year are summarized in Table 5.

2.5.2.1 Bloom start

When we examined bloom start climatology (Figure 7a), sub-regional differences over the study area became apparent and occurred across relatively short distances. For instance, the bloom started earlier in the area between 76° and 78°N . Furthermore, the bloom started earlier on the Greenland (eastern) side than on the Canadian (western) side. This feature, which was particularly noticeable in some years (Figure 21 in annex I), may reach a difference of approximately 2 months. Compared to the area lying between 76° and 78°N , the bloom also started later in the northern ($>78^{\circ}\text{N}$) part compared to the southeastern ($<76^{\circ}\text{N}$) part of Smith Sound (Figure 7a). Overall, the bloom occurred mainly between the beginning of May and June, ranging from 127 to 169 (day of year; see Table 5). Over the 17 years analyzed, the bloom start did not show a clear temporal trend ($r^2 = 0.12$, $p = 0.174$; Figure 8a). However, an advance of the bloom was noticeable if considering only the period 1998-2012 (~ -1.4 days year $^{-1}$, $r^2 = 0.36$, $p = 0.017$; regression analysis not showed). In particular, the years 2002, 2007, 2009, and 2012 were marked by the earliest bloom start dates. Interestingly, these years were also characterized by longer open-water period, bloom duration, and high SST values (Figure 9b). The regionally averaged SST (over the period 1998 to 2014) exhibited a positive trend ($r^2 = 0.35$, $p = 0.013$; Figure 8d) and showed a significant negative correlation

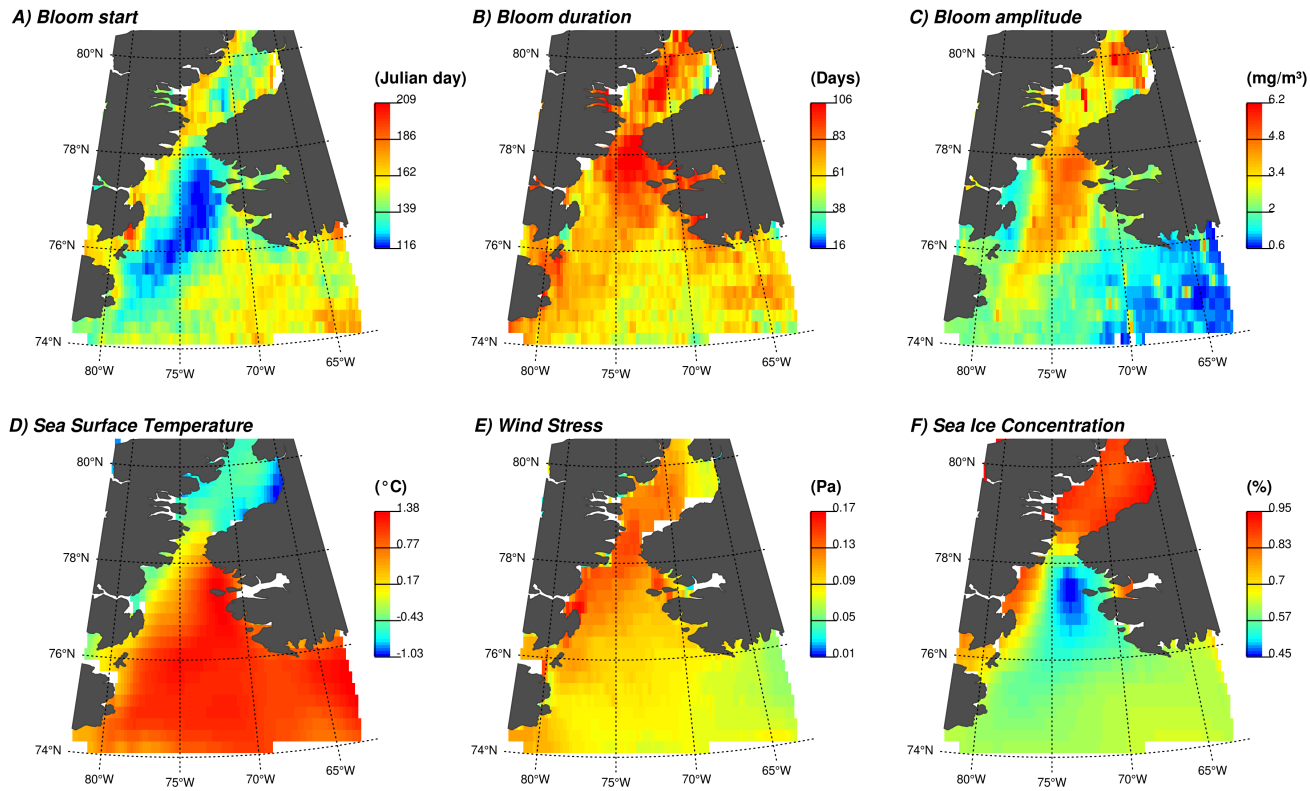


Figure 7: Climatology (1998-2014) maps of a) bloom start, b) bloom duration, c) bloom amplitude, d) sea surface temperature, e) wind stress, and f) sea-ice concentration

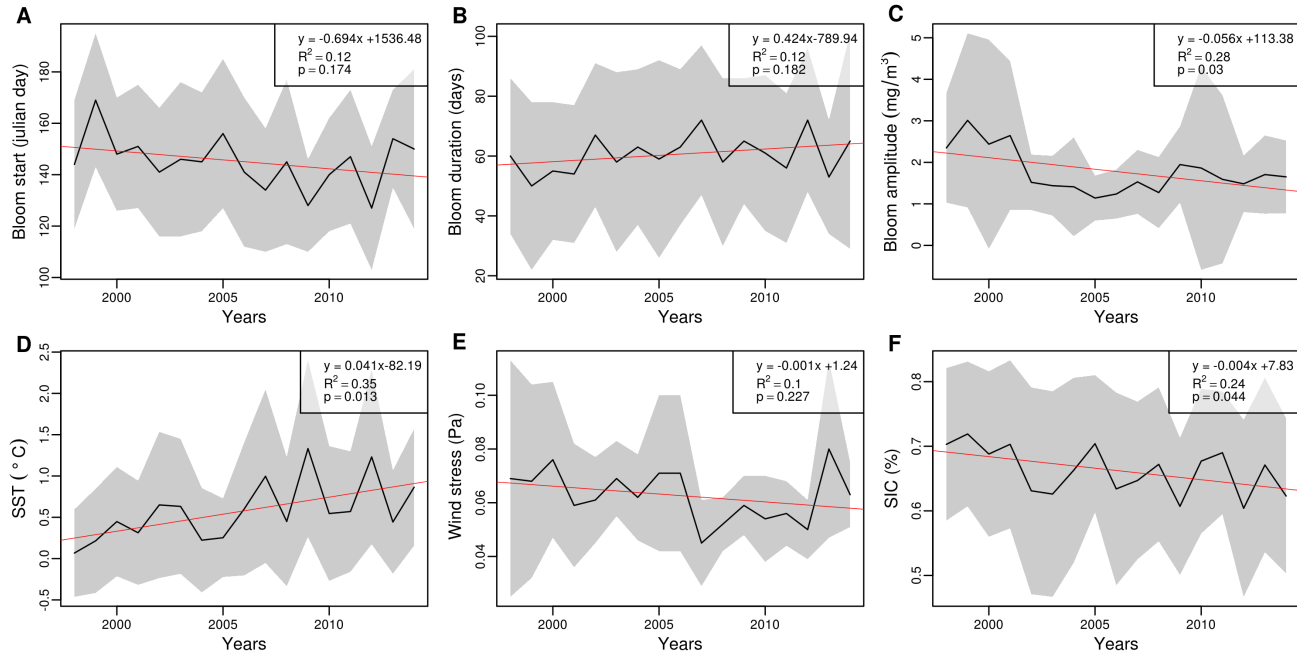


Figure 8: Time series analysis of the main bloom phenology characteristics (bloom start, bloom duration, and bloom amplitude) and environmental parameters (SST, wind stress, and SIC) averaged for the NOW polynya area. The black line is the mean \pm standard deviation (shaded grey area). The red line represents linear trend (days year⁻¹) for the 17-year time series. Coefficient of determination (r^2) and probability levels (p) is shown for each figure in the upper right box.

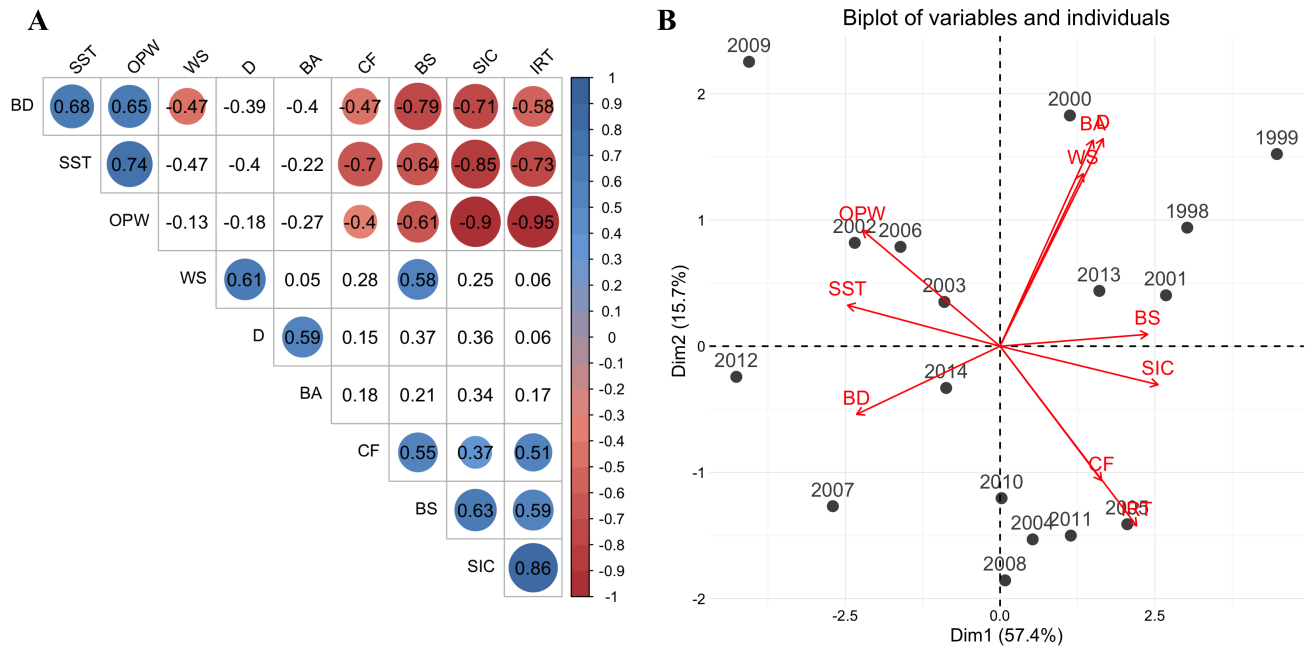


Figure 9: Spearman's rank correlation (ρ) matrix (a) between phytoplankton phenological parameters: BS (bloom start), BD (bloom duration), BA (bloom amplitude), and abiotic factors: SST (sea surface temperature), WS (wind stress), CF (cloud fraction), SIC (sea-ice concentration), SIE (sea-ice extent), IRT (ice-retreat timing), OWP (open-water period), and D (frequency of wind-driven entrainment). The red color indicates a significant ($p < 0.05$) negative correlation, while the blue color indicates a significant ($p < 0.05$) positive correlation. The color gradient (from red to blue) indicates the magnitude of the correlation. The color white means that the correlation between indicators is not significant ($p > 0.05$) according to the Spearman correlation statistical test. Principal component analysis biplot (b) of: variables (red arrows; see text above for abbreviations) and years (1998-2014) represented by dots.

with the bloom start (Figure 9a; $\rho = -0.64$, $p = 0.002$). Besides the observed negative correlation with the SST, the bloom start was also positively correlated with the surface WS (Figure 9a; $\rho = 0.58$, $p = 0.027$) and the SIC (Figure 9a; $\rho = 0.63$, $p = 0.004$). These latter environmental parameters both presented a considerable inter-annual variability (Figure 8e and 8f). In particular, while the WS was characterized by a sudden decline between the years 2007 and 2012, the SIC showed a significant but weak temporal trend ($r^2 = 0.24$, $p = 0.044$; Figure 8f). Although slightly lower if compared to that of the SIC, the bloom start was positively correlated with the ice-retreat timing (Figure 9a; $\rho = 0.59$, $p = 0.006$) and negatively correlated with the open-water period (Figure 9a; $\rho = -0.61$, $p = 0.007$). The bloom start was also positively correlated with the CF (Figure 9a; $\rho = 0.55$, $p = 0.004$). Finally, the bloom start appeared to be inversely correlated with the length of the bloom period (Figure 9a; $\rho = -0.79$, $p < 0.0001$): an early spring bloom corresponded to greater bloom duration (and *vice versa*).

2.5.2.2 Bloom duration

Geographic differences in bloom duration and pronounced inter-annual variability characterized the study region (Figure 7b and 8b). On average, the bloom duration ranged from a minimum of about two to a maximum of almost 3 months (see Table 5). The bloom duration showed considerable temporal variations but did not show any significant trend ($r^2 = 0.12$, $p = 0.182$; Figure 8b). The most evident spatial pattern of longer bloom duration encompassed the central part of the study region. This spatial trait was also particularly evident during some years (see Figure 22 in annex I). In this area the bloom tended to last longer, especially around Smith Sound (approximately between 79°N and 77°N), which corresponded to higher values of wind stress (Figure 7e). The bloom duration, however, appeared to be negatively correlated with WS (Figure 9a; $\rho = -0.472$, $p = 0.04$) and CF (Figure 9a; $\rho = -0.467$, $p = 0.003$) when considering the region as a whole. Conversely, a positive association between the

bloom duration and SST (Figure 9a; $\rho = 0.68$, $p = 0.003$) was found. Moreover, the relationship between the sea-ice dynamics and the bloom duration was highlighted by the negative correlations of the latter with the SIC (Figure 9a; $\rho = -0.71$, $p = 0.005$) and the positive correlations with the open-water period (Figure 9a; $\rho = 0.65$, $p = 0.006$). As evidenced by the PCA analysis (Figure 9b), the bloom lasted much longer during the years characterized by lower sea-ice coverage (SIC) and a longer open-water period (OPW), and the opposite also applies; the bloom was briefer in years with high SIC. Finally, no significant correlation was found between the bloom duration and the bloom amplitude (Figure 9a; $\rho = -0.4$, $p = 0.132$).

2.5.2.3 Bloom amplitude

The bloom amplitude revealed strong inter-annual variations in the spatial and temporal patterns. On average, the background Chl-a (Chl_B; Table 4) generally had lower values ($<1 \text{ mg m}^{-3}$), whereas the bloom amplitude varied approximately between 1.14 and 3.01 mg m^{-3} throughout the time period examined (see Table 5). Although the time series of the annual Chl-a cycles (see "Spatiotemporal variability of satellite chlorophyll-a" subsection and Figure 5c) showed a year-to-year variability but no trend, the annual average value of bloom amplitude showed a significant but weak declining trend (Figure 8c; $r^2 = 0.28$, $p = 0.03$) over the 17 years analyzed. In this regard, the general decrease in Chl-a was also spatially noticeable. In particular, during the years 1998 and 2000, the bloom amplitude presented a wider and intense extension of Chl-a values ($\sim 67.812 \text{ km}^2$ for Chl-a values $>3 \text{ mg m}^{-3}$). Conversely, a widespread reduction in Chl-a and in its spatial extent was particularly evident from the year 2002 onwards (see Figure 23 in annex I). Although the time series analysis of the annual Chl-a cycles (Figure 5c) showed a higher peak for the year 2014, the spatial extent of the bloom amplitude ($\sim 25.000 \text{ km}^2$ for Chl-a values $>3 \text{ mg m}^{-3}$; see also Figure 23 in annex I) and the physical conditions (see Figure 8 and 9b) were different in 2014 if compared to the

period 1998-2000.

The bloom amplitude spatial patterns are clearly noticeable in the bloom amplitude climatology (Figure 7c). Overall, higher concentrations of Chl-a were observed in northeastern Kane Basin, around the Smith Sound ($\sim 78^\circ\text{N}$) area and further down towards the southwest. Conversely, lower values of Chl-a ($< 1 \text{ mg m}^{-3}$) were usually present in the southern part of the NOW ($< 76^\circ\text{N}$) and in particular in the sector east of 75°W . The correlation analysis suggests that throughout the course of the 17 years analyzed, the year-to-year variations in bloom amplitude were positively correlated with the frequency D (see eq. 2) of wind-driven entrainment (Figure 9a; $\rho = 0.59$, $p = 0.018$). Moreover, as evidenced by the PCA analysis (Figure 9b), years of stronger WS (i.e., 1998, 1999, 2000) also had higher bloom amplitude values. Finally, no significant correlation was found between the SIC and bloom amplitude (Figure 9a; $\rho = 0.34$, $p = 0.279$).

2.6 Discussion

2.6.1 Phytoplankton bloom dynamics and phenology

At high latitudes, the sea ice and its snow cover govern the incoming light in the upper ocean (Vancoppenolle et al., 2013). In the Canadian Archipelago, phytoplankton blooms typically begin in mid-July or in early August when the ice melting stratifies the water column and a more significant fraction of sunlight is available (Tremblay et al., 2002a). An exception occurs in NOW polynya, where the onset of summer melt occurs much earlier (late March) than in the surrounding regions (Tremblay et al., 2006b). Indeed, the early exposure of the water column to sunlight allows phytoplankton to bloom as early as the beginning of May. Monthly images of climatological satellite Chl-a for the period April-September corroborate the spatial and temporal evolution of in situ measurements of Chl-a carried out during the past oceanographic surveys (e.g., Klein

[et al., 2002](#); [Odate et al., 2002](#)). In particular, Chl-a values are still low during April. However, relatively high values of Chl-a (around 1 mg m^{-3}) have been observed in late April on the eastern (Greenland) side, where the presence of sea ice is less pronounced if compared to the western side ([Mei et al., 2002](#)). The bloom peaks during the month of May and remains vigorous in June throughout the NOW polynya with a spatial extent reaching about 82.187 km^2 . During July and August, Chl-a values begin to decrease gradually over the whole region and subsequently fade away in September.

Our results highlight regional differences in bloom initiation patterns, indicating distinct areas over the NOW polynya. This spatial delay in bloom start dates occurs between the east (Greenland) and west (Canadian) sides of the polynya. More precisely, on the eastern side, the bloom starts in late April early May, while on the western side of NOW polynya at the end of May or even later. It appears that different environmental factors are responsible for the onset of the bloom. For instance, the negative correlation between the SST and bloom start suggests that accelerated surface warming can influence the bloom onset timing. A similar negative correlation field between thermal conditions and bloom start was found by [Friedland et al. \(2016\)](#) in large areas of the North Atlantic and was associated with the shoaling of the mixed layer, driven by surface heating. Overall, the correlation analysis results show that the bloom starts earlier in conditions of warm waters, and reduced sea-ice and cloud cover (i.e., more light availability). Interesting too is the inverse correlation between CF, open-water period and SST that reflects, to some extent, the atmospheric effect. For instance, measurements taken over the NOW polynya during spring and summer highlight how the effect of cloud cover predominantly cools the sea surface ([Hanafin and Minnett, 2001](#)). Our analyses do not directly address the role of the mixed layer depth, which may also be a significant driver of bloom timing, but it is plausible to hypothesize that a shallow mixed layer associated with increasing solar heating and sea-ice loss promotes optimal irradiance conditions and as a consequence the development of the bloom's early initiation. Physical conditions such as those previously described have been associated

with an early phytoplankton bloom along the eastern side (Mei et al., 2002; Tremblay et al., 2002b; Vidussi et al., 2004). Conversely, contrasting physical characteristics, such as low irradiance, temperature, and deep mixing, have been observed in April and May along the western side of the NOW polynya (Mei et al., 2002; Tremblay et al., 2002b). In this sector, the bloom starts later in the season when the same favorable environmental conditions for the phytoplankton growth are reached (Odate et al., 2002). These differences between the eastern and the western side of the NOW are attributed to different physical and climatic conditions. The western sector of the polynya receives cold water and ice from the Arctic Ocean and is characterized by strong northerly winds and deep convection (Melling et al., 2001). In the eastern sector of the polynya, a branch of the West Greenland Current brings deep warm water into the mixed layer (Melling et al., 2001) that, together with warmer air temperature (Barber et al., 2001), slow down new-ice formation. The relatively low ice cover along the Greenland coast in turn allows higher irradiance in the surface mixed layer (Mei et al., 2002) and the bloom starts in relatively warmer surface waters (Vidussi et al., 2004). A previous study (Kahru et al., 2011) showed that within Baffin Bay, the earlier start of the phytoplankton bloom was directly related to the earlier disappearance of sea ice. This result is consistent with our analysis that shows how the ice-retreat timing has an appreciable impact on the bloom start. For instance, in Antarctic coastal polynyas, the ice-retreat timing predominantly modulates light availability: earlier blooms are brought on by earlier ice-adjusted light onset (Li et al., 2016). Finally, the correlation analysis suggests that strong winds may delay the onset of the phytoplankton bloom. Wind forcing is commonly considered one of the major drivers of changes in water column stability or mixed layer depth and may exert, as shown in the North Atlantic by González Taboada and Anadón (2014), a dominant role in determining the bloom onset timing.

Although the time series does not reveal a clear trend towards earlier phytoplankton blooms, it does indicate that in the years 2002, 2007, 2009, and 2012, the bloom started much earlier. Looking at a larger scale, during these years, satellite data revealed

unusually low Arctic ice concentrations and surface, caused in part by anomalous high temperatures (Serreze et al., 2003; Comiso et al., 2008; Parkinson and Comiso, 2013). This corresponds with the observations of this study, where the SST trend analysis shows a significant increase in temperature over the 17 years analyzed, with the highest values achieved during the aforementioned years. In particular, the year 2009 was characterized by a long open-water period and a higher-than-normal SST, which in July reached approximately 5°C above the typical seasonal values (Vincent, 2013). The anomalously early bloom of 2009 was likely due to the occurrence of particularly warm environmental conditions. The Smith Sound ice arch failed to consolidate in 2009 but an ice arch formed north of Kane Basin, preventing floes from reaching the NOW polynya until late July (Vincent, 2013). This unique configuration, along with the higher SST, led to the lowest sea-ice coverage over the NOW polynya which consequently experienced unusual open-water conditions (Heide-Jørgensen et al., 2013; Vincent, 2013).

The correlation analysis also shows that the bloom start was inversely correlated with the bloom duration: earlier blooms tended to produce longer-lasting blooms. Interestingly, early bloom onsets associated with longer blooms in several ocean basins were found by Racault et al. (2012). Moreover, a consistent relationship between bloom timing and duration was also found in the North Atlantic by Friedland et al. (2016). At high latitudes, the negative correlation between bloom initiation and duration seems to suggest that grazing pressure may be relatively weak due to the wintertime decline of zooplankton that usually characterizes the beginning of the growth season (Lindemann and St John, 2014). Conversely, later in the season under warmer conditions, a later bloom could experience a higher grazing pressure (Henson et al., 2006) that may limit its duration. Within the NOW polynya, the loss of phytoplankton biomass that occurs during spring-summer (from April to July) conditions is primarily attributed to grazing activity and sinking of phytoplankton cells (Michel et al., 2002; Tremblay et al., 2006a). However, a recent mesocosm experiment (Lewandowska et al., 2014) showed that in stratified and nutrient-limited waters, the temperature influences plankton mainly through

physical mechanisms (i.e., stratification and nutrient supply). Conversely, the "grazing effects" dominate in well-mixed and nutrient-rich waters, where the phytoplankton community is typically dominated by large diatoms (Lewandowska et al., 2014). This means that differences in bloom duration should also be viewed with respect to changes in the physical environment. Variability in the upper water column structure may have a detectable effect on the length and extent of the bloom. The correlation analysis results show that although strong winds may temporarily dampen the bloom duration, blooms lasted longer during years characterized by greater open-water conditions and vice versa. In this connection, other authors have shown that an increase in open-water area or in the length of the open-water period may contribute to the length of the phytoplankton-growing season (Arrigo et al., 2008; Pabi et al., 2008; Arrigo and van Dijken, 2011). Finally, the relatively high negative correlation between CF and the bloom duration suggests that the incoming solar radiation into the surface layer is an important factor that supports the phytoplankton growth during the open-water period.

The ability of strong wind events to erode stratification by enhancing vertical mixing and to entrain nutrients into the euphotic zone is also important in relation to the seaice cover (Rainville et al., 2011; Tremblay et al., 2011). In this regard, while initial nutrient concentrations may support a more productive bloom (Mei et al., 2002; Tremblay et al., 2002b), nutrient replenishment during the growth season may contribute conspicuously to the new production in this region (Tremblay et al., 2002b). This means that over the NOW polynya, the frequency of wind-generated nutrient pulses during the open-water season may be considered an important factor controlling the magnitude of the bloom. Strong local wind events may, therefore, entrain nitrate into the surface layer and promote blooms (Rumyantseva et al., 2015). This hypothesis is supported here by the positive correlation between the bloom amplitude and the frequency D of wind-driven entrainment. For instance, a recent study (Carranza and Gille, 2015) identified regions in the Southern Ocean, where high winds correlated with high Chl-a, suggesting that the deepening of the mixed layer depth through wind mixing helped

sustain high Chl-a throughout the growing season. Recently, [Bergeron and Tremblay \(2014\)](#) reported that increased vertical stratification (over the period 1997-2011) due to a decrease in salinity and wind-driven mixing led a drastic decrease in seasonal nitrate consumption (approximately 65%) within the NOW polynya. Overall, their results indicated that nitrate drawdown (i.e., net community production) in northern Baffin Bay decreased at the mean rate of $\sim 26 \text{ mmol m}^{-2} \text{ year}^{-1}$. This change in environmental setting may, in recent years, have limited the input of nutrients to the euphotic zone ([Tremblay et al., 2002b](#); [Bergeron and Tremblay, 2014](#)). This new scenario is clearly in contrast with that of the summer 1998, during which a large portion of new production was supported by upward flux of nitrate during intermittent storm activity ([Bergeron and Tremblay, 2014](#)). Recently, direct observations ([Torres et al., 2011](#)) suggest that changes in circulation and ice formation favor an increased flow of relatively fresh waters from the Arctic Ocean into Nares Strait. Looking at a larger scale, recent hydrographic observations and sampling also provide evidence that, in recent years, the freshwater content in the Beaufort Gyre increased ([Yamamoto-Kawai et al., 2009](#); [Bourgain et al., 2013](#)). Interestingly, a three-dimensional coupled ocean and sea-ice model used to simulate the ice cover and hydrography suggests that the NOW is moving toward a future scenario characterized by longer seasonal periods of low sea-ice concentrations and increased stratification ([Rasmussen et al., 2011](#)).

In this study, no significant correlation was found between sea-ice concentration and bloom amplitude. However, [Park et al. \(2014\)](#) found a significant relationship between the year-to-year variations in sea-ice concentration and Chl-a, providing evidence that the abrupt increase in nutrients in the upper layer was primarily due to the advection of sea-ice melted water. Recent field studies have shown that sea-ice melting might influence the upper ocean layer by releasing a significant amount of nutrients, trace metals ([Tovar-Sánchez et al., 2010](#)) and other substances that may alter water transparency and the light regime ([Bélanger et al., 2013b](#)). In Baffin Bay, observational studies were carried out on the distribution of trace elements ([Campbell and Yeats, 1982](#)) and their

transfer in the NOW marine food web (Campbell et al., 2005). The high concentration of trace metals found in sea-ice and their transfer to higher trophic levels, suggests that melt water may also have a significant effect on surface water in terms of micronutrients supply.

2.6.2 Limitation of the data

Compared to in situ data collected on board ships, the main advantage of using satellite data to study phytoplankton phenology is the high temporal and spatial resolution that allows the synoptic exploration of vast areas of the world oceans. However, analyses based on satellite data sets have their limitations. For instance, given the presence of sea-ice and heavy cloud cover, quantifying the variability of the phytoplankton blooms phenology at high latitudes is not a straightforward task. The presence of data gaps in satellite ocean-color time series may entail some degree of uncertainty in phenology studies (Racault et al., 2014b). We attempted to reduce these errors by the use of the GlobColour merged satellite Chl-a product and through the application of the DINEOF method that fills data gaps by identifying the dominant spatial and temporal patterns. From an operational perspective, this approach allowed the impact of missing data to be limited and thus to increase, to some extent, accuracy when phenology metrics were applied. Moreover, the use of appropriate metrics to quantify changes in phytoplankton bloom dynamics is also of importance because different methods may lead to differences in bloom phenology patterns (Brody et al., 2013). A second limitation is that the subsurface chlorophyll maxima (SCMs), which are usually located below the pycnocline and in close association with the nitracline (Ardyna et al., 2013), may have been ignored because beyond the range of satellite ocean-color sensors. Another important point to consider is that environmental drivers controlling the bloom dynamic may co-vary and interact with each other, leading to non-linear responses within pelagic ecosystems (Hunsicker et al., 2016). This implies that empirical regression analysis,

although useful to highlight links between environmental forcing and phytoplankton bloom dynamics, may fail to fully resolve the complex interactions existing between physical and biological processes (Ji et al., 2010). In this context, the use of specific statistical models that incorporate both linear and nonlinear response curves from several environmental predictor variables might provide more specific insight on the bloom phenology variability. Finally, the potential role of the top-down grazing pressure and nutrient levels in shaping the spatial pattern of blooms should also be taken into account and quantified when phenological studies are performed.

2.7 Conclusions

Within a pelagic ecosystem, changes in phytoplankton phenology may increase the chance of trophic mismatch and, consequently, have important consequences for the structure of the marine food web. In this study, to monitor bloom phenology, we combined remote sensing data with a multi-Gaussian fitting method. The results presented here clearly suggest that a combination of different environmental drivers strongly influence phytoplankton dynamics within the NOW polynya. In particular, for the period 1998-2014, the present study provides quantitative evidence of:

1. A marked year-to-year variability in bloom onset. Results indicated that the timing of bloom onset appeared to be controlled by a delicate balance between oceanographic (e.g., surface temperature and changes in sea-ice concentration) and meteorological (e.g., cloud radiation interactions and wind stress) conditions.
2. A lack of clear positive trend in bloom duration. In particular, the correlation analysis showed that in conditions of protracted open water period blooms lasted longer. Conversely, during years with a relatively persistent ice cover blooms were of shorter duration.
3. A decline in bloom amplitude during the 17 years examined. Although caution is

needed in interpreting this result, we emphasize that the observed decline in Chl-a could be related to large-scale changes in the Arctic Ocean (i.e., increased surface temperature and freshwater content) but also to local scale forcing. For instance, in this region, the role which winds played (relative to potential change in sea-ice concentration) in entrainment of nutrient-rich water into the surface layer was of fundamental importance to fuel large phytoplankton blooms.

Overall, these findings also suggested how climate oscillations controlling fundamental environmental conditions that regulate phytoplankton growth (i.e., light availability and sea surface warming) may result in changes in size and species composition. For instance, a recent study examining the responses of two different natural Arctic phytoplankton communities to surface warming reported a decline in phytoplankton biomass and growth and as well a shift in phytoplankton size-structure and community composition (Coello-Camba et al., 2015). As far as the NOW polynya, field observations pointed out a drastic modification of the phytoplankton community structure (from large to small cells) and a drop in phytoplankton biomass between 1999 and 2011 (Blais et al., 2017). A next step would thus be to investigate the phytoplankton functional types phenology to better illustrate the phenological response of individual phytoplankton species and the environmental factors controlling it over the NOW polynya. Finally, it is noted that with respect to its sea-ice cover, the Arctic Ocean is increasingly displaying new and remarkable changes (Arrigo et al., 2012; Ardyna et al., 2014). However, the ongoing changes are not geographically homogeneous and can produce different effects in different places. Therefore, to better understand how environmental changes will affect pelagic Arctic ecosystems, it is becoming increasingly necessary to adopt a more realistic pan-Arctic perspective by focusing on specific regional studies.

Acknowledgements

This study was supported by grants from ArcticNet, the Network of Centres of Excellence of Canada and the NSERC, and the Natural Sciences and Engineering Research Council of Canada (to S.B., J.-É. T. and D.D.). C.M. received a postgraduate scholarship from Université du Québec à Rimouski (UQAR) and funded by ArcticNet. C.A. is funded by a MELS FQRNT and RAQ postdoctoral fellowship. This is a contribution to the research programs of ArcticNet and Québec-Océan. We would like to thank M. Taylor for providing useful information about the use of the DINOEF method. We are very grateful to the reviewers for their helpful comments and remarks. We also thank E. Calabretta and L. Gray for language support.

CHAPITRE 3

REGIONAL DIFFERENCES AND INTER-ANNUAL VARIABILITY IN THE TIMING OF SURFACE PHYTOPLANKTON BLOOMS IN THE LABRADOR SEA

Article in preparation

Christian Marchese¹, Laura Castro de la Guardia², Paul G. Myers², Simon Bélanger¹

¹Université du Québec à Rimouski, Département de biologie, chimie et géographie, 300 allée des Ursulines, Rimouski (Québec), G5L 3A1 Canada

²University of Alberta, Department of Earth and Atmospheric Sciences, 1-26 Earth and Atmospheric Building, Edmonton (Alberta), T6G 2E3 Canada

3.1 Résumé

L'efflorescence annuelle du phytoplancton constitue un événement marin important, dont la variabilité d'une année à l'autre est utile pour surveiller les modifications de l'écosystème pélagique et pour mieux gérer les pêches. Une analyse biogéographique, conjuguée aux données simulées à partir de l'état des connaissances actuel sur le modèle de circulation océanique, a été requise pour investiguer la variabilité de l'apparition de l'efflorescence sur l'étendue de la mer du Labrador. Le cycle saisonnier de la chlorophylle dans la mer du Labrador diffère de manière significative dans deux biorégions voisines mais distinctes : le nord ($> 60^\circ\text{N}$) et le sud ($< 60^\circ\text{N}$). Le nord voit l'efflorescence se produire plus tôt (\sim début-mi-avril) et de manière plus marquée, alors que au sud de la mer du Labrador le phénomène se produit plus tard (\sim mai) et peut durer tout l'été. Dans la biorégion du sud, le taux de croissance maximal du phytoplancton (c'est-à-dire l'apparition de l'efflorescence printanière à la surface) correspond de près au premier renversement refroidissement-réchauffement des flux de chaleur air-mer. Dans cette zone, le moment de l'efflorescence semble précéder ceux de la diminution de l'épaisseur de la couche de mélange et du développement printanier de la stratification des couches supérieures de l'océan. Or, dans la biorégion nord de la mer du Labrador, l'avènement précoce de l'efflorescence printanière est associé à la stratification de l'épaisseur de la couche de mélange et survient avant la fin du refroidissement hivernal (les flux air-mer demeurent négatifs). La différence dans le temps de réponse de l'efflorescence dans ces deux biorégions suggère de façon très nette que, par leurs interactions, la quantité de phytoplancton et l'environnement physique dépendent étroitement l'un de l'autre et, comme ils sont fonction du mécanisme de forçage dominant, peuvent fortement varier. Compte tenu de l'hétérogénéité du bassin du Labrador, cette étude insiste sur l'importance de prendre en considération les interactions physicobiologiques des couches supérieures de l'océan propres aux différentes biorégions.

Mots clés: efflorescence phytoplanctonique, biorégion marine, mer du Labrador,

forçage physique, variabilité interannuelle, Atlantique Nord subpolaire

3.2 Abstract

The annual phytoplankton bloom is an important marine event and its inter-annual variability can be used to monitor changes in the pelagic ecosystem and to manage fisheries more effectively. A biogeographic analysis in conjunction with satellite-derived ocean color observations and simulated data from a state-of-the-art ocean circulation model were used to investigate the spring bloom onset variability over the whole Labrador Sea (LS). Chlorophyll-a seasonal cycle in the LS varies markedly between two neighboring but distinct bioregions: the north ($> 60^{\circ}\text{N}$) and the south ($< 60^{\circ}\text{N}$). The north LS blooms earlier (\sim early-mid April) and more intensely, while the south LS blooms later (\sim May) and its duration may persist all summer long. In the southern LS bioregion, the maximum phytoplankton growth rate (i.e., the initiation of the surface spring bloom) coincides closely with the timing of the first cooling-to-heating shift in air-sea heat fluxes. In this area, the bloom timing tends to precede the shoaling of the mixed-layer depth and the vernal development of the upper ocean stratification. Meanwhile, in the northern LS bioregion, the early onset of the spring bloom is related to the seasonal evolution (i.e., shoaling) of the mixed-layer depth and precedes the cessation of wintertime cooling (i.e., the air-sea fluxes are still negative). The difference in bloom timing response across the two bioregions suggests that interactions among phytoplankton stock and the physical environment are strongly area-dependent and may vary significantly as a function of the dominant forcing mechanism. Given the heterogeneity of the LS basin, this study emphasizes the importance to consider the bioregion-specific differences in the upper ocean physical-biological interactions.

Keywords: phytoplankton bloom, marine bioregion, Labrador Sea, Ocean color remote-sensing, physical forcing, inter-annual variability, Sub-polar North Atlantic

3.3 Introduction

Various oceanic regions are characterized by strong seasonal variations in phytoplankton abundance. In these regions, the transition from winter to spring is characterized by a rapid and intense phytoplankton growth (Henson et al., 2006) that is easily recognizable by ocean-color satellite sensors through the increase in surface chlorophyll-a concentration (Siegel et al., 2002), a key diagnostic pigment for all phytoplankton groups (Huot et al., 2007). One of these ocean regions is undoubtedly the North Atlantic, a strongly seasonal ocean characterized by intense spring phytoplankton blooms (Siegel et al., 2002). In the North Atlantic, the pronounced seasonal growth cycle of phytoplankton has been the subject of many interdisciplinary work. In particular, much attention has been given to changes in the timing of the spring bloom (e.g., González Taboada and Anadón, 2014; Henson et al., 2009), which can result in the decoupling of phenological relationships in the pelagic food chain (Edwards and Richardson, 2004; Friedland et al., 2016) and represents a critical factor for the seasonality of the biological carbon pump (Sanders et al., 2014). The bloom timing by determining when food sources are available to both fish and marine birds, plays thus a large role in maintaining food web interactions and commercial fisheries (Racault et al., 2014a). In this connection, understand what exactly causes the spring blooms to occur and monitoring their spatial patterns is of fundamental importance.

Traditionally, the onset of the sub-polar North Atlantic phytoplankton blooms has been attributed to changes in the mixed-layer depth: in open ocean/deep water the bloom begins when the mixed-layer shoals (from winter to spring) to a depth shallower than a critical depth at which the phytoplankton net growth becomes positive (i.e., the growth of phytoplankton exceeds autotrophic respiration). The progressive shoaling of the mixed-layer depth helps phytoplankton to remain and accumulate in the brighter surface layer. Later, in late spring or early summer, nutrients become exhausted in the euphotic zone, the growth slows and the loss due to increasing grazing pressure reduces the

phytoplankton abundance to a lower level. This classical explanation for the occurrence of the spring bloom represents the so-called "critical depth hypothesis" (Sverdrup, 1953). Nowadays, the Sverdrup's critical-depth hypothesis remains the most cited and widely accepted theory and it has been used to investigate the timing of the spring bloom over high latitude regions (e.g., Henson et al., 2006). However, contemporary studies have agreed (Mahadevan et al., 2012), challenged (Behrenfeld, 2010; Boss and Behrenfeld, 2010) or merely refined the Sverdrup's model by testing if reduction in turbulent mixing within the mixed layer (rather than the decrease in the mixed layer itself) can create the appropriate conditions for the bloom onset (Chiswell, 2011; Taylor and Ferrari, 2011). Overall, in the North Atlantic the bloom onset variability has been studied extensively and it has been related to several physical drivers. For instance, large-scale climate indices such as the North Atlantic Oscillation have been linked to changes in the timing of the sub-polar bloom (Henson et al., 2009; Zhai et al., 2013).

In the Labrador Sea (LS), a sub-polar sea that connects the North Atlantic with the Arctic Ocean, few studies have investigated the bloom onset variability and its ecological significance. More specifically, satellite observations in conjunction with numerical model (Frajka-Williams and Rhines, 2010; Wu et al., 2008a), shipboard observations (Head et al., 2000) and hydrographic-based studies (Frajka-Williams et al., 2009) have identified a north-to-south progression in the spring bloom initiation. In the northern region (north of $\sim 60^\circ\text{N}$) of the LS the bloom starts earlier, and it is usually shorter but more intense compared to the central-southern region of the basin. This reversed geographical pattern represents a distinctive feature if compared to the North Atlantic where spring blooms tend to follow a general northward progression (Siegel et al., 2002). The early bloom in the north LS was related to the shallower mixed layer associated with Arctic-derived low-salinity waters. Instead, the initiation of the spring bloom in the central-southern LS was linked to the formation of the seasonal thermal stratification established by surface warming (Frajka-Williams and Rhines, 2010; Wu et al., 2008a). Recently, the difference in the bloom temporal variations was redefined

based on climatological ocean-color observations ([Lacour et al., 2015](#)): the spring bloom starts when the depth of the mixed layer shoals and regulates the phytoplankton's time exposure to sunlight. Overall, the spring bloom onset in both regions occur when the mean photosynthetically available radiation (PAR) over the mixed layer reach the same threshold of $2.5 \text{ mol photon m}^{-2} \text{ d}^{-1}$, suggesting that light-mixing regime was the main driver of the bloom onset in the whole LS basin ([Lacour et al., 2015](#)).

All these studies, using the critical depth hypothesis showed that over the LS the onset of the spring bloom is highly sensitive to the light availability and the depth of the mixed layer. However, [Townsend et al. \(1994\)](#) reported blooms in North Atlantic waters weeks before the shoaling of the mixed layer. The authors suggested that in presence of a very calm period (i.e., relaxation of atmospheric forcing), a near-surface bloom could occur without stratification. Recent observations showed evidence for widespread winter (January-March) phytoplankton blooms in a large part of the North Atlantic sub-polar gyre triggered by prolonged periods of calm ([Lacour et al., 2017](#)). Probably, these periods of calm combined with the phytoplankton cells ability to control buoyancy can maintain phytoplankton stock in the upper water column ([Lindemann and St John, 2014](#)). Numerical simulations also suggest that a net positive phytoplankton population growth in a deep mixed layer is possible when turbulence levels are not too strong and/or possibly close to a critical threshold to maintain phytoplankton in the well-lit zone ([Ghosal and Mandre, 2003](#); [Huisman et al., 2002](#)). Recently, vertical profiles from different Biogeochemical-Argo (BGC-Argo) floats that sampled the waters of the subpolar North Atlantic revealed unequivocally that phytoplankton populations start growing in early winter but at very weak rates ([Mignot et al., 2018](#)). However, the period of explosive population growth (i.e., the so-called spring bloom phase) is not observed until spring, when atmospheric cooling subsides and the mixed layer shoals ([Mignot et al., 2018](#)).

While the weak accumulation of phytoplankton in winter has no surface signature

([Ferrari et al., 2015](#); [Mignot et al., 2018](#)) the onset and magnitude of the spring bloom can be intercepted and monitored by satellite remote sensing of ocean color measures. Recently, [Ferrari et al. \(2015\)](#) used satellite data to show that over the subpolar North Atlantic the cooling-to-heating shift in air-sea heat fluxes (the so-called convection shutdown hypothesis) is a robust indicator of surface blooms. Using the air-sea heat fluxes to estimate when the mixing layer shoals, the authors demonstrated that the spring bloom onset is triggered by a reduction in turbulent mixing due to an increase in net warming at the end of winter.

Although previous studies have examined the role of convective mixing in spring blooms of the North Atlantic, none of these specifically focus on the LS (e.g., [Ferrari et al., 2015](#)), one of the few marine regions where open-ocean deep convection occurs. The goal of this study is therefore to test for the first time if the shutdown of winter convective mixing could be, on an inter-annual scale, a more suitable predictor for the spring bloom onset within the heterogeneous LS, a basin which hosts pronounced seasonal growth cycles of phytoplankton. Additionally, this study also investigates the role of the upper-ocean stratification in triggering the surface spring bloom. To achieve the aforementioned objectives, we used an integrative approach that incorporates a biogeographic analysis in conjunction with satellite-derived ocean color observations and simulated data from a state-of-the-art ocean general circulation model to identify region-specific physical determinants for the spring bloom initiation. The rationale is that spurred on by a dominant forcing mechanism, interactions among phytoplankton dynamics and the physical environment may vary across sub-regional spatial scales. Therefore, the best way to compare timing of events is to use a cross-region and inter-annual analysis. Knowing the role of blooms in drawing down atmospheric carbon dioxide and its importance in food web interactions, a better understanding of the mechanisms governing the timing of the LS's spring bloom is of particular relevance.

3.4 Material and methods

3.4.1 Satellite chlorophyll-a time series

The area lying between 67°N - 52°N and 65°W - 42°W was selected to study the inter-annual variability in phytoplankton bloom onset over the LS (Figure 10a). Daily time series (from 1998 to 2015) of surface satellite-derived chlorophyll-a (mg m^{-3}) at 25 km ($\sim 0.25^\circ$) of spatial resolution were obtained from the GlobColour Project (<http://hermes.acri.fr>). The surface chlorophyll-a values are gathered by using the Garver-Siegel-Maritorena (GSM) model (Maritorena et al., 2002) combining, when possible, data from different sensors (i.e., SeaWiFS, MERIS, MODIS and VIIRS), and ultimately providing a merged product with elevated spatiotemporal coverage (Maritorena et al., 2010). The GlobColour dataset represents thus a common and appropriate choice for phytoplankton phenology studies because it improves coverage in both space and time by combining observations from multiple sensors (Ferreira et al., 2014). Additionally, the dataset performs relatively well when compared with the SeaWiFS Bio-optical Archive and Storage System (SeaBASS) database and other in situ datasets (see Cole et al. 2015, and the references therein).

In order to facilitate comparison with the model output time-series (see subsection 3.4.4), to further increase spatial coverage and to reduce extreme values in the data, the daily images of chlorophyll-a were averaged on a pixel-by-pixel basis (by using the geometric mean that is less affected by extreme value than the arithmetic mean) to create a 10-day composite time-series. Due to the low incidence sun angle in winter the temporal coverage of the chlorophyll-a time-series is from early March to the end of September, and it contains twenty-four 10-day periods. The aforementioned time period is thus used to characterize exclusively the spring bloom phase over the LS.

3.4.2 Clustering K-means analysis

Using the 10-day composite chlorophyll-a time-series, a bio-regionalization analysis was carried out using the cluster K-means analysis (Hartigan and Wong, 1979). The Calinski-Harabasz index (Caliński and Harabasz, 1974) was used to evaluate the optimal number of clusters (see Figure 25 in annex II). The K-means analysis method regroups pixels with a similar seasonal cycle shape (i.e., phenology). This method was previously applied successfully at the global scale (D’Ortenzio et al., 2012), in the Mediterranean Sea (D’Ortenzio and Ribera d’Alcalà, 2009), over the North Atlantic (Lacour et al., 2015) and more recently in the Southern Ocean (Ardyna et al., 2017). The analysis was performed on a pixel-by-pixel basis: each pixel within the study area was averaged over the period 1998-2015 to create a 10-day climatological time-series of chlorophyll-a concentration that was subsequently normalized in order to scale values between 0 and 1. However, pixels with more than two 10-day periods of missing data (i.e., due the continued presence of clouds or sea-ice) were excluded from the analysis. The cluster analysis, by condensing the spatiotemporal variations of the surface chlorophyll-a concentration identifies groups representative of a characteristic seasonal cycle (i.e., a distinctive phenological regime). Basically, the spatial distribution of each group constitutes a specific bioregion. Finally, using bathymetry data, the bioregions were redefined to exclude shelf areas (shallower than ~ 200 m) where the chlorophyll-a seasonal cycle may be different.

3.4.3 Mixed-layer depth from ARGO data

The mixed-layer depth (MLD) represents a hydrographically defined region in which turbulent mixing has homogenized some range of depths. We obtained daily MLD data for the period 2002-2014 from the Scripps Institution of Oceanography and the University of California, San Diego (<http://mixedlayer.ucsd.edu/>). This MLD is

estimated using salinity and temperature profiles from an Array of Real-time Geostrophic Oceanography (ARGO) and a hybrid temperature-density algorithm (Holte and Talley, 2009). The algorithm, recently tested in the Labrador and Irminger Seas seems to produce MLDs more accurate than those calculated with a density threshold method (Holte et al., 2017). That being said, other criteria to define the MLD can be found in the literature. However, applying the most accurate MLD criteria presents challenges because they all have limitations.

From the daily mean profiles, we calculated 10-day LS regional means. The 10-day mean excluded outliers, i.e., floats with MLD values that were more than 2 standard deviations away from the corresponding 10-day temporal mean. To assure the best temporal quality, the mean was calculated when at least five individual profiling floats were available within the 10-day period (after removing outliers). However, the seasonal and inter-annual evolution of the MLD was still subject to temporal gaps and estimation errors due to spatial coverage (see section 4) that would have introduced biases to our analysis of phytoplankton phenology. For this reason, the 10-day regional MLD mean derived from ARGO data was mainly used to evaluate the simulated MLD (derived from NEMO3.4; see next subsection).

3.4.4 Simulated mixed-layer depth and heat fluxes

A numerical simulation using the Nucleus for European Modeling of the Ocean version 3.4 (NEMO3.4; Madec 2008) was applied to capture the MLD and heat fluxes (HFs) time evolution (i.e., seasonal and inter-annual) over the LS. The model domain covers the Arctic and the Northern Hemisphere Atlantic with a horizontal resolution of 0.25° (ANHA4). This regional configuration has two open boundaries, one close to the Bering Strait in the Pacific Ocean and the other one at 20°S across the Atlantic Ocean. Further details about the model configuration and set up can be found in Dukhovskoy et al. (2016) and Gillard et al. (2016).

The simulation was integrated from January 2002 to December 2014 with initial conditions (3D temperature, salinity, horizontal velocities, sea surface height and sea-ice) from the Global Ocean Reanalysis and Simulations (GLORYS2v3) product from MERCATOR (Ferry et al., 2010). The open boundary conditions (ocean temperature, salinity, and velocities) were extracted from the GLORYS2v3 product as well. At the surface, the model was driven with hourly 33-km resolution atmospheric forcing data (10 m wind, 2 m air temperature and humidity, downwelling and long wave radiation flux, and total precipitation) from the Canadian Meteorological Centers Global Deterministic Prediction System (CMC-GDPS; Smith et al. 2014). Monthly inter-annual runoff from Dai et al. (2009) as well as Greenland melt-water provided by Bamber et al. (2012) was also carefully remapped onto the model grid to give a more realistic freshwater input to the ocean. No temperature or salinity restoring was applied in the simulation.

The HFs were computed on the fly (i.e. every model step) using the bulk formula developed by Large and Yeager (2004). The model produced five-day mean HFs fields as well as the 3D ocean temperature and salinity. The latter two fields were used to calculate the MLD by employing the algorithm developed by Holte and Talley (2009) that was recently adapted for ocean general circulation models by Courtois et al. (2017).

To align the time series of physical variables with the chlorophyll-a concentration time-series, we averaged two consecutive 5-day means from the model output to obtained 10-day-mean fields of MLD and HFs. The high-frequency 10-day mean of simulated data were thus used to consider the inter-annual relationships with surface chlorophyll-a. Finally, as previously noted, we evaluated the 10-day mean simulated MLD values within the LS with the ARGO MLD.

3.4.5 Surface bloom onset and physical timing metrics

In order to better analyze the chlorophyll-a cycles in the bioregions identified by the cluster analysis, 10-day annual cycles were created by spatial averaging all pixels within the bioregions. If compared to a simple data-box selection, averaging data within the bioregions represents a more accurate method because each bioregion is representative of a distinctive phenological regime. To ensure sufficient data to identify the onset of the surface bloom, only data covering the period 2002-2014 were used, given that at least three out of the four sensors were operational during this period. The growth rate is used as a proxy for the net increase of surface phytoplankton biomass. For each year and for each bioregion, the growth rate (i.e., the rate of chlorophyll-a increase), gr (day^{-1}), was computed as follows:

$$gr = \frac{1}{Chla} \times \frac{Chla}{dt} \quad (1)$$

where $Chl a$ is the averaged surface chlorophyll-a concentration. Similarly, to [Lacour et al. \(2015\)](#), the surface bloom onset was defined as the date on which the biomass reaches the maximum growth rate.

Two additional timing metrics (see also Table 6 for definitions) were selected based on previous and relevant studies of bloom dynamics (e.g., [Cole et al., 2015](#); [Ferrari et al., 2015](#)). The physical timing metrics were calculated for each year and for each bioregion. For each HF's annual cycle, the date on which the HF's became positive for at least 20-days (two consecutive time step) was used as a proxy to indicate the end of winter convection and the beginning of less turbulent conditions. Similarly, the date of the steepest gradient in MLD that occurs between its maximum and minimum (i.e., date on which the MLD became shallower) was estimated each year and used as a proxy to distinguish between vertically well mixed waters (> 100 m) and stratified water ($<$

100 m). This threshold was also used in previous studies (i.e., [Lacour et al., 2015, 2017](#)).

Finally, the Brunt-Väisälä frequency (N^2) in the upper 25 m of the water column was also used as an indicator of the upper water column stratification. Specifically, we calculated the Brunt-Väisälä frequency using the vertical gradient of potential density: this computation uses the polynomial expression of [McDougall \(1987\)](#) and the 5-day-mean output temperature and salinity from NEMO.

Table 6: Description of physical metrics

Metric name	Definition	Reference
*HFs turn positive	The date on which the air-sea heat fluxes became positive for at least 20 days (two consecutive time step)	Taylor and Ferrari (2011); Ferrari et al. (2015)
**MLD shoaling	The date of the steepest gradient in mixed-layer depth that occur between its maximum and minimum (i.e., the date on which the MLD became shallower)	Cole et al. (2015)

* Heat Fluxes

** Mixed Layer Depth

3.5 Results and Discussion

3.5.1 Bioregionalization and phytoplankton seasonal cycles differences

The bioregionalization of the LS identified two distinct bioregions on either side of the 60°N parallel (Figure 10a) and matched those identified by [Lacour et al. \(2015\)](#). The two bioregions respectively indicated as the northern bioregion (yellow area; Figure 10a) and the southern bioregion (green area; Figure 10a), have marked differences in bloom initiation patterns. In northern bioregion, the bloom starts in early-mid April, peaks later in May, and usually declines in June (Figure 10b). Conversely, in the southern

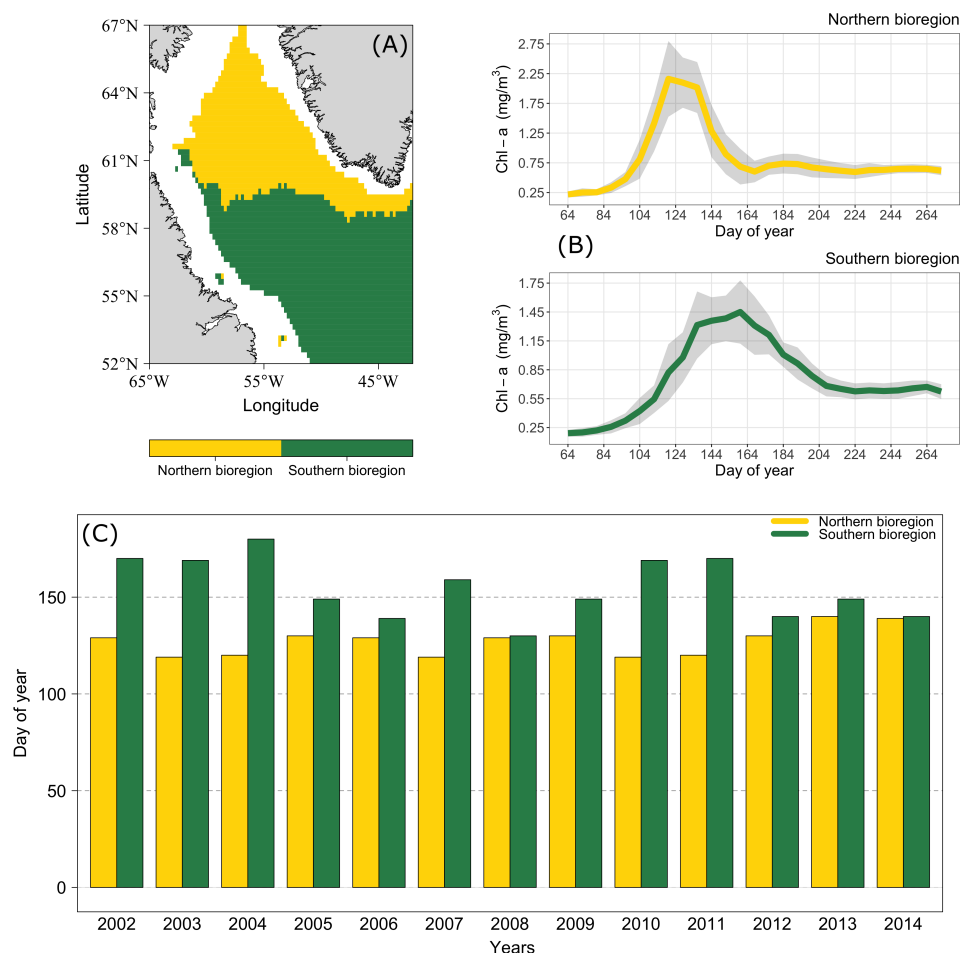


Figure 10: (a) Spatial distribution of the clusters obtained from the K-means analysis and (b) the mean biomass (chlorophyll-a) annual cycles in each cluster ± 1 standard deviation (light grey area). The spatial distribution of each cluster constitutes a specific bioregion representative of a characteristic seasonal cycle. (c) Time (day of the year) of the maximum chlorophyll-a amplitude (i.e., the date at which the chlorophyll-a reaches its maximum value) for each bioregion.

bioregion the bloom starts in May, peaks in June, and fades away approximately towards the end on July (Figure 10b). This temporal delay in bloom start dates clearly shows that, over the LS, the bloom does not follow the general south-to-north progression usually associated with the seasonal increase in surface light availability (Lacour et al., 2015; Wu et al., 2008a). A Hovmöller diagram (Figure 26 in annex II) also gives

a synthetic representation of the reversed latitudinal bloom gradient. Furthermore, the southern bioregion has a longer bloom and lower bloom amplitude compared to northern bioregion. However, differences in bloom phenology (i.e., onset, amplitude and duration) between the north and the south LS can be more or less pronounced, depending on the year. For instance, the northern bioregion, which typically has higher surface chlorophyll-a concentrations, had a less intense bloom compared to the southern bioregion during 2005 (Frajka-Williams et al., 2009). Moreover, during spring 2008 satellite data showed a spatially large phytoplankton bloom in the LS with the north and south blooms observed nearly simultaneously. Both regions bloomed within a few days of each other, reaching their maximum peaks with a difference of only few days (Frajka-Williams and Rhines, 2010).

Overall, with the exception of some years (e.g., 2008 and 2014; Figure 10c) in which the difference in bloom phenology between bioregions is less marked, the northern bioregion starts and reaches its maximum amplitude earlier (Figure 10c). On average, in the northern bioregion the bloom peaks in early May (126 ± 7 day of year) while in the southern bioregion the bloom peaks later in early June (154 ± 15 day of year). These observations confirm that on an inter-annual basis, mechanisms triggering spring blooms differ between the two bioregions making the onset of the spring bloom strongly area dependent. Indeed, the distinctions in dominant physical characteristics between bioregions may play a crucial role in affecting the inter-annual variability of the bloom.

3.5.2 The southern bioregion

In winter, over the North Atlantic subpolar gyre, strong winds and surface cooling deepen the mixed layer impacting on light and the upward flux of nutrients into the euphotic zone (Barton et al., 2015). In the LS's southern bioregion, which hosts the convection area (south of 58°N and up to ~ 300 km wide along the western side of the basin; Lab Sea Group 1998), the pelagic ecosystem is heavily shaped by convective

mixing. For instance, profiling floats reveal convection reaching depths of more than 800-1000 m or even greater than 1500 m during some years (Frajka-Williams et al., 2009; Yashayaev and Loder, 2016). In this bioregion, the shoaling of the MLD were assumed to be a critical environmental factor for the bloom onset (Wu et al., 2008a). To investigate if over the southern bioregion other physical drivers were responsible for the inter-annual variability in bloom initiation, the convection shutdown hypothesis was tested following the approach of Ferrari et al. (2015). In the southern bioregion, the surface seasonal bloom is visible as a sudden increase in chlorophyll-a concentration (solid green line in Figure 11). The surface chlorophyll-a maximum (i.e., the bloom peak value) is systematically preceded by the date at which the HFs turn positive (dotted black vertical lines in Figure 11). The HFs annual cycle is made up by negative values (cooling) in winter (grey shade in Figure 11), which favors convective mixing over the bioregion, and by positive values (heating) in spring-summer (period between grey shade in Figure 11). On an inter-annual timescale, the timing of the spring bloom (i.e., maximum phytoplankton growth rate) is well-correlated ($r = 0.64$, $p = 0.018$) with the timing of the first shift from cooling to heating in HFs (the end of wintertime convection). Cole et al. (2015) found a similar correlation (i.e., $r = 0.61$) in the sub-polar North Atlantic. The authors indicated the onset of positive HFs as a basin wide driver for the bloom initiation date. Brody et al. (2013), also showed that over most of the subpolar North Atlantic the spring bloom initiation dates, gained by three different methods, were approximately in sync with the HFs turning positive. It is also interesting to note that in correspondence of the date at which the HFs turn positive (dotted black vertical lines in Figure 11) the model-derived MLD (green area in Figure 11) is markedly still deep when chlorophyll-a starts increasing (solid green line in Figure 11). The site of deep convection is located in this bioregion and a rapid increase in the mean MLD occurs during winter months, as a result of convective mixing. As the HFs start to increase from its winter minimum the MLD also shoals gradually from winter into spring. However, over the southern bioregion, the correlation between the timing of MLD shoaling and the

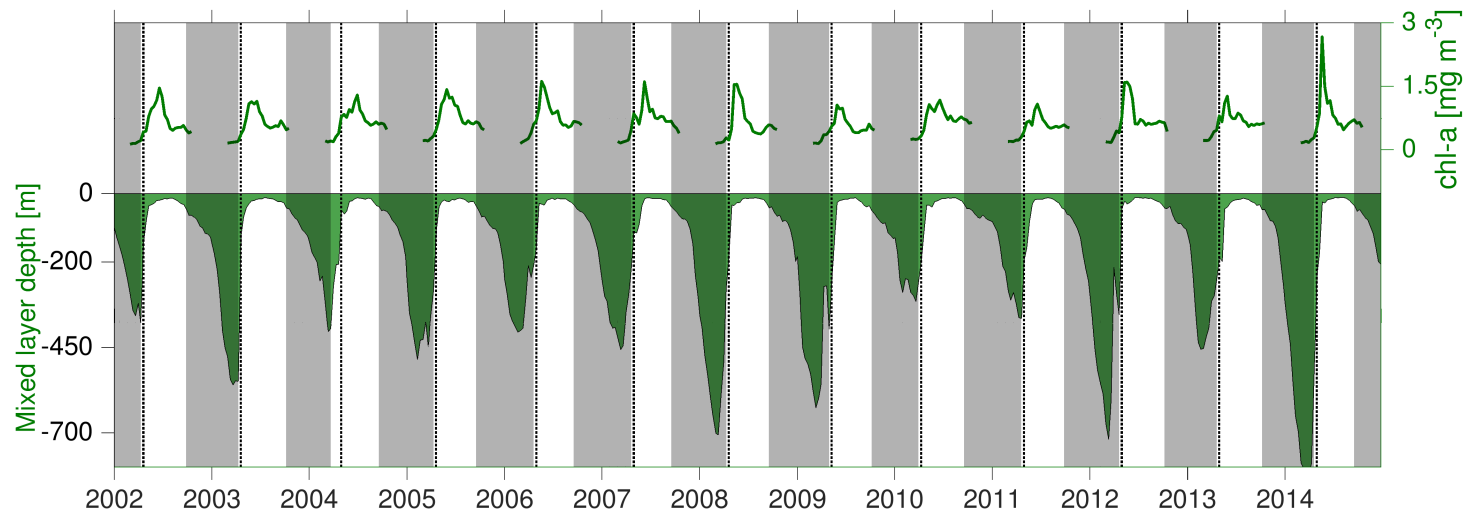


Figure 11: Time series (2002-2014) of chlorophyll-a (green solid line), heat fluxes (the shaded areas show negative values in winter) and simulated mixed layer depth (green area) over the southern bioregion. The heat fluxes annual cycle is made up by negative values (cooling) in winter (grey shaded areas), which favors convective mixing and by positive values in spring-summer (period between grey shaded areas). The vertical (black dotted) lines represent the date (for each year) on which the heat fluxes became positive for a minimum of 20 consecutive days (note one time-step is 10-days). The mixed layer is still deep when chlorophyll-a starts growing at the end of winter and the heat fluxes change sign (black dotted lines).

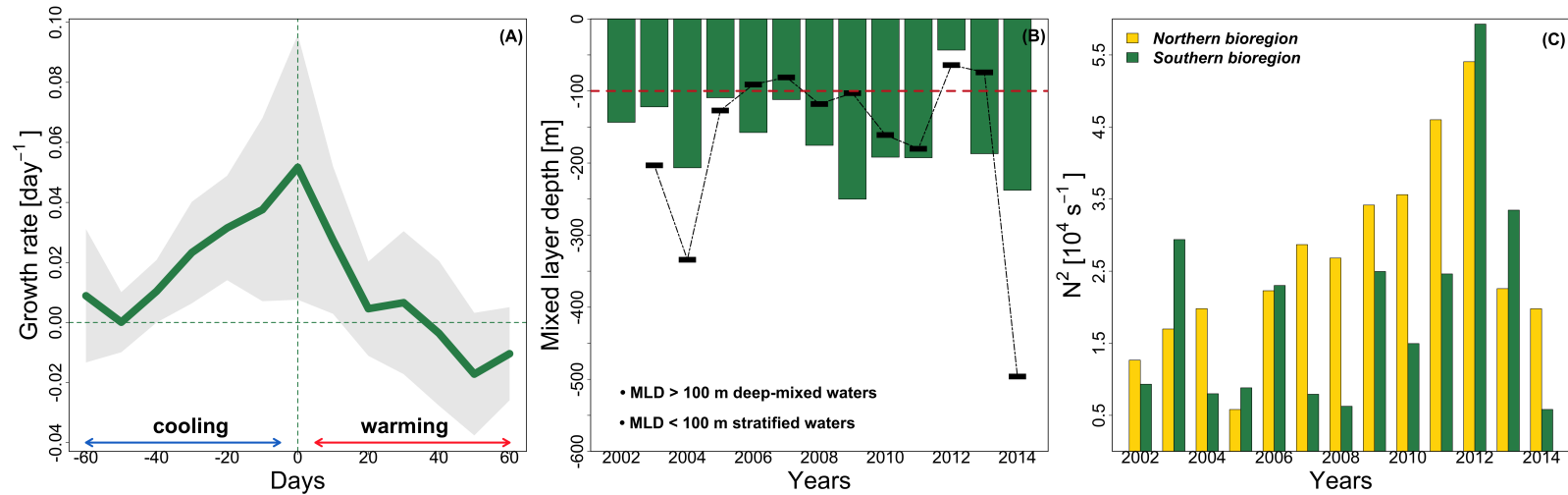


Figure 12: (a) Net surface growth rate increase averaged over the southern bioregion (green solid line ± 1 standard deviation) as a function of the days since the net heat fluxes turns positive. The average net surface growth rate is much larger closer to the date when the heat fluxes turns positive (i.e., day zero). (b) The mixed layer depth (from 2002 to 2014) at the time when the air-sea heat flux turned positive over the southern bioregion. Green bars represent the modeled mixed layer depth, while the black two-dashed line with successive segments represents the ARGO mixed layer depth (note that for the year 2002 no ARGO data were available at the time when the air-sea heat flux turned positive). In both cases, when heat fluxes first exceed zero the depth of the mixed layer is often deeper than 100 m. (c) The stratification index for both bioregions (see different colors) at the time when the HF's change sign over the southern bioregion (green bars). In 8 out of 13 years ($\sim 62\%$) the stratification is stronger (i.e., larger N^2) in the northern bioregion (yellow bars).

timing of the maximum phytoplankton growth rate was no significant. In the sub-polar North Atlantic, [Cole et al. \(2015\)](#) found a weak correlation (i.e., $r = 0.25$) between the date of MLD shoaling and the spring bloom initiation. Although different datasets and a somewhat different time-period are used here, our results are in accordance with previous observations obtained in the North Atlantic.

More quantitative evidence that in southern bioregion the convection shutdown events strongly drive the bloom initiation is found when the net surface growth rate is plotted as a function of the days since HFs turn positive (Figure 12a). Relative to any other time of the year, the averaged net surface growth rate (green solid line ± 1 standard deviation in Figure 12a, computed over the study period 2002-2014) is much larger closer to the date when the HFs turn positive (i.e., day zero in Figure 12a). This result suggests that the maximum phytoplankton accumulation rate (i.e., the onset of the surface spring bloom) occur approximately when the convection shutdown, as revealed by the change in HFs sign. The simulated (vertical green bars) and ARGO (black two-dashed line with successive segments) MLD at the time when the HFs change sign are shown in Figure 12b. It is noteworthy that the depth of the mixed-layer has been traditionally identified as the crucial physical control for the timing of the spring bloom. However, at the surface bloom onset time, in 12 out of 13 years ($\sim 92\%$) the simulated MLD remained beneath 100 m. Likewise, in 8 out of 12 (note that for the year 2002 no ARGO data were available at the time when the HFs turned positive) years ($\sim 67\%$) the MLD calculated from ARGO floats was deeper than 100 m. Basically, the MLD remains noticeably deep but turbulence likely decreases. Interestingly, in 8 out of 13 years ($\sim 62\%$) on the same date when the HFs change sign over the southern bioregion, the stratification is weaker (Figure 12c) compared to northern bioregion (see next subsection).

All together these results suggest that the spring bloom onset coincides with the period of decreasing turbulence as the HFs become positive. This implies that over

the southern bioregion the shutdown of winter convective mixing closely matches the timing of phytoplankton growth. However, it is also possible that both a decrease in turbulence (i.e., HFs close to zero) and MLD shoaling (~ 50 m) occur together to trigger the spring bloom (e.g., year 2012 in Figure 11 and 12b). A similar concomitance of mechanisms is not unusual and was previously observed in sub-polar North Atlantic by [Cole et al. \(2015\)](#). Furthermore, it is interesting to note that although the maximum accumulation rate of chlorophyll-a coincides closely with the date when the HFs turn positive, the net surface chlorophyll-a growth rate is already positive and started to increase several weeks earlier (Figure 12a). [Behrenfeld \(2010\)](#) and [Boss and Behrenfeld \(2010\)](#), argued that phytoplankton blooms might also start in midwinter, largely triggered by the dilution of phytoplankton and grazer populations during mixed-layer deepening. Basically, the deepening of the mixed-layer reduces grazer encounters and allows the phytoplankton stock to increase. According to the hypothesis, rather than with an increase in division rates, the phytoplankton accumulation starts because of a decrease in zooplankton grazing rate (i.e., loss rates). A recent experiment, using the marine diatom *Thalassiosira weissflogii* as a model organism showed that phytoplankton cells during deep winter convection are able to use fluctuating light (i.e., rapid change in light exposures) for growth, even if growth rates are very low ([Walter et al., 2014](#)). Fieldwork conducted in the northern North Atlantic, Icelandic and Norwegian Sea, also revealed a winter stock of living phytoplankton in the open ocean ([Backhaus et al., 2003](#)). The authors, concluded that the winter stock may form the inoculum for the spring production in the open ocean. More recently, [Mignot et al. \(2018\)](#) using time series collected by BGC-Argo floats in North Atlantic subpolar gyre showed that accumulation of phytoplankton biomass starts in winter, at a time when the mixed layer was still deepening. However, during this period the net population growth rates were weak ($\sim 0.01 - 0.02 \text{ d}^{-1}$). Instead, the authors report a sudden increase in net population growth rates ($\sim 0.08 \text{ d}^{-1}$) that clearly shows the increase in division at the beginning of the spring bloom, as the cooling ends. These findings are in agreement with our

results which show a similar increase in the net population growth rate, with a maximum occurring in spring before significant shoaling of the MLD and the development of stable density stratification (Figure 12a and 12b).

3.5.3 The northern bioregion

The northern bioregion is an area characterized by high eddy kinetic energy (De Jong et al., 2016). The East Greenland Current (EGC), a boundary current that flows southward along the east coast of Greenland, turns west (at Cape Farewell, the southern tip of Greenland) and then north into the LS, forming the West Greenland Current (WGC). The latter provides a source of cold freshwater in its upper layers and warm, salty Irminger Water at intermediate depths (Lacour et al., 2015; Wu et al., 2008a). Other possible freshwater sources include elevated precipitation rates (Wu et al., 2008a) and enhanced Greenland ice-sheet melt (Böning et al., 2016; Luo et al., 2016; Gillard et al., 2016). However, as the topography of the West Greenland slope steepens around 61°N, the WGC becomes unstable generating an eddy kinetic energy maximum (Lilly et al., 2003). Mesoscale eddies, likely associated with instability of the WGC, mix and spread the low salinity water from the Greenland coast to the northern LS (see also Figure 27 in annex II), controlling the haline stratification (Lilly et al., 2003; Gelderloos et al., 2011; Frajka-Williams et al., 2009; Frajka-Williams and Rhines, 2010; Wu et al., 2008a). The high kinetic energy that characterizes the northeastern LS, along with the large number of eddies shading off the boundary current system (De Jong et al., 2016) may also inject additional nutrients from deeper waters. For instance, eddy-kinetic-energy was shown to positively correlate with bloom intensity in the northern area of the LS (Frajka-Williams and Rhines, 2010). In the same area, sea-glider observations revealed that fluorescence (a proxy for phytoplankton concentration) was elevated within and around several mesoscale eddies (Frajka-Williams et al., 2009).

These environmental peculiarities make the northern bioregion fairly different from

the previously discussed southern bioregion, which hosts the deep convection site. The surface freshwater flux and mesoscale eddies dynamics that characterize the northern bioregion, counteract the mixing generated by surface cooling (i.e., reduce the convective activity) and contribute to the restratification and shoaling of the MLD (Chanut et al., 2008). For instance, the results of Mahadevan et al. (2012) demonstrated the role of mixed-layer eddies in creating stratification and thus initiating surface blooms in the absence of net positive heat input. Over the northern bioregion, the cooling-to-heating shift in air-sea heat flux (dashed red vertical lines in Figure 13) occurs, on average 1.9 ± 1.4 time-steps (note that one time-step is 10-days) after the shoaling of the MLD (dotted black vertical lines in Figure 13) and in concomitance or after the bloom peak. Further inspection of data shows that in this bioregion, at the time of the cooling-to-heating shift in air-sea heat flux, phytoplankton growth rates values are weak or already negative (i.e., declining biomass; Figure 14a). Therefore, in the northern bioregion contrary to the southern bioregion, the maximum phytoplankton growth rate (i.e., the initiation of the surface spring bloom) tends to precede the cessation of wintertime cooling (i.e., the air-sea fluxes are still negative). In northern bioregion, the date of the spring bloom initiation had similar timing to the date of the MLD shoaling (dotted black vertical lines in Figure 13). Both are well-correlated ($r = 0.67$, $p = 0.012$), suggesting that the inter-annual variability in the date of bloom initiation is more closely related to the thickness of the mixed layer. To provide more quantitative evidence that in the northern bioregion the shoaling of the MLD strongly influences the bloom onset variability, the averaged net surface growth rate (yellow solid line ± 1 standard deviation in Figure 14b) was plotted as a function of the maximum MLD shoaling time (i.e., days since the MLD reached the steepest gradient that occurs between its maximum and minimum). The average net surface growth rate is larger closer to the date on which the steepest gradient in MLD occurred (i.e., becoming shallower; Figure 14b). This result clearly suggests that phytoplankton growth rates over the northern bioregion are sensitive to the seasonal evolution of the MLD. However, even in this bioregion, the net surface growth

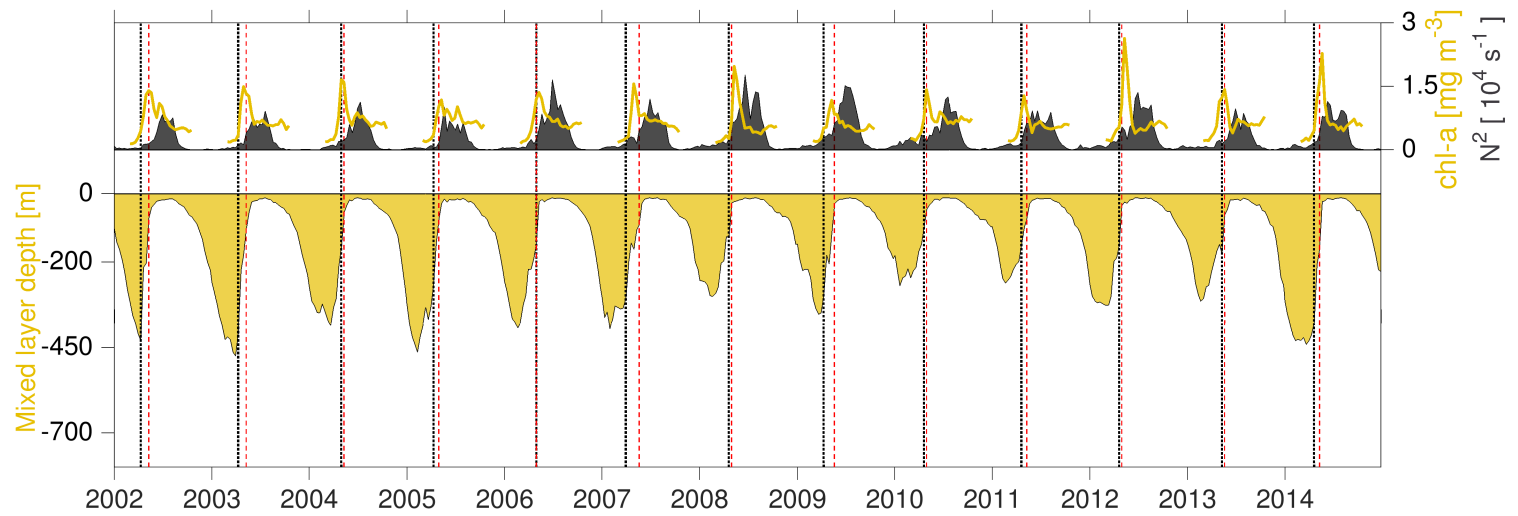


Figure 13: Time series (2002-2014) of chlorophyll-a (yellow solid line), stratification (grey areas), and simulated mixed layer depth (yellow area) over the northern bioregion. As the MLD shoals the stratification within the upper 25 m of the ocean increases. The vertical (black dotted) lines represent the date (for each year) of maximum mixed layer shoaling (i.e., the steepest gradient that occurs between its maximum and minimum). The vertical (red dashed) lines represent the date (for each year) on which the heat fluxes became positive. The cooling-to-heating shift in air-sea heat flux (red dashed lines) occurs, on average 1.9 ± 1.4 time-steps (with a range spanning from a minimum of 0 to a maximum of 5; note that one time-step is 10-days) after the shoaling of the MLD (black dotted lines).

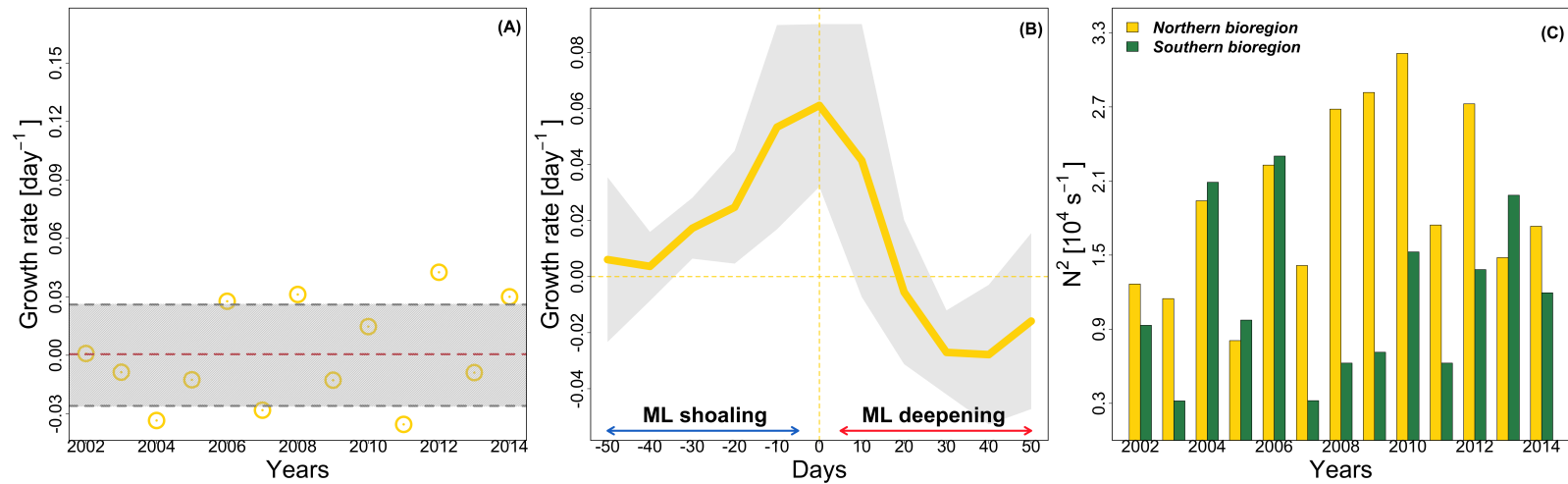


Figure 14: Phytoplankton growth rates values at the time of the cooling-to-heating shift in air-sea heat flux over the northern bioregion. The red dashed line represents the average value, while the light grey area is ± 1 standard deviation from the mean. Growth rates are near-zero or already negative (i.e., declining biomass). (b) Net surface growth rate increase averaged over the northern bioregion (yellow solid line ± 1 standard deviation) as a function of the days since the mixed layer depth reaches the steepest gradient (i.e., becoming shallower) that occurs between its maximum and minimum. The average net surface growth rate is larger closer to the date on which the mixed layer depth became shallower (i.e., day zero). (b) The stratification index for both bioregions (see different colors) at the time when the mixed layer depth reaches the steepest gradient in the northern bioregion. In 9 out of 13 years, the upper ocean stratification is much stronger over the northern bioregion.

rate is already positive and starts to increase several weeks earlier than the shoaling of the MLD. Recent studies clearly show that weak mixed layer biomass accumulations prior the spring bloom phase are possible across the whole North Atlantic subpolar gyre (Lacour et al., 2017; Mignot et al., 2018). Finally, the stratification index (larger N^2 , stronger stratification) at the time when the MLD reaches the steepest gradient (i.e., maximum MLD shoaling) in northern bioregion is shown for both bioregions in Figure 14c. In 9 out of 13 years ($\sim 69\%$), the upper ocean stratification is much stronger over the northern bioregion. This result, once again, suggests that on an inter-annual basis stratification may play a major role in driving the timing of the surface spring bloom in the northern bioregion.

3.5.4 Limitation

The outcomes presented in this study must be interpreted within the limitations of the satellite data and the ocean model adopted. Remotely sensed ocean color data provides key information about phytoplankton bloom phenology. In this study, the combined use of satellite data and model outputs allowed to better address the seasonal and inter-annual variability of both type of parameters (i.e., physical and biological). However, it should be noted that our analysis applies only to surface blooms (i.e., the spring bloom phase) since satellite remote sensing of ocean color is unable to track the complete winter-spring evolution of phytoplankton biomass. Another partial limitation of the method concerns the fact that the boundaries of the bioregions are defined on a climatological basis and thus "static". The LS is a region characterized by a strong environmental variability that can lead to the development of heterogeneous blooms that may step outside the boundaries. When this happens, the bioregionalization of the study area may become less efficient in delimiting the bioregion-specific linkages between physical factors and phytoplankton dynamics. However, it is worth restating that the results presented in this study relate on a sufficiently long time-series (2002-2014;

13-years) to quantitatively highlight the bioregion-specific differences in the upper ocean physical-biological interactions.

Furthermore, evaluation of the model MLD with ARGO floats suggest that the model overestimates the MLD during deep convection with mean biases of 53 meters (Figure 28 in annex II). This error may be partially modulated by the ARGO regional coverage, for example, in years where the ARGO coverage within the convection region was relatively poor, model biases were larger relative to years when ARGO coverage was good. Simulated MLD biases may also be attributed to the 0.25-degree resolution of the ocean model simulation, which although is the same as the satellite data resolution, limits the representation of many of the small eddies shed by the boundary currents (De Jong et al., 2016) that are key in the re-stratification process, therefore our model simulation has lower skills in counterbalancing the heat loss due to the atmospheric forcing. However, the simulation captures the seasonality of the MLD in the LS and provides a good estimation of the shallower MLD (~ 200 m) with biases of only 8 meters deeper (Figure 28 in annex II; see small panel on the right). This latter outcome allows us to be more confident with the results of our analysis that only takes in consideration the spring bloom phase and the hydrographic conditions of the upper ocean (0-200 m).

Furthermore, it is worth remarking that role of other factors such as grazing pressure, nutrients and wind mixing that may also be significant drivers for the spring bloom timing were not explicit assessed in this paper. Holdsworth and Myers (2015) suggests that wind events are crucial to deep winter vertical mixing, through the role the wind plays in enhancing latent and sensible heat losses. Other authors suggest that wind events contribute less to winter vertical mixing (e.g., Ferrari et al., 2015). Recently, emphasizing the role of wind, Brody and Lozier (2014) predicted blooms to occur when negative heat fluxes weaken, and the mixing mechanism shifts from convection to wind. Certainly, the depth and intensity of the wind-driven mixing may become more important later in the season, because of the ability to entrain (i.e., by

eroding stratification) nutrients into the euphotic zone (Wu et al., 2008b).

Finally, it is becoming increasingly clear that not only the biological (i.e., top-down grazing pressure) and physical (i.e., bottom-up factors) external controls modulate phytoplankton dynamics but also phytoplankton adaptive qualities (i.e., plasticity) such as physiological rates, photo-adaptation to low light, nutrient kinetics, and grazing resistance are of fundamental importance in determining phytoplankton community structure and their dynamics (Gaedke et al., 2010; Lewandowska et al., 2015; Lindemann et al., 2015; Walter et al., 2014).

3.6 Conclusion

We have examined the inter-annual variability of phytoplankton spring blooms over the LS in response to different environmental factors (i.e., mixed-layer depth and air-sea heat fluxes). Our study using a biologically (i.e., exclusively based on the chlorophyll-a) regionalization has spatially characterized two distinct sub-regions with different phenological regimes. As a consequence, it was possible to recognize region-specific physical drivers for the spring bloom timing.

Our findings suggest that over the southern bioregion the end of wintertime convection nearly matches the timing of phytoplankton growth. More precisely, the initiation of the spring bloom coincides closely with the timing of the first shift from cooling to heating at the end of winter (i.e., when turbulent mixing becomes weak), possibly before significant shoaling of the mixed layer and the development of stable stratification. This is in opposition to blooms that occur in a thin layer near the surface (usually shallower than ~ 100 m). The change in sign of heat fluxes that typically precedes the mixed-layer shoaling may thus provide a more suitable indicator for the spring bloom initiation date over the southern bioregion. On the other hand, in the northern bioregion, the early onset of the spring bloom is related with the development

of stable stratification and precedes the cooling-to-heating shift in heat fluxes. As described above, this result is probably linked to the intrinsic characteristics of the northern bioregion. In this area, freshwater exchanges may eventually suppress vertical mixing while the air-sea fluxes are still negative. It follows that the early shoaling of the mixed layer triggers the onset of the phytoplankton spring bloom.

The present study, focusing on the influence of turbulent convection on the timing of the spring bloom extended previous qualitative knowledge and provided a basin-wide picture of the spring bloom dynamics over the LS. The difference in spring bloom timing response across the two bioregions clearly indicate that interactions among phytoplankton dynamics and the physical environment may vary significantly at sub-regional spatial scales and as a function of the dominant forcing mechanism. Overall, results contain useful information on the bioregion-dependent phytoplankton bloom dynamics and therefore give an indication of the sensitivity of phytoplankton growth to the physical complexity and heterogeneity of the pelagic ecosystem within the LS basin. Future work will however need to better disentangle sub-regional variability of the physical mechanisms controlling the phytoplankton bloom phenology in the LS. In this connection, long time series of biogeochemical *in situ* measurements, as those collected by the growing network of Bio-Argo floats (<http://biogeochemical-argo.org/>), will no doubt be even more of significant help to complement satellite observations and simulated bio-physical parameters.

Acknowledgements

Ocean-color satellite data were made available by the European Space Agency's GlobColour project (<http://www.globcolour.info>). The Argo (Array for Real Time Geostrophic Oceanography) data were collected and made freely available by the International Argo Program and the national programs that contribute to it (<http://www.argo.ucsd.edu>).

[//www.argo.ucsd.edu](http://www.argo.ucsd.edu);<http://argo.jcommops.org>). The Argo Program is part of the Global Ocean Observing System. Bathymetry was extracted from the General Bathymetric Chart of the Oceans, version 2014 (<http://www.gebco.net>). CMC-GDPS atmospheric forcing fields used in our simulation were made available by Environment and Climate Change Canada. This study was supported by grants from ArcticNet (Network of Centres of Excellence of Canada) (grant to S.B.) the Natural Sciences and Engineering Research Council of Canada (NSERC) (355774 to S.B.; 04357 to P. M.) and Université du Québec à Rimouski (to S.B. and C.M.). This is a contribution to Québec-Océan and VITALS (Ventilation, Interactions and Transports Across the Labrador Sea; grant number 433898) research programs.

CHAPITRE 4

ANOMALOUS MESOSCALE ACTIVITY LEADS TO MASSIVE PHYTOPLANKTON SPRING BLOOM IN THE LABRADOR SEA

Article in preparation

Christian Marchese¹, Laurent Oziel², Igor Yashayaev³, Simon Bélanger¹

¹Université du Québec à Rimouski, Département de biologie, chimie et géographie, 300 allée des Ursulines, Rimouski (Québec), G5L 3A1 Canada

²Takuvik Joint International Laboratory, Université Laval, Pavillon Alexandre-Vachon, 1045 av. de la Médecine, Québec G1V 0A6 Canada

³Fisheries and Oceans Canada, Bedford Institute of Oceanography, 1 Challenger Dr, Dartmouth (Nova Scotia), B2Y 4A2 Canada

4.1 Résumé

La mer du Labrador subit à la fois d'intenses efflorescences printanières et de profondes convections hivernales. Il en résulte, du fait de sa contribution significative au rabattement du CO₂ atmosphérique, que cette région s'avère d'une grande importance du point de vue biogéochimique. En mai 2015, l'efflorescence de phytoplancton printanière a été la plus forte enregistrée jusqu'ici en termes de magnitude et d'étendue grâce aux données satellitaires de la couleur de l'océan. Pour identifier les facteurs environnementaux en cause dans cet événement biologique exceptionnel, nous avons utilisé une combinaison d'observations par satellite et in situ, et d'indices climatiques. Or l'année 2015 a été caractérisée par un régime d'oscillation nord-atlantique (NAO) très élevé qui a mené à des conditions hivernales plus froides que la normale et à l'une des plus profondes convections observées. Une augmentation d'énergie cinétique sans précédent a alors succédé à ces rares conditions hivernales relevées dans tout le bassin intérieur de la mer du Labrador, probablement en raison du nombre élevé de caractéristiques dynamiques de type turbulence. Le bilan est clair : l'intense et étendue efflorescence de 2015 suit une période de convection profonde et correspond à une phase d'énergie cinétique maximale. La convection hivernale peut ainsi jouer un rôle majeur dans l'approvisionnement nutritif au cours du préconditionnement de l'efflorescence printanière. Les observations suggèrent que le taux d'énergie cinétique élevé est l'élément clé d'une productivité saisonnière accrue. En effet, des processus à méso-échelles ont pu augmenter la stratification printanière, et ainsi la productivité de tout le bassin du Labrador. Plus généralement, les résultats démontrent que la poussée phytoplanctonique massive de 2015 a été fortement favorisée par une période d'anomalies océanographiques temporaire ressentie dans tout le bassin du Labrador.

Mots clés : efflorescence phytoplanctonique, forçage physique, convection profonde, activité tourbillonnaire, mer du Labrador

4.2 Abstract

The Labrador Sea (LS) experiences intense spring phytoplankton blooms following deep winter convection events. As a consequence, due to its large contribution to the drawdown of atmospheric CO₂, the LS is a region of great biogeochemical importance. In May 2015, the spring phytoplankton bloom was by far the most intense in term of magnitude and area ever observed throughout the LS by satellite ocean color data. Here we use a combination of satellite-derived data, climate indices and in situ observations to identify environmental factors responsible for this exceptional biological event. The year 2015 was characterized by a highly positive NAO regime that lead to colder than usual winter conditions and to one of the deepest winter convection event on record. These exceptional winter conditions were followed by an unprecedented kinetic energy increase over the interior LS basin, due to an enhanced number of eddy-like dynamic features. The balance of evidence suggests that the intense and widespread 2015 spring phytoplankton bloom follows a deep convection period and coincides with the phase of maximum kinetic energy. Winter convection may play a key role in supplying nutrients during the preconditioning period of the spring bloom. Observations suggest that the high level of eddy kinetic energy to be key in the seasonal increase of primary production. Mesoscale processes may have enhanced the springtime restratification and thus the productivity of the whole LS basin. Overall, results provide evidence of how the massive 2015 phytoplankton bloom was actively promoted by a temporary period of anomalous oceanographic conditions over the LS basin.

Keywords: Phytoplankton bloom, deep convection, eddy kinetic energy, Labrador Sea

4.3 Introduction

High-latitude oceans usually harbor highly productive springtime phytoplankton blooms (Siegel et al., 2002). The high levels of phytoplankton biomass and primary production that occur during these blooms strongly contribute to the global photosynthetic fixation and export of carbon to the deep ocean (Daniels et al., 2015). The Labrador Sea (LS, hereafter), a sub-polar sea that connects the North Atlantic with the Arctic Ocean, represents not only an ocean "sink" region for atmospheric carbon dioxide, but also a marine region with a highly variable biological production and a pronounced seasonal growth cycle of phytoplankton (Harrison et al., 2013). For instance, the LS is one of the few marine sites where the functioning of the pelagic ecosystem is subject to nutrient replenishment by the deepest mixing in the Northern Hemisphere (Frajka-Williams et al., 2009). Open-ocean deep convection, a key and physical process by which deep and intermediate waters are formed, is an annual event in the LS with a high degree of inter-annual variability (Yashayaev and Loder, 2016). Profiling floats reveal convection reaching depths of more than 800-1000 m or even greater than 1500 m during some years (Yashayaev and Loder, 2017). In the LS, deep winter convection contributing to the Atlantic meridional overturning circulation (AMOC) makes this marine site a "hotspot" for the global climate system (Våge et al., 2009; Yashayaev et al., 2015). The main factor controlling convection events is the atmospheric forcing (e.g., cooling and evaporation) of water column density. During winter conditions, extreme surface cooling and strong winds generate convective and wind-induced turbulence that deepen the mixed-layer depth (MLD) and entrain nutrients from the deep ocean to the euphotic zone (Severin et al., 2014). Low solar radiation and vertical mixing limit winter phytoplankton biomass accumulation in the water column, although a recent analysis shows positive phytoplankton growth starting in winter (Lacour et al., 2017). However, the positive relationship between vertical mixing and nutrient concentrations creates favorable conditions for phytoplankton growth in spring and summer (Harrison

et al., 2013). The spring bloom phase thus initiates later in spring, when phytoplankton stock takes advantage of either the increase in light exposure or the winter nutrient pool (Siegel et al., 2002). Eventually, the bloom ends when the available amount of nutrients and the grazing pressure significantly limit its growth (Lacour et al., 2015). Occasionally, less intense summer phytoplankton blooms may be triggered by high wind events (i.e., storms) that entrain nutrients into the euphotic zone by eroding the surface stratification (Wu et al., 2008b).

In the North Atlantic, the distribution of bloom patterns has been studied extensively (see Friedland et al. 2016 and the references therein). Many studies have shown how environmental factors that modulate the phytoplankton dynamics are complex. Light and nutrients are modulated by a host of physical processes (Lindemann and St John, 2014). Recently, it has been suggested by Lacour et al. (2015) that, on a climatological scale, the first-order mechanism controlling the timing of the onset of the spring bloom over the LS is the light-mixing regime (i.e., the concomitant influence of surface light and mixing). The seasonal increase in light availability from the decrease in MLD modulates phytoplankton's time exposure to light, enhancing primary production. However, physical forcing may vary significantly within or between years and, in particular, unpredictable fluctuations (i.e., unusual but efficient mechanisms) may be of particular relevance to understanding bloom dynamics under climate change. For instance, an increased transport of meltwater from the Greenland ice sheet towards the northern and central LS may strongly influence circulation patterns, nutrient reservoirs and biogeochemical processes (Arrigo et al., 2017; Luo et al., 2016).

In this study, we provide evidence for the occurrence of a spectacular springtime phytoplankton bloom that is unprecedented in nearly 20-years of satellite observations over the LS basin. The 2015 spring bloom developed nearly simultaneously over nearly the whole LS reaching its maximum in mid-May. The oceanographic survey of the Atlantic Zone Off-Shelf Monitoring Program (AZOMP) annual survey of the Department

of Fisheries and Oceans (DFO) of Canada (Kieke and Yashayaev, 2015) confirmed the exceptional character of the phytoplankton bloom, which was largely dominated by the presence of *Phaeocystis sp.* (Schoemann et al., 2005). This intense bloom was preceded by exceptionally deep wintertime convection that occurred across the entire sub-polar gyre, driven by large oceanic heat loss (Fröb et al., 2016). More precisely, in the central LS during the 2014-2015, winter convection depths were among the deepest ones in the historical record (Yashayaev and Loder, 2016). The LS is considered an important atmospheric carbon dioxide sink and biogeochemical transitional zone between waters of the Arctic and the North Atlantic Oceans. Knowing therefore the role of the North Atlantic blooms in drawing down atmospheric CO₂, exporting carbon to the ocean interior and influencing the marine foodweb, the main objective of this study is to gain a better understanding of the possible mechanisms that stirred up the anomalous 2015 spring bloom. A combination of satellite-derived data, large-scale climate indices and in situ observations was therefore used to investigate whether unusual forcing events were responsible for the anomalous phytoplankton bloom.

4.4 Material and Methods

4.4.1 Satellite-derived data and eddy kinetic energy

Satellite-derived surface chlorophyll-a (Chl-a) data were used as a proxy to evaluate phytoplankton variability patterns in the LS basin. The level-3 mapped Chl-a data (units of mg/m³) were acquired at 4.6-km and 8-day resolution from the European Space Agency (ESA)'s Ocean Colour Climate Change Initiative Group (OC-CCI; <http://www.esa-oceancolour-cci.org>) for the period 1998-2015. The OC-CCI dataset is created by merging data from different satellite sensors (SeaWiFS, MERIS, MODIS and VIIRS) and by following a procedure to estimate per-pixel uncertainty (Belo Couto et al., 2016). Surface Chl-a concentrations are computed using the version 6 of the Ocean-

Colour-4 algorithm (OC4v6), an updated version of a four-band blue-green reflectance ratio empirical algorithm developed for SeaWiFS (O'Reilly et al., 2000). With respect to the use of a single satellite sensor, this method limits missing data (usually associated with cloud cover) by providing a greater spatial-temporal resolution and thus useful in climate change prediction studies.

Absolute Dynamic Topography (MADT) gridded data, extracted from the delayed time (DT) multi-mission (merging of TP/ERS-1/2, Jason-1/Envisat, and Jason-2/Envisat missions), were used to characterize the sea-level variability over the period 1998-2015. The MADT is routinely provided by the Archiving, Validation, and Interpretation of Satellite Oceanographic data program (AVISO; www.aviso.oceanobs.com) with a spatial resolution of ~ 25 km ($1/4^\circ$ latitude by $1/4^\circ$ longitude grid) and with 1-day temporal resolution. The data set is corrected for atmospheric attenuation, satellite orbit errors, sea-state and tidal influence (Ablain et al., 2009). To improve the reliability of the dataset, we excluded MADT values with error estimates (percentage of the signal variance) higher than 50%. However, errors were relatively small and typically below 10% of the signal variance. The eddy kinetic energy (EKE; unit: cm^2/s^2) time series (1998-2015) was derived from the processed MADT and calculated as:

$$EKE = \frac{1}{2} (U^2 + V^2) \quad (1)$$

where U and V are the zonal and meridional velocity components. Values of U and V are calculated as $-\left(\frac{g}{f}\right) \left(\frac{\partial h}{\partial y}\right)$ and $\left(\frac{g}{f}\right) \left(\frac{\partial h}{\partial x}\right)$ respectively, where g is gravity, f is the Coriolis parameter, and h is the MADT.

4.4.2 Large-scale climate indices

Along with the previous satellite datasets, climate indices, such as the North Atlantic Oscillation (NAO) and the Sub Polar Gyre (SPG-I), were also employed to investigate ecosystem changes. Both indices synthesize (being related to several physical elements) complex space and time climatic-weather variability into simple measures that may explain a significant portion of the local and/or regional variability in marine ecosystems. The NAO represents the dominant climate pattern in the North Atlantic region and refers to a north-south alternation in atmospheric mass between the subtropical Atlantic and the Arctic (Hurrell and Deser, 2010). Significant changes in ocean surface temperature and heat content, ocean currents and sea-ice cover in the Arctic and subarctic regions are also induced by changes in the NAO. The winter (December-March) NAO time series based on station sea level pressures was downloaded from the U.S. Global Climate Observing System (GCOS) website (http://www.esrl.noaa.gov/psd/gcos_wgsp/Time-series). In addition to the NAO index, the SPG-I (defined as the first principle component of the sea level anomaly in the North Atlantic; Berx and Payne 2017), a physical metric reflecting the strength and extent of the North Atlantic sub-polar gyre, was downloaded from the Marine Scotland Data web-platform (<http://data.marine.gov.scot>). The sub-polar gyre, a counter-clockwise rotating large body of relatively cold and low-saline subarctic water, is the dominant features of the surface circulation of the North Atlantic Ocean, which is subject to inter-annual and decadal variability. Positive values of SPG-I are associated with a strong sub-polar gyre circulation. In comparison, negative values of SPG-I are associated with a weak sub-polar gyre and westward retraction. Full details of the data processing and calculation of the SPG-I can be found in Berx and Payne (2017).

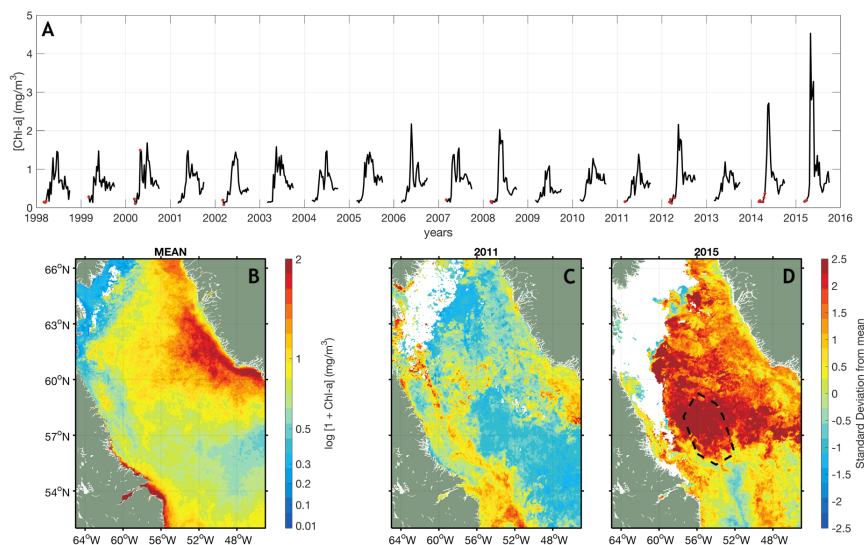


Figure 15: Temporal and spatial characterization of remotely sensed surface, chlorophyll-a concentration over the Labrador Sea. (a) Time-series (1998-2015) obtained from the mean of all chlorophyll-a values (in mg m^{-3}) available from eight-day composites of the Labrador Sea area between March 1998 and September 2015. Chlorophyll-a values (red dots) that were obtained from less than 30% of all pixels contained in the Labrador Sea area are also indicated. Maps showing (b) climatological (1998-2015) monthly mean of chlorophyll-a concentration for May; (c) monthly anomaly of chlorophyll-a for May 2011; and (d) monthly anomaly of chlorophyll-a for May 2015. In (d) the area of deepest mixing is indicated by the dashed black line.

4.5 Results and Discussion

In the global ocean, there are very few areas where ocean ventilation and atmospheric carbon dioxide sequestration occur. One of these locations, where surface water is exchanged with the deep and intermediate ocean, is the LS. In this area, deep convection efficiently transferring atmospheric gases and biogeochemical components (such as oxygen and inorganic and organic carbon) to the deep and intermediate waters contributes to the ventilation of the mesopelagic and bathypelagic layers. Furthermore,

during the winter season, deep convective mixing also injects nutrients to the surface ocean sustaining an increase in surface production (Severin et al., 2014).

In the LS, the phytoplankton spring bloom is a recurrent feature, but higher surface Chl-a concentrations have been recorded over the years (e.g., 2008, 2012, 2014) with stronger winter convection (Yashayaev and Loder, 2016). In May 2015, however, satellite observations showed concentrations of Chl-a to be among the highest values ever recorded for the LS basin (the 2015 bloom amplitude is over 4 mg m^{-3} ; Figure 15a). This extreme ocean manifestation occurred after two (2014 and 2015) deep ($> 1500 \text{ m}$) winter convection events (Yashayaev and Loder, 2016). On average, in May, the bloom (Figure 15b) reaches its maximum in the northern part ($> 60^\circ\text{N}$) of the basin, with higher values close to the Greenland coast. South of 60°N the spring bloom occurs later reaching its maximum in June (Frajka-Williams and Rhines, 2010; Lacour et al., 2015). Beside the climatological mean, Chl-a concentrations for the month of May 2011 and 2015 (Figure 15c and 15d) are shown for comparison. During May 2015, the spring bloom was extensively larger to nearly covering the entire basin. Compared to the year 2011 (Figure 15c), the 2015 spring bloom was particularly intense and a remarkable shift toward a pattern of positive anomaly in the phytoplankton biomass was clearly observable over the whole basin (Figure 15d; see also Figure 29 in annex III). In mid-May (17th to 24th of May), the surface area with Chl-a concentration greater than 5 mg m^{-3} and 10 mg m^{-3} reached as much as $\sim 620\,000 \text{ km}^2$ and $\sim 490\,000 \text{ km}^2$, respectively. For comparison, the 2015 bloom spatial extent was 3-fold greater than the 2014 bloom, which was also an exceptional year in the satellite time series (see Figure 15a). Conversely, the winter 2011 was characterized by relatively weak ($< 1000 \text{ m}$) convection (Yashayaev and Loder, 2016). That year, the bloom reached its maximum extent in early May (1st to 8th of May) with Chl-a concentration greater than 5 mg m^{-3} and 10 mg m^{-3} reaching only $162\,000 \text{ km}^2$ and $76\,000 \text{ km}^2$, respectively. The unusually high Chl-a concentration in May 2015 is also confirmed by comparison of *in situ* ARGO float measurements with those of May 2013 (see Figure 30 in annex III).

The winter (December-March) 2014-15 was much more severe than the previous winters in terms of ocean heat loss (Yashayaev and Loder, 2016). Since 2012, the NAO (excluding the 2013) has mostly been in a high positive phase, which was strongly positive in 2015, the highest one on record (~ 1.5 , Figure 16a). This is consistent with the fact that a positive phase is often linked to strong winter atmospheric cooling (i.e., heat loss) and deep convection (Yashayaev and Loder, 2009). Compared to previous winters, the 2014-2015 was exceptional in terms of winter heat loss and strong wind event occurrences (Piron et al., 2017). Although there is a good correlation ($r = 0.62$, $p < 0.01$) between convection depths and the NAO index (Figure 16b), preconditioning plays an important role in regulating convection depths and the NAO explains only a fraction of the regional atmospheric circulation variability (Våge et al., 2009). The convection in winter 2014-2015 was the fourth deep-water (~ 1650 m) formation event following those in winters 2007-2008 (~ 1545 m), 2011-2012 (~ 1290 m) and 2013-2014 (~ 1520 m) (Yashayaev and Loder, 2016). Although with certain exceptions, winter convection processes may enhance nutrient concentration in surface waters (Ólafsson, 2003). However, a recent analysis suggests that, rather than the depth reached by the convective mixing, the upper-ocean nutrient replenishment can also be determined by the convection area extension (Severin et al., 2014). During the winter 2014-2015 deep convection occurred over an incomparably wide region in the subpolar North Atlantic (Fröb et al., 2016; Piron et al., 2017). Strong winter cooling over the Labrador-Irminger Seas during the winter 2014-2015 might have elevated the nutrients concentrations over the LS basin. In this connection, a statistically significant ($r = 0.71$, $p < 0.01$) and positive correlation (Figure 16c) between the depths of the winter convection and the surface Chl-a (average from May to June) over the period 1998-2015 was found. A similar correlation ($r = 0.60$, $p < 0.01$; data not shown) was found between the depths of the winter convection and the Chl-a surface maxima. Recent observations show that nutrient concentrations in the Labrador Sea and Irminger Sea are highly correlated with the sub-polar gyre index (Hátún et al., 2017). During years characterized by

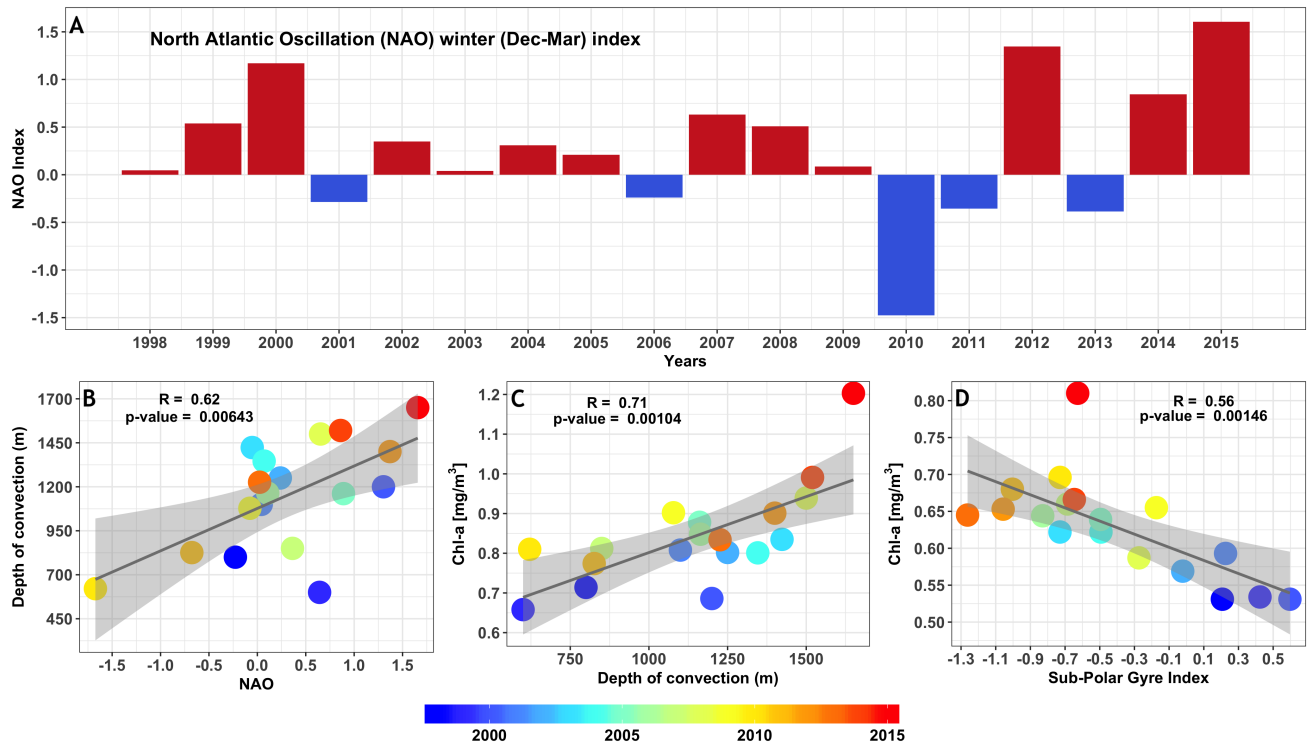


Figure 16: (a) Time-series of the winter (December to March average) of the NAO index. (b) Correlation between the NAO and the convection depths. (c) Correlation between the depths of the winter convection and the surface chlorophyll-a (area-averaged from May to June) over the period 1998-2015. (d) Correlation between the Sub-Polar Gyre Index (SPG-I) and the area-averaged surface chlorophyll-a between 1998 and 2015.

exceptional deep wintertime convection, the subpolar gyre expands. The SPG-I increased in 2014 and even more in 2015, reflecting thus the cold anomaly that developed the gyre-scale deep convection over the Labrador-Irminger Sea (Hátún *et al.*, 2017). Changes in the strength (and extent) of the sub-polar gyre, as characterized by the SPG-I, are correlated ($r = 0.56$, $p < 0.01$) with surface Chl-a concentrations (Figure 16d). Such a link has been reported previously suggesting that the sub-polar gyre dynamics may regulate phytoplankton abundance and higher trophic levels, but the exact mechanisms involved remain unknown (Hátún *et al.*, 2009). However, it is interesting to note that in both correlations (Figure 16c and 16d), the 2015 bloom stands out. These non-linear responses of the 2015 spring bloom suggest that other physical mechanisms may have fueled the exceptional increase in phytoplankton biomass. We speculate that highly anomalous hydrographic settings in the region may have created persistence of optimal bloom conditions throughout the LS basin.

In the LS, the altimetry-derived surface EKE is subject to significant inter-annual variations (Figure 17a). The most prominent feature of the EKE time series in the LS interior basin was the rise of spring EKE that started in 2014 and reached its maximum in 2015. The annual mean EKE (Figure 17b) field in the LS shows distinct sub-regional differences: kinetic energy is moderated over most of the basin with a maximum along the boundary current system (i.e., the West Greenland Current (WGC) and the Labrador Current (LC) flowing over the continental slope). In particular, a large EKE signal extends from the West Greenland coast into the interior of the Labrador Sea near 61-62°N: as the topography of the West Greenland slope steepens, the WGC becomes unstable generating significant EKE levels (Luo *et al.*, 2011). This is a well-known feature of the northern LS and has been the subject of numerous studies (Lilly *et al.*, 2003; Frajka-Williams and Rhines, 2010; Luo *et al.*, 2011, 2016; Gelderloos *et al.*, 2011). These studies indicate that mesoscale eddies, generated in the WGC area, may propagate southward into the central LS. Their presence over the central LS may thus speed up restratification process and as consequence minimize the time required for

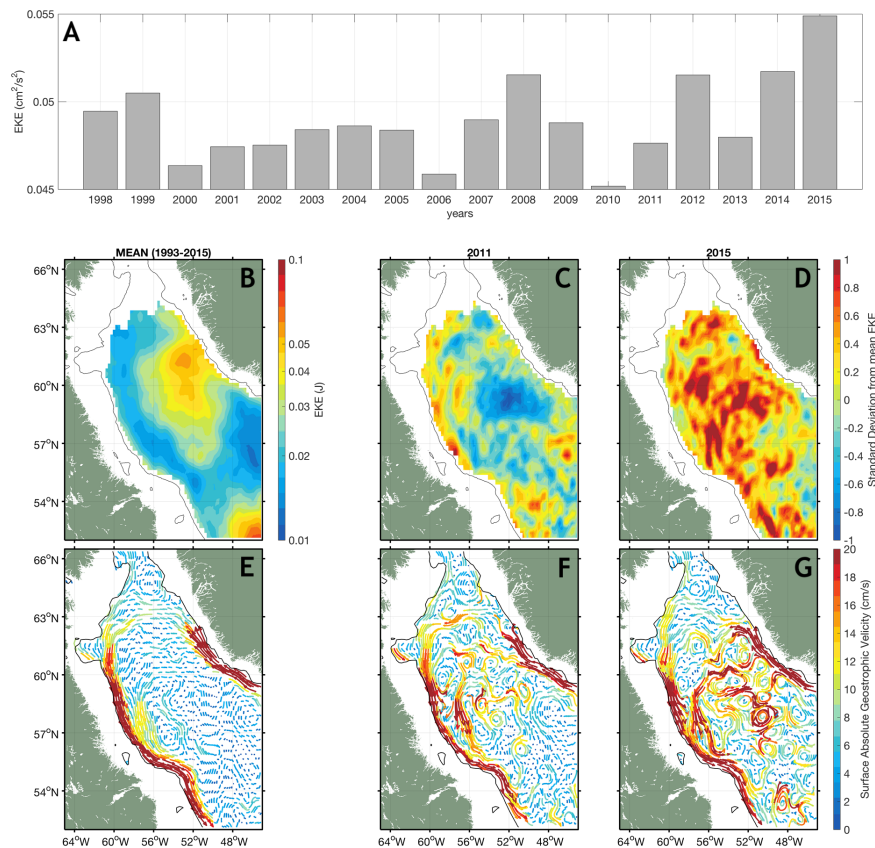


Figure 17: Temporal and spatial characterization of altimetry-derived surface EKE (Eddy Kinetic Energy) and absolute geostrophic velocities over the Labrador Sea. (a) Time-series of altimetry-derived EKE in the Labrador Sea averaged between April and May (spring), for the period 1998-2015. Maps showing (b) the climatological (1998-2015) mean distribution of surface EKE in the Labrador Sea; (c) monthly anomaly of EKE in spring 2011; (d) monthly anomaly of EKE in spring 2015; (e) absolute geostrophic velocities average (May 1st; 1993-2015); (f) absolute geostrophic velocities on May 1st 2015 and (g) 2011.

restratification (Lilly et al., 2003; Gelderloos et al., 2011). However, a recent analysis, suggests that the significant southward propagation only occurs when the EKE signal is very strong (Zhang and Yan, 2018). Beside the climatological mean (Figure 17b), the spring 2011 and the 2015 EKE anomalies (Figure 17c and 17d) are shown for comparison. It is apparent from the 2011 EKE map (Figure 17c), that except for the area along the Labrador continental slope the EKE signal was weak over most of the basin. A very different situation characterizes the year 2015: the EKE signal is weaker along the boundary current system but is significantly higher over the central basin (Figure 17d). The central LS is capable of generating its own eddies (i.e., convective eddies) that are usually linked to convection strength (Luo et al., 2011). The latter, was particularly strong during winters 2014 and 2015. Consequently, considerable contribution to the central LS EKE may be given by the activity of convective eddies (Zhang and Yan, 2018). Therefore, the large kinetic energy reservoir hosted in the central LS during spring 2015 points out a local change in circulation patterns and likely an intensification of the mesoscale dynamics. The near-surface surface absolute geostrophic velocities (mean state in Figure 17e), derived from the absolute dynamic topography that provide circulation maps, clearly show that as opposed to May 2011 (Figure 17f) a pronounced mesoscale eddy dynamic in May 2015 is present (Figure 17g).

Looking at the 2015 EKE seasonal cycle from the central LS basin (Figure 18), the peak of highest EKE is at the end of April- beginning of May, after the period of the convective season and in correspondence with the Chl-a maximum. Such an instantaneous increase in satellite-derived EKE levels in March-April has been previously reported by Brandt et al. (2004) in 1993-1995 and 1997 in the whole central LS. The authors, suggested that the enhanced EKE levels were largely generated by the collapse of the convective regime at the end of the convective season. In this study, a significant correlation ($r = 0.58$, $p < 0.01$; data not shown) was found between the 2015 seasonal cycles of EKE and Chl-a. On an inter-annual time scale (1998-2008), EKE was also shown to correlate with the bloom peak in the northern part of the LS (Frajka-Williams

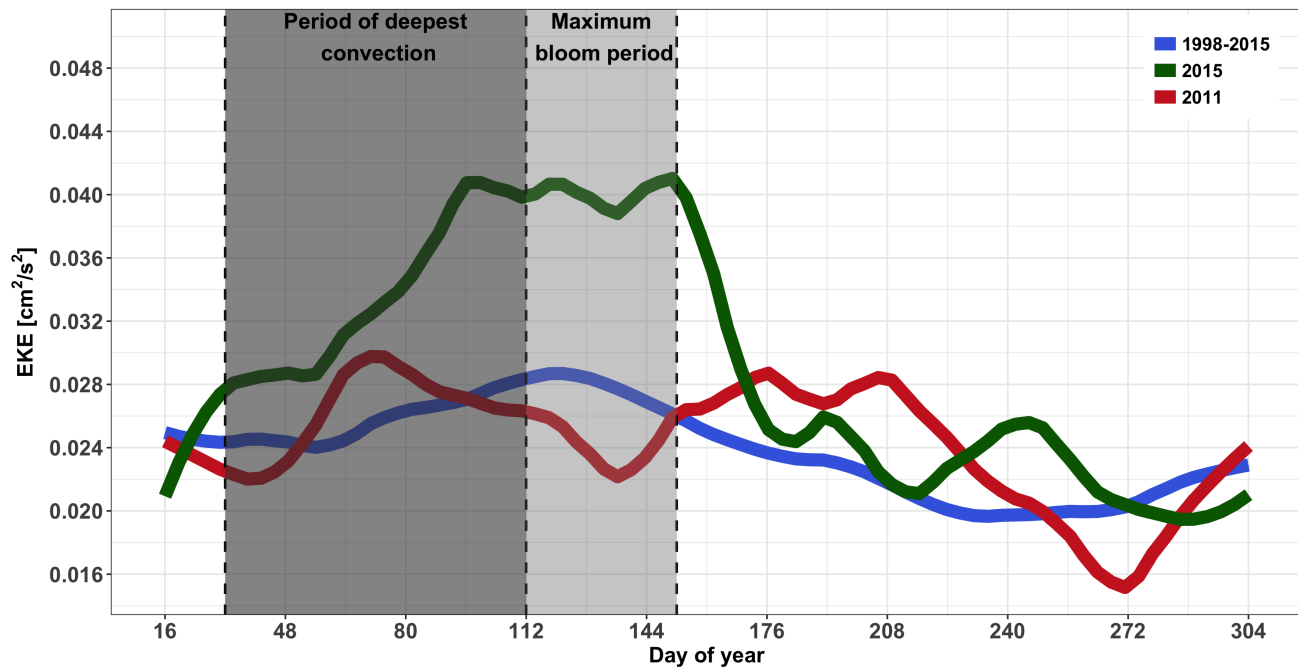


Figure 18: Eddy Kinetic Energy (EKE) seasonal cycle in the Labrador Sea for the years 2015 (green), 2011 (red) and the mean period (blue). The dark gray area indicates the period of deepest convection (February-April). The pale gray area indicates the bloom period (from late April to the end of May) over the year 2015. The 2015 spring bloom seems to coincide with a phase of increased eddy activity.

and Rhines, 2010). A similar correlation (for the period 1998-2015) was also found in this study ($r = 0.7$, $p < 0.01$; data not shown).

As previously reported, during May 2015, the surface Chl-a maximum coincides with a period of strongly enhanced kinetic energy signal (Figure 18), which is indicative of eddies structures which may have trigger the 2015 spring bloom. For instance, full resolution (750-m pixel) of Chl-a and sea surface temperature (SST) clearly show numerous small cyclonic eddies within the bloom area (Figure 19). According to the literature, the presence of cyclonic eddies seems unusual. For example, Lilly et al. (2003) documented 33 eddies in the Labrador Sea, out of which 31 were anticyclonic (downwelling core). However, although there is still much to learn about the propagation and contribution of the different eddy types to the restratification processes after deep convection (Chanut et al., 2008; Gelderloos et al., 2011), modeling and field studies (Brody et al., 2016; Mahadevan et al., 2012) have recently shown the importance of eddy-driven stratification in shaping the spring bloom onset over the North Atlantic. Moreover, sea-glider observations (Frajka-Williams et al., 2009) revealed that fluorescence (a reliable proxy for phytoplankton biomass) was elevated within and around several mesoscale eddies. Other in situ observations showed low-salinity and high-oxygen patterns during the passage of a single intense eddy (Körtzinger et al., 2008).

In conclusion, this study, provided evidence that the strong kinetic energy signal and its intra-seasonal variation might have had a large effect on the phytoplankton dynamic during spring 2015. Overall, observations suggest that the massive 2015 spring bloom was driven by a combination of two factors: (1) the gyre-scale deep convection over the Labrador-Irminger Sea that played a key role in supplying nutrient during the preconditioning period of the spring bloom and (2) the higher EKE level that enhanced the springtime restratification and thus the productivity of the whole LS basin. Yet, it should be noted that other mechanisms may also have been responsible for the 2015 bloom. In this respect, ongoing analysis of Argo profiles together with

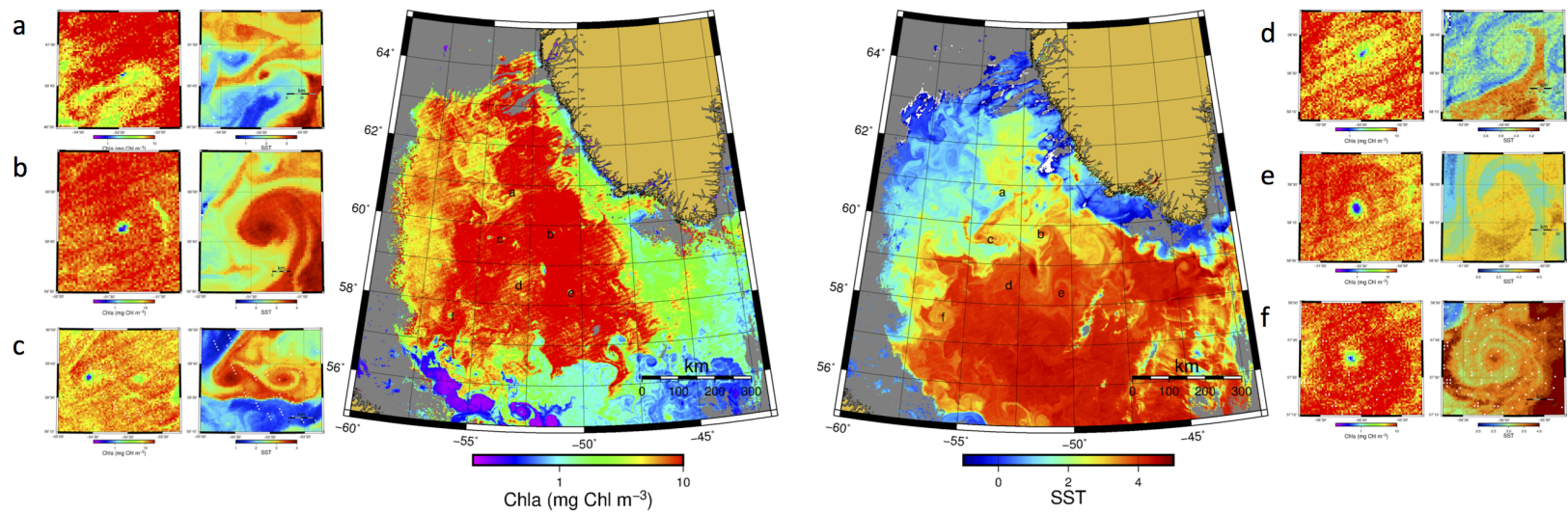


Figure 19: High-resolution images of chlorophyll-a (Chl-a) and Sea Surface Temperature (SST) the 17th of May 2015. On both sides, small boxes (from a to f) of Chl-a and SST show more in details some of the small cyclonic eddies within the bloom area.

Biogeochemical-Argo measurements and the cruise data collected as part of the 2015 AZOMP annual survey may reveal some additional clues to the causes of the anomalous bloom. Therefore, future work could confirm these proposed mechanisms using more detailed observations and also provide a better understanding of the importance of unusual and short-term environmental events.

Acknowledgements

The Ocean Colour Climate Change Initiative (OC-CCI) dataset (Version 3.1) was made available by the European Space Agency (<http://www.esa-oceancolour-cci.org/>). The altimetry-derived data were provided by AVISO/CNES and were accessible via their website (<https://www.aviso.altimetry.fr/en/data/data-access.html>). Biogeochemical-Argo data are freely available via ftp (<ftp://ftp.ifremer.fr/ifremer/argo/dac/coriolis>). This work is a contribution to Québec-Ocean and the VITALS (Ventilation, Interactions and Transports Across the Labrador Sea) research program.

CONCLUSION GÉNÉRALE

In a nutshell : context and originality

The Earth's climate is undergoing a major transformation. In particular, the Northern Hemisphere is probably experiencing some of the most visible and severe climate change. Scientific evidence for high-latitude climate warming is currently provided by observational and satellite studies that highlight changes in glaciers, sea-ice and snow-cover patterns. The progressive reduction of the sea-ice cover and the warming of the surface ocean layer are altering the physical, biogeochemical and biological linkages within the pelagic ecosystem. In particular, trends toward the earlier onset of seasonal sea-ice melt and increased duration of the annual melt season are going to limit the habitat range for cold-adapted biota and possibly alter the timing of trophic interactions in Arctic and sub-arctic marine food webs. All of these climate-related effects could potentially lead the Northern Hemisphere to reach a new state, with characteristics different than those observed previously. In the context of a "changing Arctic Ocean" there is therefore a need for an improved understanding of the biological-physical interactions.

High-latitude phytoplankton blooms are at the root of trophic interactions within food webs and play an important role in oceanic uptake of atmospheric carbon dioxide. In this regard, the research presented in this dissertation was primarily focused on identifying seasonal to inter-annual variations in phytoplankton phenology in two important and especially sensitive marine regions : the North Water (NOW) polynya (northern of Baffin Bay) and the Labrador Sea. The chapters presented in this dissertation each have an original aspect. Chapter 1 is the first comprehensive review on the general concept of biodiversity hotspots with a link to highly productive marine ecosystems. For instance, in pelagic ecosystems, phytoplankton blooms can be considered dynamic

biological hotspots because their timing and location dictate the life cycles and migration patterns of higher trophic levels. Chapter 2 is the first study to specifically monitor, by using seventeen years of remote-satellite data, changes in phytoplankton phenology in the NOW polynya. For this purpose, an improved interpolation scheme together with multiple Gaussian models was combined in a novel framework to capture the variability in bloom characteristics (i.e., onset, amplitude, duration). Chapter 3 presents a pertinent and objective regionalization of the Labrador Sea used to specifically test for the first time the shutdown of winter convective mixing (i.e., reduction in turbulent mixing caused by changes in the atmospheric forcing) as the most effective mechanism influencing the inter-annual variability of the spring bloom onset. Chapter 4 presents the first attempt to investigate whether unusual forcing events were responsible for the massive 2015-phytoplankton spring bloom, which occurred after two deep winter (2014 and 2015) convection events.

Overview : main findings, limitations and future directions

In this study, the main findings have mainly been achieved through the use of ocean-color observations together with various types of satellite data (e.g., wind speed and sea-ice concentration). A reason of strong interest for using remote sensing data in oceanography is its potential to allow the synoptic exploration (at high temporal and spatial resolution) of vast ocean regions. However, in high-latitude marine regions the use of ocean-color observations is not a straightforward task because missing data can affect the quality of phenology estimates (Cole et al., 2012; Brody et al., 2013). The optical complexity of seawater and the impact of sea-ice on remotely sensed reflectance (Bélanger et al., 2007, 2008) despite accounting for uncertainty in chlorophyll-a estimates, affect fewer phenological studies. Therefore, the presence of persistent clouds and fog remains the main limit to enabling resolution of timing of seasonal events with sufficient precision.

In Chapter 2, perhaps the most challenging aspect in providing the first quantitative investigation of the phenology of phytoplankton in the NOW polynya was dealing with missing data. One way to potentially minimize data gaps in ocean-color datasets is to use climatological values or relatively simple interpolation methods such as the linear or the nearest neighbour weighted method. However, such an approach may result in perturbations in the time-series by masking inter-annual variability. We addressed this issue by utilising a recently developed method ([Beckers and Rixen, 2003](#)) that fills data gaps by identifying the dominant spatial and temporal patterns. Finally, the interpolation scheme together with a multiple-Gaussian fitting approach was combined in a novel framework to examine phytoplankton phenological patterns. From an operational perspective, the framework proposed in this research allows us to encompass different shapes and concentration ranges in chlorophyll-a seasonal cycles and may therefore be extended to monitor inter-annual variability of phytoplankton seasonality in other Arctic and subarctic marine ecosystems with a pronounced seasonal growth cycle.

In Chapter 2, results clearly suggest that a combination of different environmental drivers strongly influences phytoplankton dynamics within the NOW polynya. In particular, results provide a local-scale assessment of the year-to-year variability in bloom timing : earlier blooms occur during years with warm temperatures and an earlier disappearance of sea-ice. Moreover, blooms last longer during years characterized by a longer open-water period and are shorter during those characterized by greater sea-ice coverage. In addition to the remarkable effects of temperature and sea-ice concentration, the work revealed the important contribution of wind vertical-mixing in modulating bloom phenology. For instance, the positive relationship between bloom magnitude and the frequency of wind-driven entrainment is consistent with the idea that when light is not limiting, wind mixing enhances nutrient input into the euphotic zone, leading to higher chlorophyll-a concentrations. In this regard, the decline in bloom amplitude during the seventeen years examined is also notable. The observed decline in biomass may thus reflect a stringent phytoplankton nutrient limitation due to changes

in stratification-destratification cycles during the productive period. However, this result must be considered keeping in mind that the relationship between variability in surface-layer chlorophyll-a and variability in subsurface chlorophyll-a maxima (a common feature in Arctic Ocean ; [Ardyna et al. 2013](#)) was not explicitly evaluated. Basically, the implicit assumption is that surface-layer chlorophyll-a variability reflects whole-water column variability. That being said, accounting for subsurface chlorophyll-a maxima, recent field observations in the north of Baffin Bay have shown a modification of the phytoplankton community structure (from large to small cells) and a sharp decline in phytoplankton biomass between 1999 and 2011 ([Blais et al., 2017](#)). All together these results emphasize the importance of different bottom-up processes in shaping phytoplankton phenology, community structure and regimes. Changes in phytoplankton community structure may influence carbon export and the transfer of energy through the NOW polynya food web structure. We suggest that this may be a fruitful and important area for future research. For instance, phytoplankton functional types (PFTs) satellite products are now being improved even more, validated ([Brewin et al., 2017](#); [Mouw et al., 2017](#)) and used for phenological studies ([Kostadinov et al., 2017](#)) although remain to be tested in the optically complex waters of the Arctic. However, it is well known that standing stocks of chlorophyll-a reflect the influence of both bottom-up processes and top-down effects. Grazing activity by zooplankton may therefore also contribute to changes in the patterns of bloom shape and dynamics ([Friedland et al., 2016](#)). Our analysis did not address this hypothesis and further work is needed to resolve the uncertainty about the impacts of grazing. To date, a relatively small number of studies focus on zooplankton phenology, especially in high-latitude marine ecosystems ([Ji et al., 2010](#)). Future work in this research line should specifically link zooplankton timing variability to changes in phytoplankton species composition and phenology.

Different approaches can be taken to further explore variability patterns and determine differences in phytoplankton phenology. In Chapter 3, the spatial distribution of the surface chlorophyll-a was characterized by a biogeographic analysis to spatially

identify bloom regions with similar phytoplankton seasonal cycles within the heterogeneous Labrador Sea basin. Basically, the spatial distribution of each bioregion is representative of a distinctive phenological regime. As a consequence, it was possible to identify region-specific physical environmental determinants for the bloom onset timing. The cross-region and inter-annual (a thirteen-year period was considered) analysis has delimited the boundaries of two distinct bioregions in the Labrador Sea : the north ($> 60^{\circ}\text{N}$) and the south ($< 60^{\circ}\text{N}$). South of 60°N , the bloom timing precedes the shoaling of the mixed layer depth and the vernal development of stratification. Specifically, in this area the bloom onset coincides closely with the timing of the first shift from cooling to heating at the end of winter. Conversely, north of 60°N , the bloom starts before heat fluxes become positive, hence no relation was found between the cooling-to-heating shift in air-sea heat flux and the bloom timing response. In particular, in this specific bloom region the early onset of the spring bloom was related to stratification and shoaling of the mixed-layer depth. Overall, findings suggest that in the southern bioregion (south of 60°N) the end of wintertime convection closely matches the timing of phytoplankton growth. In this bioregion the initiation of the spring bloom coincides closely with the timing of the first shift from cooling to heating at the end of winter (i.e., when turbulent mixing becomes weak), possibly before significant shoaling of the mixed layer and the development of stable stratification. In the northern bioregion (north of 60°N), the early onset of the spring bloom is related with the development of stable stratification and precedes the cooling-to-heating shift in heat fluxes. This result is probably linked to the intrinsic characteristics of the bioregion, where mesoscale processes may eventually suppress vertical mixing while the air-sea fluxes are still negative. To the best of our knowledge, these results were not reported previously for the study area. Furthermore, albeit in a more speculative way (since the analysis was restricted primarily to surface-layer chlorophyll-a) findings also support the disturbance-recovery hypothesis, which predicts a net increase in phytoplankton biomass due to a "dilution effect" during the deepening of the mixed-layer ([Behrenfeld and Boss, 2014](#)). In fact, although the results

clearly showed that the maximum surface phytoplankton growth rates may occur with the development of stable stratification in the northern bioregion or close with the cooling-to-heating shift in the southern bioregion, in both bioregion the growth rate starts to be positive earlier in the season.

Overall, results from Chapter 3 emphasize the view that the impact of the physical environment on biological processes can vary markedly between bioregions, thus providing a basin-wide picture of the complexity of bloom dynamics over the Labrador Sea. Interactions between phytoplankton and the physical environment are therefore expected to vary significantly depending on the intrinsic characteristics and/or geographical features of the marine region and the dominant forcing mechanism. In this regard, a parallelism can be done with the NOW marine ecosystem (Chapter 2). The ice bridge, which represents the northern extent of the NOW polynya, prevents sea ice from drifting southward into northern Baffin Bay and allows strong northerly winds to promote open-water conditions. The Smith Sound ice-arch failed to consolidate in 2009 but an ice-arch formed north of Kane Basin, preventing floes from reaching the NOW until late July (Vincent, 2013). This unique configuration, along with the higher sea surface temperature, led to the lowest sea-ice coverage over the NOW which consequently experienced unusual open-water conditions and an anomalously early and lasting bloom.

In Chapter 3, the boundaries of the two bloom regions were delimited by a biologically (i.e., exclusively based on the chlorophyll-a) regionalization. Perhaps, the main limitation of the method concerns the fact that the boundaries of the bioregions are fixed on a climatological basis and thus "static". In the pelagic zone, environmental variability can lead to the development of temporary periods of anomalous oceanographic and biological conditions that may step outside boundaries (see Chapter 4). Given this limitation, the bioregionalization, however, provides a framework that can be used in conjunction with models to further test hypotheses on the interactions between phytoplankton dynamics and climate forcing.

To end with, an interesting outcome of this study was the observed widespread and strong phytoplankton bloom throughout the Labrador Sea basin during May 2015. Two events occurred during 2015, which could have had the potential to promote the unusual bloom. The intense 2015 spring bloom occurred after a severe winter characterized by a high NAO regime and deep convection. Winter convection processes in the Labrador-Irminger Seas have been suggested to enhance biological production by bringing up nutrients from deep to euphotic layers. The convection in winter 2014-2015 was the fourth deep-water (~ 1650 m) formation event following those in winters 2007-2008 (~ 1545 m), 2011-2012 (~ 1290 m) and 2013-2014 (~ 1520 m). These exceptional winter conditions were followed by an unprecedented kinetic energy increase over the interior Labrador Sea basin, probably due to an enhanced number of eddy-like dynamic features. Mesoscale processes may play an important role in enhancing the seasonal restratification and thus primary production. The resulting picture is that the combined effect of these two key events may have stimulated the massive and unusual bloom. However, although phytoplankton bloom and diversity may be associated with regimes of instability and enhanced eddy kinetic energy (Clayton et al., 2013), this does not rule out the possibility that other factors may have contributed to fuel the sharp bloom in May 2015. For instance, the massive bloom may also have been influenced by reduced grazing pressure. Future research following up on these results from Chapter 4 should accurately resolve both mesoscale and intra-seasonal processes to better elucidate the causes of the anomalous bloom.

Finally, a partial limitation of this thesis arises from the use of traditional statistical approaches (i.e., regression and curve-fitting analyses). The latter, although useful to highlight links between environmental forcing and bloom dynamics, may fail to fully resolve the complex interactions within pelagic ecosystems. Therefore, a potential line of future research to explore mechanisms underlying changes in phytoplankton dynamics could be to use machine learning-based methods, such as the Random Forest (Breiman, 2001). In marine ecosystem studies, the use of machine-learning algorithms still remains

an unexplored area. Random Forest algorithms can cope with complex datasets, mixed data types, outliers and missing data. Furthermore, they offer a simple and powerful alternative to enable the detection of nonlinear relationships between environmental predictor and response variables. Finally, Random Forest models can provide measures of relative variable importance that can be used to further disentangle the effects of the individual environmental variables in shaping phytoplankton patterns.

To conclude, the phenological methods proposed in this study have been used to relate phytoplankton blooms to changes in the near-surface physical environment. Overall, the observations presented in this thesis provide valuable insight into the sensitivity of the phytoplankton seasonal cycle to environmental forcing. Findings suggest that a single mechanism for what drives spring blooms in high latitude marine ecosystems may be an oversimplification : often it is a combination of environmental variable changes that strongly influence phytoplankton bloom phenology. Furthermore, observations clearly show that phytoplankton dynamics can vary over relatively short distances. For instance, spurred on by a dominant forcing mechanism, interactions among phytoplankton dynamics and the physical environment may vary across sub-regional spatial scales. Finally, the biotic response can be different or even unexpected where local physical processes create a highly variable environment.

As a whole, the observations presented in this research emphasize the view that only a careful integration of satellite data, in situ time series, and model output can provide a solid basis upon which to explore the complexity of the phytoplankton dynamics. Moreover, to accurately understand the sensitivity of the pelagic ecosystem and related changes in phytoplankton phenology targeted and tailor-made observational programs must be conducted at spatiotemporal scales that are relevant for ecosystem dynamics and phytoplankton growth. Finally, the research reinforces the role of phytoplankton as a key biotic element for evaluating high-latitude marine ecosystem responses to climate change.

ANNEXE I

CHAPITRE 2 : MATÉRIEL SUPPLÉMENTAIRE

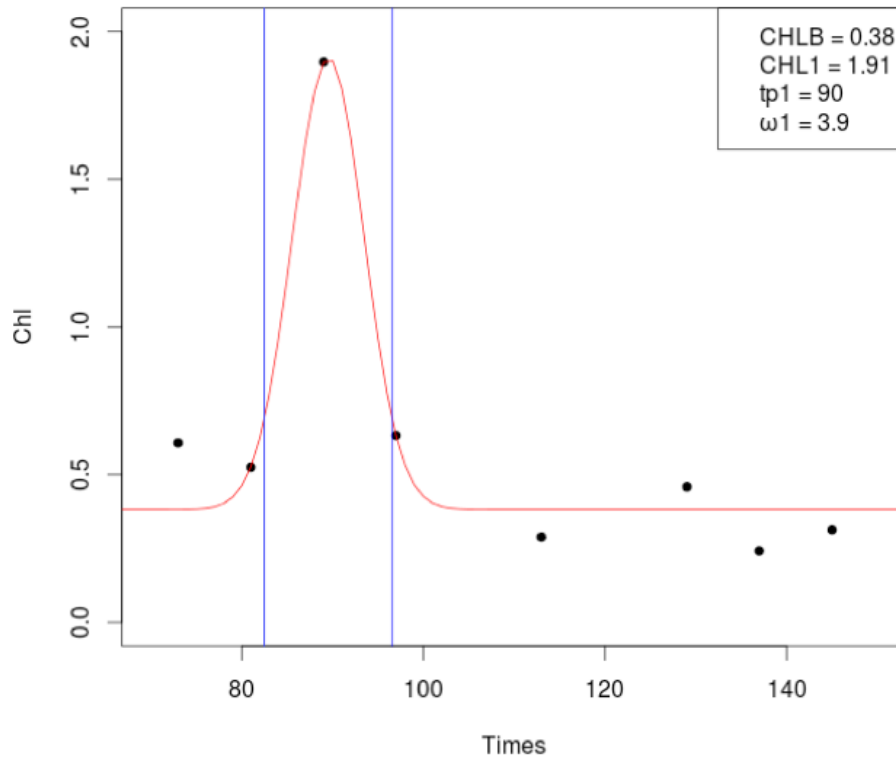


Figure 20: An example of fit. CHL_B (0.38 mg/m^3) corresponds to the background chlorophyll-a determined by the fitted function (red line). CHL_1 (1.91 mg/m^3) correspond to the peak amplitude, ω_1 is the standard deviation of the Gaussian curve and define the temporal width of the bloom, and tp_1 (day 90 of year) define the peak timing, i.e. the day of the year at which the maximum of bloom occurs. The bloom start is determined using a relative threshold : it is the date (day of the year) at which the fitted function reaches the threshold of 20% (blue line) of its maximum amplitude. The same criterion was used to define the bloom end in the downslope of the Gaussian curve. The time interval, represented in figure by the blue lines, gives the bloom duration (the difference between bloom end and bloom start).

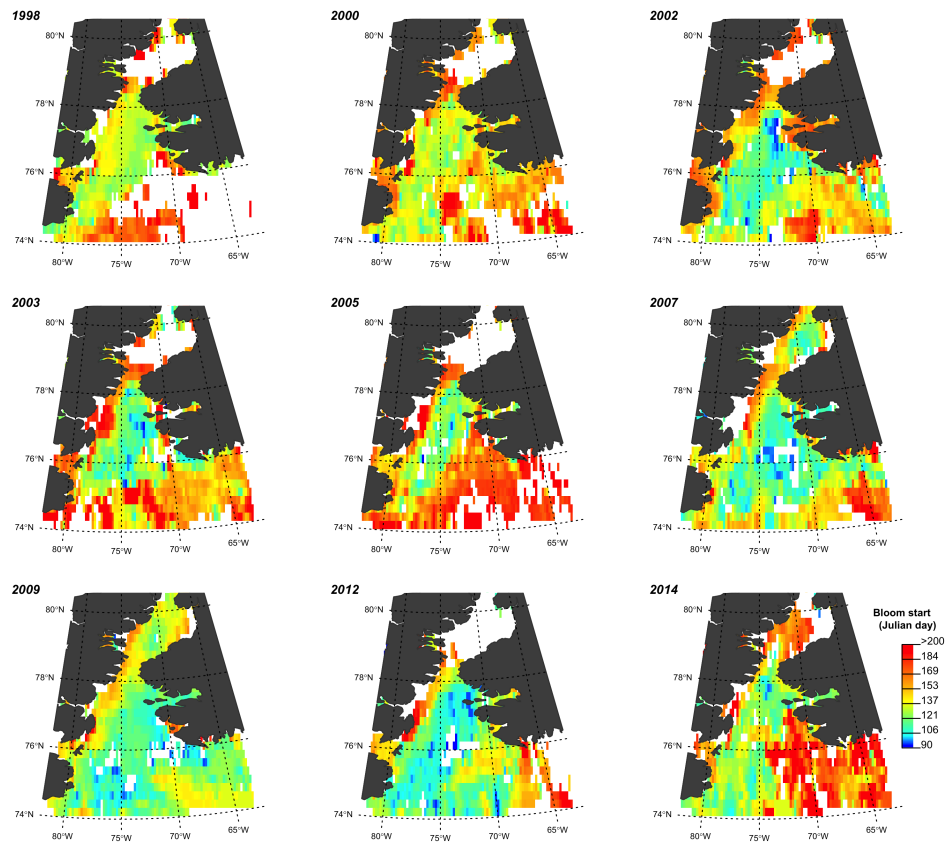


Figure 21: Bloom start phenology : inter-annual differences for selected years (1998-2000, 2002, 2003, 2005, 2007, 2009, 2012, 2014) over the study region. White areas represent pixels with low variability or persistent periods of missing data. Highest values are represented by the red color and lowest values by the blue color.

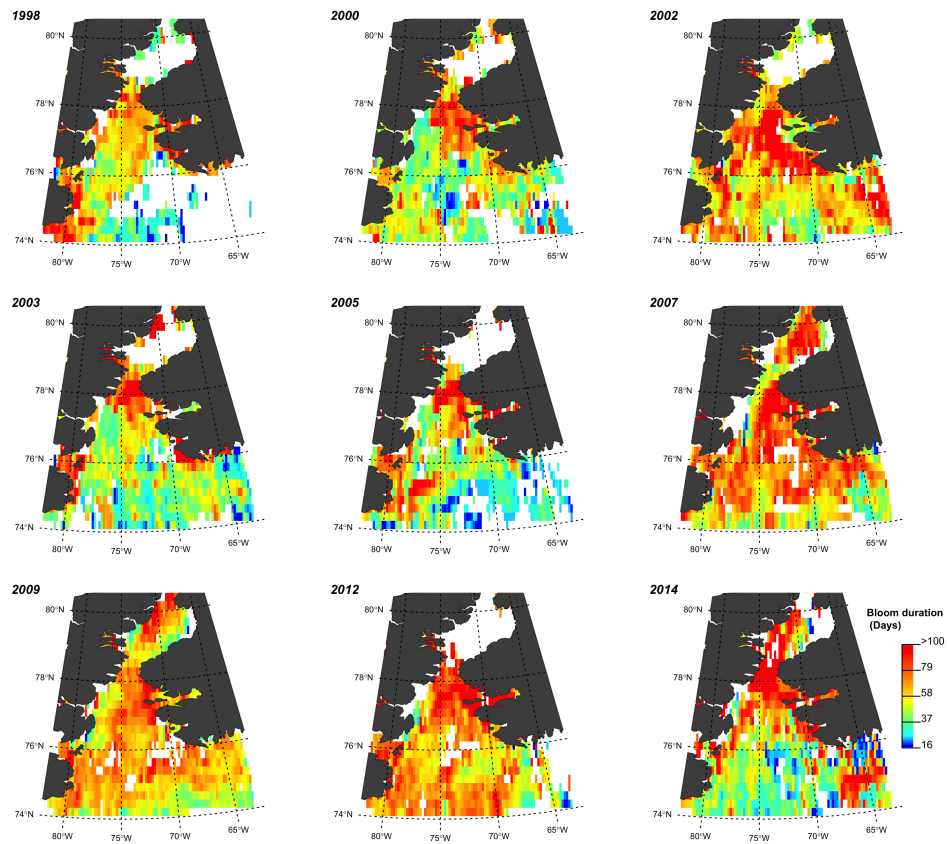


Figure 22: Bloom duration phenology : inter-annual differences for selected years (1998-2000, 2002, 2003, 2005, 2007, 2009, 2012, 2014) over the study region. White areas represent pixels with low variability or persistent periods of missing data. Highest values are represented by the red color and lowest values by the blue color.

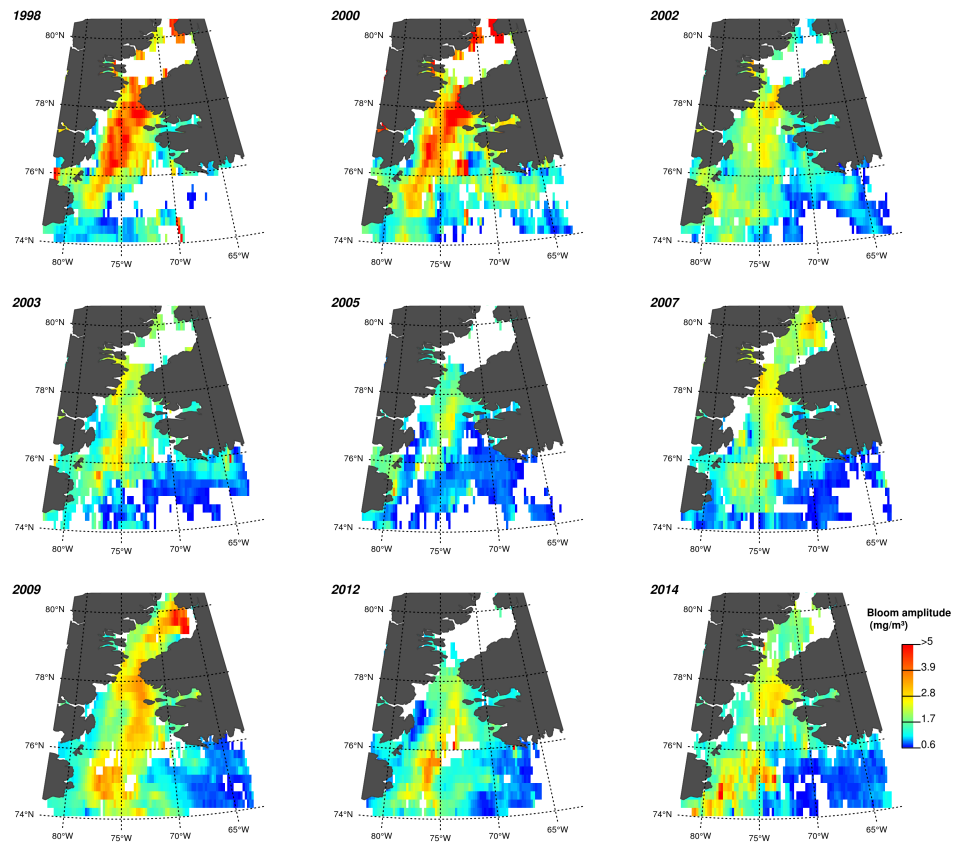


Figure 23: Bloom amplitude phenology : inter-annual differences for selected years (1998-2000, 2002, 2003, 2005, 2007, 2009, 2012, 2014) over the study region. White areas represent pixels with low variability or persistent periods of missing data. Highest values are represented by the red color and lowest values by the blue color

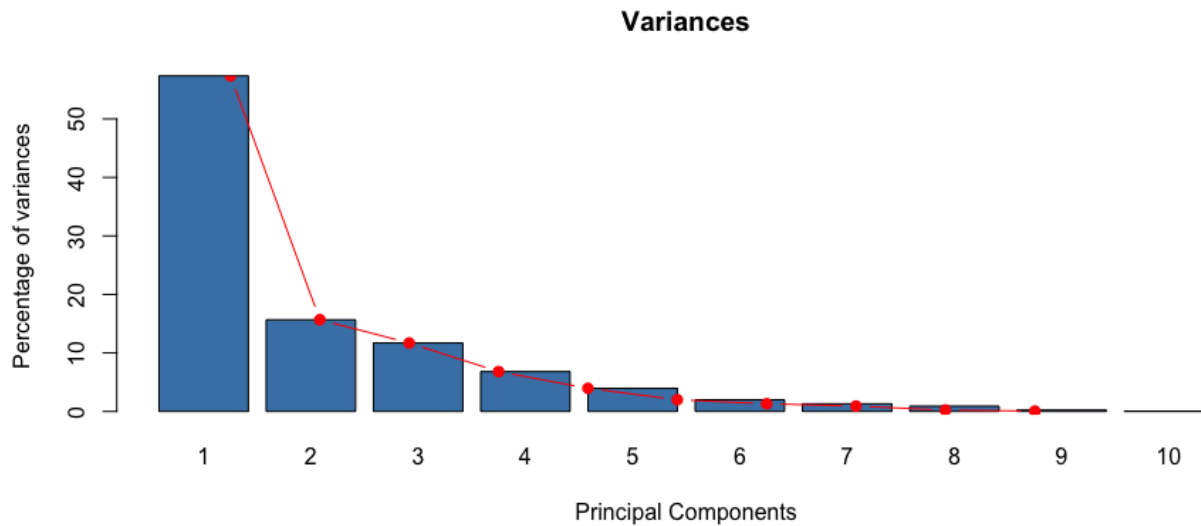


Figure 24: Plot of the proportion of variances (y-axis) explained by the components (x-axis) of annual change in phytoplankton phenology and physical parameters across the years (1998-2014). Based on this figure, we decided to retain 4 principal components and to focus only on the two most important that represent more than 70% of the proportion of variances (Axe 1 = 57.4%; Axe 2 = 15.7%)

ANNEXE II

CHAPITRE 3 : MATÉRIEL SUPPLÉMENTAIRE

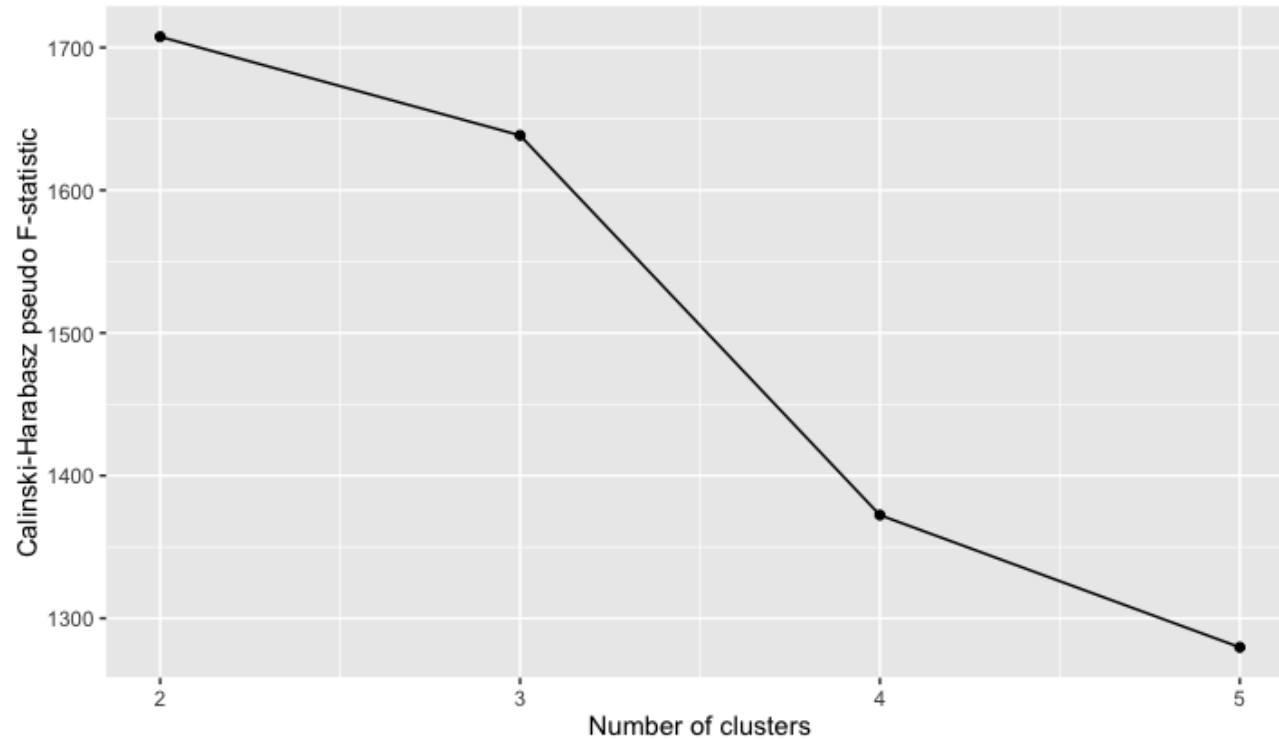


Figure 25: The Calinski-Harabasz index used to estimate the optimal number of cluster to bio-regionalize the Labrador Sea. The index measures the ratio between the dispersion of the observations (i.e., chlorophyll-a data) within a cluster and the dispersion between the clusters. The optimal clustering is the one with the highest value for the pseudo F-statistic.

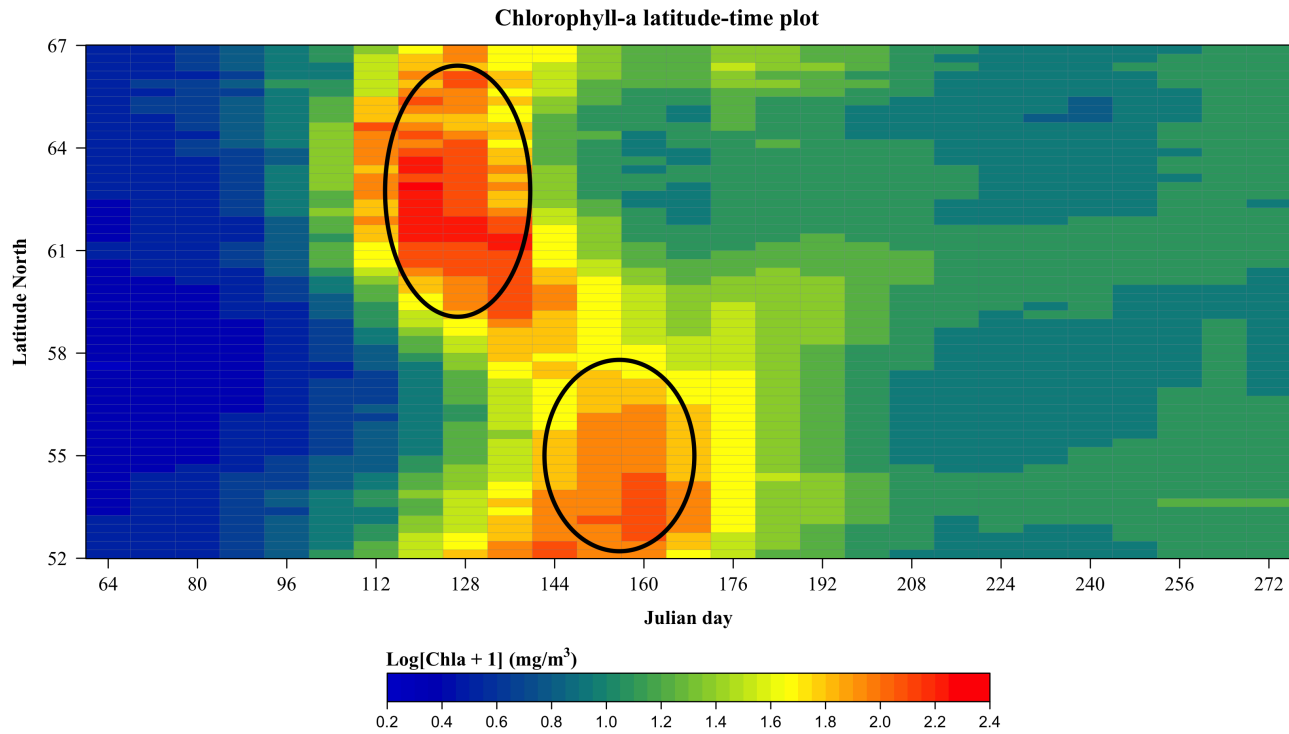
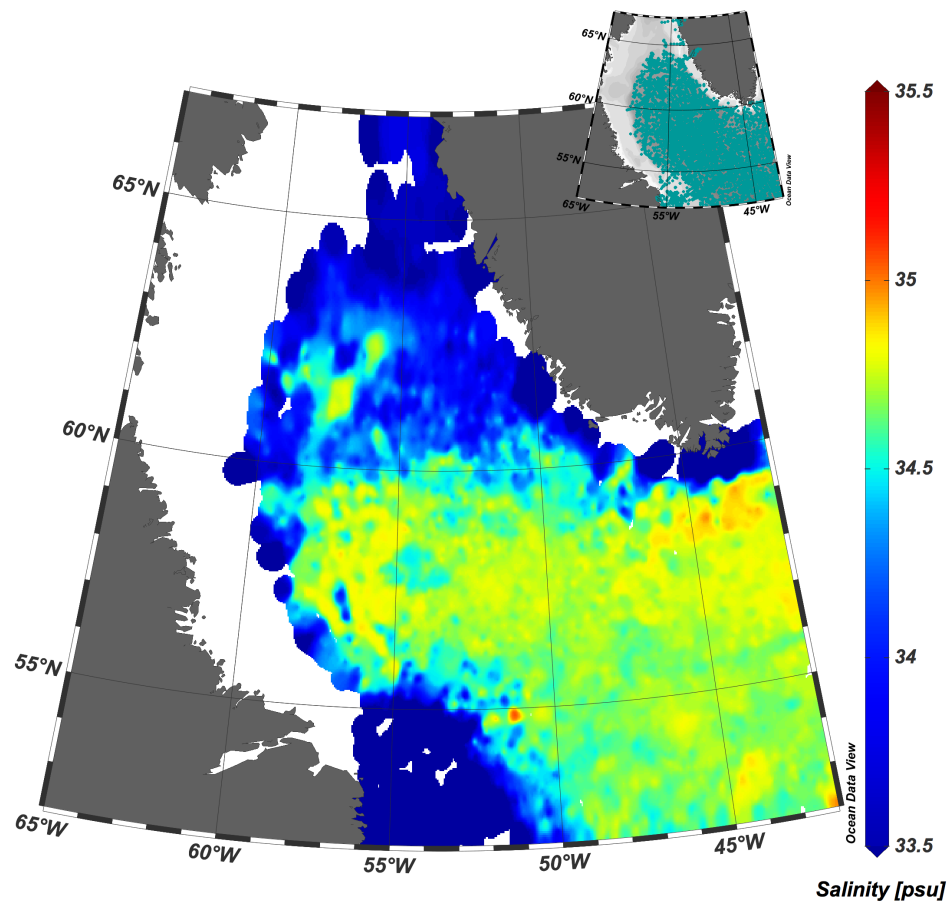


Figure 26: Hovmöller diagram used to plot the latitudinal evolution of the 10-days climatological (2002-2014) chlorophyll-a mean as function of the time over the Labrador Sea. Compared to the North Atlantic where blooms tend to follow the general south-to-north progression, the reversed pattern within the Labrador Sea represents a distinctive feature.



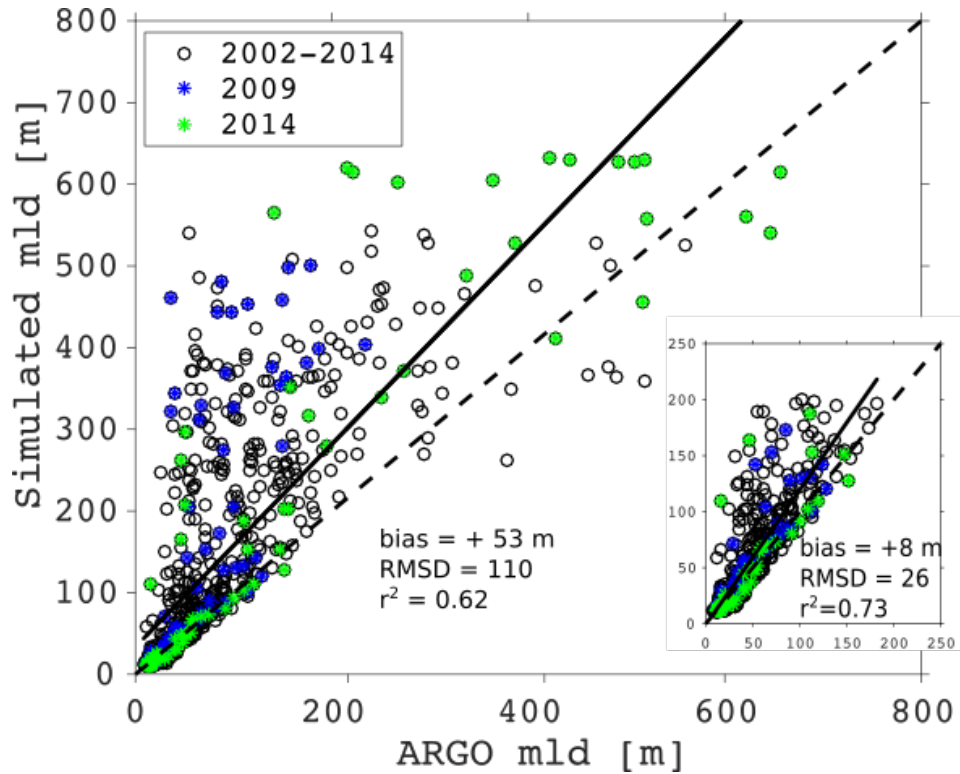


Figure 28: Scatter plot comparing the time-series of mean MLD computed with the ANHA4 configuration and ARGO-floats using the density criteria. The mean from ARGO-floats was computed when there were more than five floats available after outliers were removed. Outliers were defined as values being more than two standard deviations from the mean. The model represents relatively well the shallower MLD (<200 m) with biases of only 8 meters (small panel on the right).

ANNEXE III

CHAPITRE 4 : MATÉRIEL SUPPLÉMENTAIRE

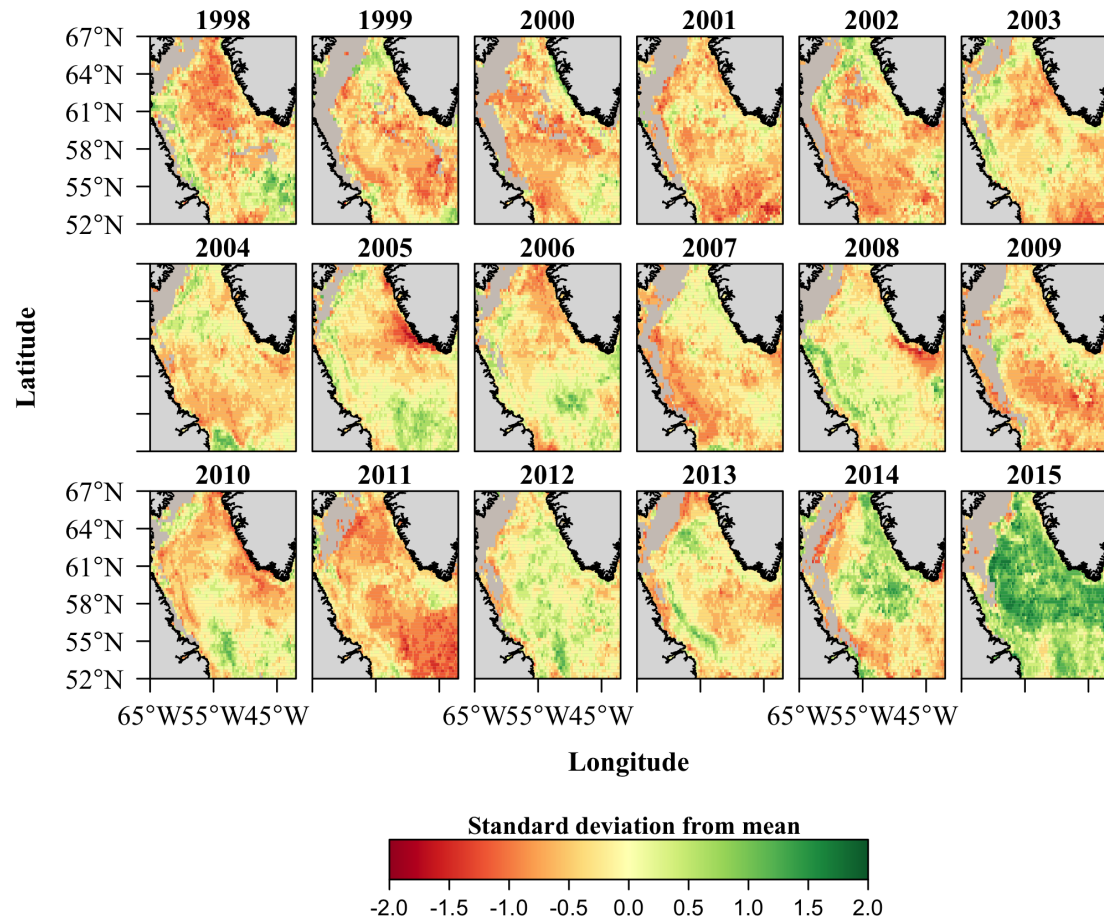


Figure 29: Standardized monthly anomalies maps of surface chlorophyll-a for the month of May over the period 1998-2015. Satellite data indicates elevated phytoplankton biomass in the Labrador Sea during May 2015 when compared to data for the eighteen-year period (1998-2015).

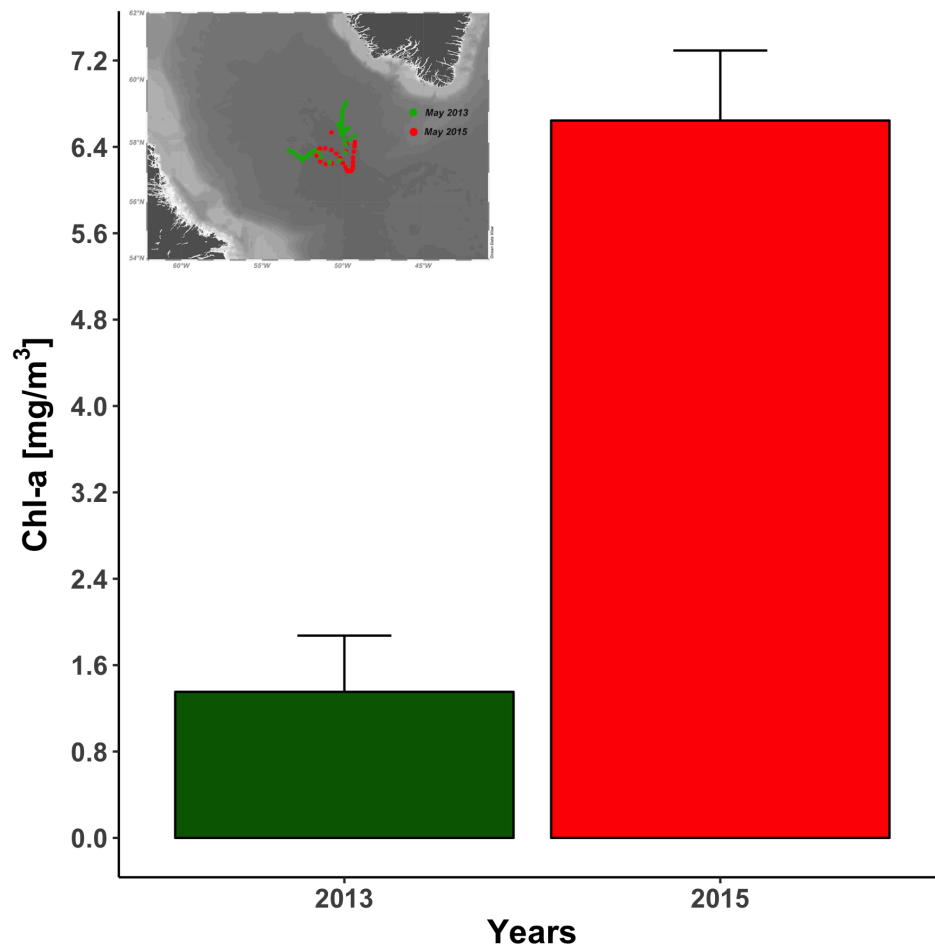


Figure 30: Depth-averaged (0-25 m) chlorophyll-a concentration in the central Labrador Sea derived from Biogeochemical-Argo (BGC-Argo) float measurements in May 2013 and 2015. The box in the upper left shows the free-drifting profiling floats position taken into account.

RÉFÉRENCES

- Ablain, M., Cazenave, A., Valladeau, G., Guinehut, S., 2009. A new assessment of the error budget of global mean sea level rate estimated by satellite altimetry over 1993-2008. *Ocean Science* 5 (2), 193–201.
- Alvera-Azcárate, A., Barth, A., Rixen, M., Beckers, J.-M., 2005. Reconstruction of incomplete oceanographic data sets using empirical orthogonal functions: application to the adriatic sea surface temperature. *Ocean Modelling* 9 (4), 325–346.
- Ardyna, M., Babin, M., Gosselin, M., Devred, E., Bélanger, S., Matsuoka, A., Tremblay, J.-É., 2013. Parameterization of vertical chlorophyll a in the arctic ocean: impact of the subsurface chlorophyll maximum on regional, seasonal, and annual primary production estimates. *Biogeosciences* 10 (6), 4383.
- Ardyna, M., Babin, M., Gosselin, M., Devred, E., Rainville, L., Tremblay, J.-É., 2014. Recent arctic ocean sea ice loss triggers novel fall phytoplankton blooms. *Geophysical Research Letters* 41 (17), 6207–6212.
- Ardyna, M., Claustre, H., Sallée, J.-B., D'Ovidio, F., Gentili, B., Dijken, G., D'Ortenzio, F., Arrigo, K. R., 2017. Delineating environmental control of phytoplankton biomass and phenology in the southern ocean. *Geophysical Research Letters* 44 (10), 5016–5024.
- Arrigo, K. R., Dijken, G. L., Castelao, R. M., Luo, H., Rennermalm, Å. K., Tedesco, M., Mote, T. L., Oliver, H., Yager, P. L., 2017. Melting glaciers stimulate large summer phytoplankton blooms in southwest greenland waters. *Geophysical Research Letters* 44 (12), 6278–6285.
- Arrigo, K. R., Perovich, D. K., Pickart, R. S., Brown, Z. W., Van Dijken, G. L., Lowry, K. E., Mills, M. M., Palmer, M. A., Balch, W. M., Bahr, F., et al., 2012. Massive phytoplankton blooms under arctic sea ice. *Science*, 1215065.
- Arrigo, K. R., Perovich, D. K., Pickart, R. S., Brown, Z. W., van Dijken, G. L., Lowry, K. E., Mills, M. M., Palmer, M. A., Balch, W. M., Bates, N. R., et al., 2014. Phytoplankton blooms beneath the sea ice in the chukchi sea. *Deep Sea Research Part II: Topical Studies in Oceanography* 105, 1–16.
- Arrigo, K. R., van Dijken, G., Pabi, S., 2008. Impact of a shrinking arctic ice cover on marine primary production. *Geophysical Research Letters* 35 (19).
- Arrigo, K. R., van Dijken, G. L., 2011. Secular trends in arctic ocean net primary production. *Journal of Geophysical Research: Oceans* 116 (C9).
- Arrigo, K. R., van Dijken, G. L., 2015. Continued increases in arctic ocean primary production. *Progress in Oceanography* 136, 60–70.

- Ateweberhan, M., Feary, D. A., Keshavmurthy, S., Chen, A., Schleyer, M. H., Sheppard, C. R., 2013. Climate change impacts on coral reefs: synergies with local effects, possibilities for acclimation, and management implications. *Marine pollution bulletin* 74 (2), 526–539.
- Babin, M., Bélanger, S., Ellingsen, I., Forest, A., Le Fouest, V., Lacour, T., Ardyna, M., Slagstad, D., 2015. Estimation of primary production in the arctic ocean using ocean colour remote sensing and coupled physical–biological models: strengths, limitations and how they compare. *Progress in Oceanography* 139, 197–220.
- Backhaus, J. O., Hegseth, E. N., Wehde, H., Irigoien, X., Hatten, K., Logemann, K., 2003. Convection and primary production in winter. *Marine Ecology Progress Series* 251, 1–14.
- Baird, A. H., Bellwood, D. R., Connell, J. H., Cornell, H. V., Hughes, T. P., Karlson, R. H., Rosen, B. R., 2002. Coral reef biodiversity and conservation. *Science* 296 (5570), 1026–1028.
- Balmford, A., Bruner, A., Cooper, P., Costanza, R., Farber, S., Green, R. E., Jenkins, M., Jefferiss, P., Jessamy, V., Madden, J., et al., 2002. Economic reasons for conserving wild nature. *science* 297 (5583), 950–953.
- Bamber, J., den Broeke, M., Ettema, J., Lenaerts, J., Rignot, E., 2012. Recent large increases in freshwater fluxes from greenland into the north atlantic. *Geophysical Research Letters* 39 (19).
- Barber, D., Hanesiak, J., Chan, W., Piwowar, J., 2001. Sea-ice and meteorological conditions in northern baffin bay and the north water polynya between 1979 and 1996. *Atmosphere-Ocean* 39 (3), 343–359.
- Barber, D. G., Massom, R. A., 2007. The role of sea ice in arctic and antarctic polynyas. *Elsevier Oceanography Series* 74, 1–54.
- Barnosky, A. D., Hadly, E. A., Bascompte, J., Berlow, E. L., Brown, J. H., Fortelius, M., Getz, W. M., Harte, J., Hastings, A., Marquet, P. A., et al., 2012. Approaching a state shift in earth’s biosphere. *Nature* 486 (7401), 52.
- Barton, A. D., Lozier, M. S., Williams, R. G., 2015. Physical controls of variability in north atlantic phytoplankton communities. *Limnology and Oceanography* 60 (1), 181–197.
- Bass, M. S., Finer, M., Jenkins, C. N., Kreft, H., Cisneros-Heredia, D. F., McCracken, S. F., Pitman, N. C., English, P. H., Swing, K., Villa, G., et al., 2010. Global conservation significance of ecuador’s yasuní national park. *PloS one* 5 (1), e8767.

- Beckers, J.-M., Rixen, M., 2003. Eof calculations and data filling from incomplete oceanographic datasets. *Journal of atmospheric and oceanic technology* 20 (12), 1839–1856.
- Behrenfeld, M. J., 2010. Abandoning sverdrup’s critical depth hypothesis on phytoplankton blooms. *Ecology* 91 (4), 977–989.
- Behrenfeld, M. J., Boss, E. S., 2014. Resurrecting the ecological underpinnings of ocean plankton blooms. *Annu. Rev. Mar. Sci.* 6, 167–94.
- Bélanger, S., Babin, M., Larouche, P., 2008. An empirical ocean color algorithm for estimating the contribution of chromophoric dissolved organic matter to total light absorption in optically complex waters. *Journal of Geophysical Research: Oceans* 113 (C4).
- Bélanger, S., Babin, M., Tremblay, J.-E., 2013a. Increasing cloudiness in arctic damps the increase in phytoplankton primary production due to sea ice receding. *Biogeosciences* 10 (6), 4087.
- Bélanger, S., Cizmeli, S., Ehn, J., Matsuoka, A., Doxaran, D., Hooker, S., Babin, M., 2013b. Light absorption and partitioning in arctic ocean surface waters: impact of multiyear ice melting. *Biogeosciences* 10 (10), 6433–6452.
- Bélanger, S., Ehn, J. K., Babin, M., 2007. Impact of sea ice on the retrieval of water-leaving reflectance, chlorophyll a concentration and inherent optical properties from satellite ocean color data. *Remote Sensing of Environment* 111 (1), 51–68.
- Bellard, C., Bertelsmeier, C., Leadley, P., Thuiller, W., Courchamp, F., 2012. Impacts of climate change on the future of biodiversity. *Ecology letters* 15 (4), 365–377.
- Bellard, C., Leclerc, C., Courchamp, F., 2014a. Impact of sea level rise on the 10 insular biodiversity hotspots. *Global Ecology and Biogeography* 23 (2), 203–212.
- Bellard, C., Leclerc, C., Leroy, B., Bakkenes, M., Veloz, S., Thuiller, W., Courchamp, F., 2014b. Vulnerability of biodiversity hotspots to global change. *Global Ecology and Biogeography* 23 (12), 1376–1386.
- Bellwood, D. R., Hughes, T. P., Folke, C., Nyström, M., 2004. Confronting the coral reef crisis. *Nature* 429 (6994), 827.
- Belo Couto, A., Brotas, V., Mélin, F., Groom, S., Sathyendranath, S., 2016. Inter-comparison of oc-cci chlorophyll-a estimates with precursor data sets. *International Journal of Remote Sensing* 37 (18), 4337–4355.
- Bentamy, A., Grodsky, S. A., Carton, J. A., Croizé-Fillon, D., Chapron, B., 2012. Matching ascats and quikscats winds. *Journal of Geophysical Research: Oceans* 117 (C2).

- Bergeron, M., Tremblay, J.-É., 2014. Shifts in biological productivity inferred from nutrient drawdown in the southern beaufort sea (2003–2011) and northern baffin bay (1997–2011), canadian arctic. *Geophysical Research Letters* 41 (11), 3979–3987.
- Berke, S. K., Jablonski, D., Krug, A. Z., Valentine, J. W., 2014. Origination and immigration drive latitudinal gradients in marine functional diversity. *PLoS One* 9 (7), e101494.
- Berteaux, D., Blois, S. d., Angers, J.-F., Bonin, J., Casajus, N., Darveau, M., Fournier, F., Humphries, M. M., McGill, B., Larivée, J., et al., 2010. The cc-bio project: studying the effects of climate change on quebec biodiversity. *Diversity* 2 (11), 1181–1204.
- Berx, B., Payne, M. R., 2017. The sub-polar gyre index—a community data set for application in fisheries and environment research. *Earth System Science Data* 9 (1), 259.
- Bhagabati, N. K., Ricketts, T., Sulistyawan, T. B. S., Conte, M., Ennaanay, D., Hadian, O., McKenzie, E., Olwero, N., Rosenthal, A., Tallis, H., et al., 2014. Ecosystem services reinforce sumatran tiger conservation in land use plans. *Biological Conservation* 169, 147–156.
- Blais, M., Ardyna, M., Gosselin, M., Dumont, D., Bélanger, S., Tremblay, J.-É., Gratton, Y., Marchese, C., Poulin, M., 2017. Contrasting interannual changes in phytoplankton productivity and community structure in the coastal canadian arctic ocean. *Limnology and Oceanography* 62 (6), 2480–2497.
- Bøhn, T., Amundsen, P.-A., 2004. Ecological interactions and evolution: Forgotten parts of biodiversity? *AIBS Bulletin* 54 (9), 804–805.
- Böning, C. W., Behrens, E., Biastoch, A., Getzlaff, K., Bamber, J. L., 2016. Emerging impact of greenland meltwater on deepwater formation in the north atlantic ocean. *Nature Geoscience* 9 (7), 523.
- Boss, E., Behrenfeld, M., 2010. In situ evaluation of the initiation of the north atlantic phytoplankton bloom. *Geophysical Research Letters* 37 (18).
- Bourgain, P., Gascard, J.-C., Shi, J., Zhao, J., 2013. Large-scale temperature and salinity changes in the upper canadian basin of the arctic ocean at a time of a drastic arctic oscillation inversion. *Ocean Science* 9 (2), 447.
- Bowen, B. W., Rocha, L. A., Toonen, R. J., Karl, S. A., et al., 2013. The origins of tropical marine biodiversity. *Trends in Ecology & Evolution* 28 (6), 359–366.
- Brandt, A., Griffiths, H., Gutt, J., Linse, K., Schiaparelli, S., Ballerini, T., Danis, B., Pfannkuche, O., 2014. Challenges of deep-sea biodiversity assessments in the southern ocean. *Advances in Polar Science* 25 (3), 204–212.

- Brandt, P., Schott, F. A., Funk, A., Martins, C. S., 2004. Seasonal to interannual variability of the eddy field in the labrador sea from satellite altimetry. *Journal of Geophysical Research: Oceans* 109 (C2).
- Breiman, L., 2001. Random forests. *Machine learning* 45 (1), 5–32.
- Brewin, R. J., Ciavatta, S., Sathyendranath, S., Jackson, T., Tilstone, G., Curran, K., Airs, R. L., Cummings, D., Brotas, V., Organelli, E., et al., 2017. Uncertainty in ocean-color estimates of chlorophyll for phytoplankton groups. *Frontiers in Marine Science* 4, 104.
- Brewin, R. J., Sathyendranath, S., Lange, P. K., Tilstone, G., 2014. Comparison of two methods to derive the size-structure of natural populations of phytoplankton. *Deep Sea Research Part I: Oceanographic Research Papers* 85, 72–79.
- Bring, A., Shiklomanov, A., Lammers, R. B., 2017. Pan-arctic river discharge: Prioritizing monitoring of future climate change hot spots. *Earth's Future* 5 (1), 72–92.
- Brody, S. R., Lozier, M. S., 2014. Changes in dominant mixing length scales as a driver of subpolar phytoplankton bloom initiation in the north atlantic. *Geophysical Research Letters* 41 (9), 3197–3203.
- Brody, S. R., Lozier, M. S., Dunne, J. P., 2013. A comparison of methods to determine phytoplankton bloom initiation. *Journal of Geophysical Research: Oceans* 118 (5), 2345–2357.
- Brody, S. R., Lozier, M. S., Mahadevan, A., 2016. Quantifying the impact of submesoscale processes on the spring phytoplankton bloom in a turbulent upper ocean using a lagrangian approach. *Geophysical Research Letters* 43 (10), 5160–5169.
- Brooks, T. M., Mittermeier, R. A., da Fonseca, G. A., Gerlach, J., Hoffmann, M., Lamoreux, J. F., Mittermeier, C. G., Pilgrim, J. D., Rodrigues, A. S., 2006. Global biodiversity conservation priorities. *science* 313 (5783), 58–61.
- Budikova, D., 2009. Role of arctic sea ice in global atmospheric circulation: A review. *Global and Planetary Change* 68 (3), 149–163.
- Burnham, K. P., Anderson, D. R., Huyvaert, K. P., 2011. Aic model selection and multimodel inference in behavioral ecology: some background, observations, and comparisons. *Behavioral Ecology and Sociobiology* 65 (1), 23–35.
- Butchart, S. H., Scharlemann, J. P., Evans, M. I., Quader, S., Arico, S., Arinaitwe, J., Balman, M., Bennun, L. A., Bertzky, B., Besancon, C., et al., 2012. Protecting important sites for biodiversity contributes to meeting global conservation targets. *PloS one* 7 (3), e32529.

- Butchart, S. H., Walpole, M., Collen, B., Van Strien, A., Scharlemann, J. P., Almond, R. E., Baillie, J. E., Bomhard, B., Brown, C., Bruno, J., et al., 2010. Global biodiversity: indicators of recent declines. *Science*, 1187512.
- Cadotte, M. W., Jonathan Davies, T., 2010. Rarest of the rare: advances in combining evolutionary distinctiveness and scarcity to inform conservation at biogeographical scales. *Diversity and Distributions* 16 (3), 376–385.
- Cadotte, M. W., Jonathan Davies, T., Regetz, J., Kembel, S. W., Cleland, E., Oakley, T. H., 2010. Phylogenetic diversity metrics for ecological communities: integrating species richness, abundance and evolutionary history. *Ecology Letters* 13 (1), 96–105.
- Caliński, T., Harabasz, J., 1974. A dendrite method for cluster analysis. *Communications in Statistics-theory and Methods* 3 (1), 1–27.
- Camathias, L., Bergamini, A., Küchler, M., Stofer, S., Baltensweiler, A., 2013. High-resolution remote sensing data improves models of species richness. *Applied Vegetation Science* 16 (4), 539–551.
- Campbell, J., Yeats, P., 1982. The distribution of manganese, iron, nickel, copper and cadmium in the waters of baffin-bay and the canadian arctic archipelago. *Oceanologica Acta* 5 (2), 161–168.
- Campbell, L. M., Norstrom, R. J., Hobson, K. A., Muir, D. C., Backus, S., Fisk, A. T., 2005. Mercury and other trace elements in a pelagic arctic marine food web (northwater polynya, baffin bay). *Science of the Total Environment* 351, 247–263.
- Cañadas, E. M., Fenu, G., Peñas, J., Lorite, J., Mattana, E., Bacchetta, G., 2014. Hotspots within hotspots: Endemic plant richness, environmental drivers, and implications for conservation. *Biological Conservation* 170, 282–291.
- Carranza, M. M., Gille, S. T., 2015. Southern ocean wind-driven entrainment enhances satellite chlorophyll-a through the summer. *Journal of Geophysical Research: Oceans* 120 (1), 304–323.
- Cavender-Bares, J., Kozak, K. H., Fine, P. V., Kembel, S. W., 2009. The merging of community ecology and phylogenetic biology. *Ecology letters* 12 (7), 693–715.
- Ceballos, G., Ehrlich, P. R., 2006. Global mammal distributions, biodiversity hotspots, and conservation. *Proceedings of the National Academy of Sciences* 103 (51), 19374–19379.
- Chanut, J., Barnier, B., Large, W., Debreu, L., Penduff, T., Molines, J. M., Mathiot, P., 2008. Mesoscale eddies in the labrador sea and their contribution to convection and restratification. *Journal of Physical Oceanography* 38 (8), 1617–1643.

- Chao, A., Chiu, C.-H., Hsieh, T., Davis, T., Nipperess, D. A., Faith, D. P., 2015. Rarefaction and extrapolation of phylogenetic diversity. *Methods in Ecology and Evolution* 6 (4), 380–388.
- Chassot, E., Bonhommeau, S., Reygondeau, G., Nieto, K., Polovina, J. J., Huret, M., Dulvy, N. K., Demarcq, H., 2011. Satellite remote sensing for an ecosystem approach to fisheries management. *ICES Journal of Marine Science* 68 (4), 651–666.
- Chernokulsky, A., Mokhov, I. I., 2012. Climatology of total cloudiness in the arctic: An intercomparison of observations and reanalyses. *Advances in Meteorology* 2012.
- Chiswell, S. M., 2011. Annual cycles and spring blooms in phytoplankton: don't abandon sverdrup completely. *Marine Ecology Progress Series* 443, 39–50.
- Clark, M., Rowden, A., Schlacher, T., Williams, A., Consalvey, M., Stocks, K., Rogers, A., O'Hara, T., White, M., Shank, T., et al., 2010. The ecology of seamounts: structure, function, and human impacts. *Annual Review of Marine Science* 2, 253–278.
- Clark, M. R., Rowden, A. A., Schlacher, T. A., Guinotte, J., Dunstan, P. K., Williams, A., O'Hara, T. D., Watling, L., Niklitschek, E., Tsuchida, S., 2014. Identifying ecologically or biologically significant areas (ebsa): a systematic method and its application to seamounts in the south pacific ocean. *Ocean & coastal management* 91, 65–79.
- Clayton, S., Dutkiewicz, S., Jahn, O., Follows, M. J., 2013. Dispersal, eddies, and the diversity of marine phytoplankton. *Limnology and Oceanography: Fluids and Environments* 3 (1), 182–197.
- Coello-Camba, A., Agustí, S., Vaqué, D., Holding, J., Arrieta, J. M., Wassmann, P., Duarte, C. M., 2015. Experimental assessment of temperature thresholds for arctic phytoplankton communities. *Estuaries and coasts* 38 (3), 873–885.
- Cole, H., Henson, S., Martin, A., Yool, A., 2012. Mind the gap: The impact of missing data on the calculation of phytoplankton phenology metrics. *Journal of Geophysical Research: Oceans* 117 (C8).
- Cole, H. S., Henson, S., Martin, A. P., Yool, A., 2015. Basin-wide mechanisms for spring bloom initiation: how typical is the north atlantic? *ICES Journal of Marine Science* 72 (6), 2029–2040.
- Comiso, J. C., Parkinson, C. L., Gersten, R., Stock, L., 2008. Accelerated decline in the arctic sea ice cover. *Geophysical research letters* 35 (1).
- Cook, J., Nuccitelli, D., Green, S. A., Richardson, M., Winkler, B., Painting, R., Way, R., Jacobs, P., Skuce, A., 2013. Quantifying the consensus on anthropogenic global warming in the scientific literature. *Environmental research letters* 8 (2), 024024.

- Cook, J., Oreskes, N., Doran, P. T., Anderegg, W. R., Verheggen, B., Maibach, E. W., Carlton, J. S., Lewandowsky, S., Skuce, A. G., Green, S. A., et al., 2016. Consensus on consensus: a synthesis of consensus estimates on human-caused global warming. *Environmental Research Letters* 11 (4), 048002.
- Corliss, B., Brown, C., Sun, X., Showers, W., 2009. Deep-sea benthic diversity linked to seasonality of pelagic productivity. *Deep Sea Research Part I: Oceanographic Research Papers* 56 (5), 835–841.
- Corredor-Acosta, A., Morales, C. E., Hormazabal, S., Andrade, I., Correa-Ramirez, M. A., 2015. Phytoplankton phenology in the coastal upwelling region off central-southern Chile (35° S–38° S): Time-space variability, coupling to environmental factors, and sources of uncertainty in the estimates. *Journal of Geophysical Research: Oceans* 120 (2), 813–831.
- Coupe, P., Ruiz-Pino, D., Sicre, M.-A., Chen, J., Lee, S., Schiffrine, N., Li, H., Gascard, J.-C., 2015. The impact of freshening on phytoplankton production in the Pacific Arctic Ocean. *Progress in Oceanography* 131, 113–125.
- Courtois, P., Hu, X., Pennelly, C., Spence, P., Myers, P. G., 2017. Mixed layer depth calculation in deep convection regions in ocean numerical models. *Ocean Modelling* 120, 60–78.
- Cowman, P. F., Bellwood, D. R., 2013. The historical biogeography of coral reef fishes: global patterns of origination and dispersal. *Journal of Biogeography* 40 (2), 209–224.
- Dai, A., Qian, T., Trenberth, K. E., Milliman, J. D., 2009. Changes in continental freshwater discharge from 1948 to 2004. *Journal of Climate* 22 (10), 2773–2792.
- Daily, G. C., Polasky, S., Goldstein, J., Kareiva, P. M., Mooney, H. A., Pejchar, L., Ricketts, T. H., Salzman, J., Shallenberger, R., 2009. Ecosystem services in decision making: time to deliver. *Frontiers in Ecology and the Environment* 7 (1), 21–28.
- Dalton, R., 2000. Biodiversity cash aimed at hotspots. *Nature* 406, 818.
- Daniels, C., Poulton, A. J., Mario, E., Paulsen, M. L., Bellerby, R., St John, M., Martin, A. P., 2015. Phytoplankton dynamics in contrasting early stage North Atlantic spring blooms: composition, succession, and potential drivers.
- Danovaro, R., Canals, M., Gambi, C., Heussner, S., Lampadariou, N., Vanreusel, A., 2009. Exploring benthic biodiversity patterns and hotspots on European margin slopes. *Oceanography* 22 (1), 16–25.
- Danovaro, R., Corinaldesi, C., D’Onghia, G., Galil, B., Gambi, C., Gooday, A. J., Lampadariou, N., Luna, G. M., Morigi, C., Olu, K., et al., 2010. Deep-sea biodiversity in the Mediterranean Sea: The known, the unknown, and the unknowable. *PLoS one* 5 (8), e11832.

- Danovaro, R., Gambi, C., Dell'Anno, A., Corinaldesi, C., Fraschetti, S., Vanreusel, A., Vincx, M., Gooday, A. J., 2008. Exponential decline of deep-sea ecosystem functioning linked to benthic biodiversity loss. *Current Biology* 18 (1), 1–8.
- Danovaro, R., Snelgrove, P. V., Tyler, P., 2014. Challenging the paradigms of deep-sea ecology. *Trends in ecology & evolution* 29 (8), 465–475.
- Daru, B. H., Bank, M., Davies, T. J., 2015. Spatial incongruence among hotspots and complementary areas of tree diversity in southern africa. *Diversity and Distributions* 21 (7), 769–780.
- Davies, T. J., Cadotte, M. W., 2011. Quantifying biodiversity: does it matter what we measure? In: *Biodiversity hotspots*. Springer, pp. 43–60.
- De Jong, M. F., Bower, A. S., Furey, H. H., 2016. Seasonal and interannual variations of iringer ring formation and boundary–interior heat exchange in flame. *Journal of Physical Oceanography* 46 (6), 1717–1734.
- Deardorff, J., 1983. A multi-limit mixed-layer entrainment formulation. *Journal of physical oceanography* 13 (6), 988–1002.
- Díaz, S., Fargione, J., Chapin III, F. S., Tilman, D., 2006. Biodiversity loss threatens human well-being. *PLoS biology* 4 (8), e277.
- Diehl, S., Berger, S. A., Soissons, Q., Giling, D. P., Stibor, H., 2015. An experimental demonstration of the critical depth principle. *ICES Journal of Marine Science* 72 (6), 2051–2060.
- Doney, S. C., Ruckelshaus, M., Duffy, J. E., Barry, J. P., Chan, F., English, C. A., Galindo, H. M., Grebmeier, J. M., Hollowed, A. B., Knowlton, N., et al., 2012. Climate change impacts on marine ecosystems. *Annu. Rev. Mar. Sci* 4, 4–1.
- D'Ortenzio, F., Antoine, D., Martinez, E., Ribera d'Alcalà, M., 2012. Phenological changes of oceanic phytoplankton in the 1980s and 2000s as revealed by remotely sensed ocean-color observations. *Global Biogeochemical Cycles* 26 (4).
- D'Ortenzio, F., Ribera d'Alcalà, M., 2009. On the trophic regimes of the mediterranean sea: a satellite analysis. *Biogeosciences* 6 (2), 139–148.
- Drinkwater, K. F., Beaugrand, G., Kaeriyama, M., Kim, S., Ottersen, G., Perry, R. I., Pörtner, H.-O., Polovina, J. J., Takasuka, A., 2010. On the processes linking climate to ecosystem changes. *Journal of Marine Systems* 79 (3-4), 374–388.
- Duffy, J. E., Amaral-Zettler, L. A., Fautin, D. G., Paulay, G., Rynearson, T. A., Sosik, H. M., Stachowicz, J. J., 2013. Envisioning a marine biodiversity observation network. *Bioscience* 63 (5), 350–361.

- Duke, J. M., Dundas, S. J., Messer, K. D., 2013. Cost-effective conservation planning: lessons from economics. *Journal of Environmental Management* 125, 126–133.
- Dukhovskoy, D. S., Myers, P. G., Platov, G., Timmermans, M.-L., Curry, B., Proshutinsky, A., Bamber, J. L., Chassignet, E., Hu, X., Lee, C. M., et al., 2016. Greenland freshwater pathways in the sub-arctic seas from model experiments with passive tracers. *Journal of Geophysical Research: Oceans* 121 (1), 877–907.
- Dumont, D., Gratton, Y., Arbetter, T. E., 2009. Modeling the dynamics of the north water polynya ice bridge. *Journal of Physical Oceanography* 39 (6), 1448–1461.
- Durant, S., Wachter, T., Bashir, S., Woodroffe, R., Ornellas, P., Ransom, C., Newby, J., Abáigar, T., Abdelgadir, M., El Alqamy, H., et al., 2014. Fiddling in biodiversity hotspots while deserts burn? collapse of the sahara’s megafauna. *Diversity and Distributions* 20 (1), 114–122.
- D’agata, S., Mouillot, D., Kulbicki, M., Andréfouët, S., Bellwood, D. R., Cinner, J. E., Cowman, P. F., Kronen, M., Pinca, S., Vigliola, L., 2014. Human-mediated loss of phylogenetic and functional diversity in coral reef fishes. *Current Biology* 24 (5), 555–560.
- Edwards, M., Richardson, A. J., 2004. Impact of climate change on marine pelagic phenology and trophic mismatch. *Nature* 430 (7002), 881.
- Elzhov, T. V., Mullen, K. M., Bolker, B., 2016. minpack.lm:r interface to the levenberg-marquardt nonlinear least-squares algorithm found in minpack. URL: <http://CRAN.R-project.org/package=minpack.lm>.
- Ferrari, R., Merrifield, S. T., Taylor, J. R., 2015. Shutdown of convection triggers increase of surface chlorophyll. *Journal of Marine Systems* 147, 116–122.
- Ferreira, A., Hátún, H., Counillon, F., Payne, M., Visser, A., 2015. Synoptic-scale analysis of mechanisms driving surface chlorophyll dynamics in the north atlantic. *Biogeosciences* 12 (11), 3641–3653.
- Ferreira, A. S., Visser, A. W., MacKenzie, B. R., Payne, M. R., 2014. Accuracy and precision in the calculation of phenology metrics. *Journal of Geophysical Research: Oceans* 119 (12), 8438–8453.
- Ferry, N., Parent, L., Garric, G., Barnier, B., Jourdain, N. C., et al., 2010. Mercator global eddy permitting ocean reanalysis glorys1v1: Description and results. *Mercator-Ocean Quarterly Newsletter* 36, 15–27.
- Fetterer, F., Knowles, K., Meier, W., Savoie, M., 2002. Sea ice index. boulder, colorado usa: National snow and ice data center. Digital media, updated 2009, 2002.

- Frajka-Williams, E., Rhines, P. B., 2010. Physical controls and interannual variability of the labrador sea spring phytoplankton bloom in distinct regions. *Deep Sea Research Part I: Oceanographic Research Papers* 57 (4), 541–552.
- Frajka-Williams, E., Rhines, P. B., Eriksen, C. C., 2009. Physical controls and mesoscale variability in the labrador sea spring phytoplankton bloom observed by seaglider. *Deep Sea Research Part I: Oceanographic Research Papers* 56 (12), 2144–2161.
- Frey, K. E., Perovich, D. K., Light, B., 2011. The spatial distribution of solar radiation under a melting arctic sea ice cover. *Geophysical Research Letters* 38 (22).
- Friedland, K. D., Record, N. R., Asch, R. G., Kristiansen, T., Saba, V. S., Drinkwater, K. F., Henson, S., Leaf, R. T., Morse, R. E., Johns, D. G., et al., 2016. Seasonal phytoplankton blooms in the north atlantic linked to the overwintering strategies of copepods. *Elem Sci Anth* 4.
- Fröb, F., Olsen, A., Våge, K., Moore, G., Yashayaev, I., Jeansson, E., Rajasakaren, B., 2016. Irminger sea deep convection injects oxygen and anthropogenic carbon to the ocean interior. *Nature communications* 7, 13244.
- Fujiwara, A., Hirawake, T., Suzuki, K., Imai, I., Saitoh, S.-I., 2014. Timing of sea ice retreat can alter phytoplankton community structure in the western arctic ocean. *Biogeosciences* 11 (7), 1705–1716.
- Gaedke, U., Ruhlenstroth-Bauer, M., Wiegand, I., Tirok, K., Aberle, N., Breithaupt, P., Lengfellner, K., Wohlers, J., Sommer, U., 2010. Biotic interactions may overrule direct climate effects on spring phytoplankton dynamics. *Global Change Biology* 16 (3), 1122–1136.
- Gambi, C., Pusceddu, A., Benedetti-Cecchi, L., Danovaro, R., 2014. Species richness, species turnover and functional diversity in nematodes of the deep mediterranean sea: searching for drivers at different spatial scales. *Global ecology and biogeography* 23 (1), 24–39.
- Gelderloos, R., Katsman, C. A., Drijfhout, S. S., 2011. Assessing the roles of three eddy types in restratifying the labrador sea after deep convection. *Journal of Physical Oceanography* 41 (11), 2102–2119.
- Ghosal, S., Mandre, S., 2003. A simple model illustrating the role of turbulence on phytoplankton blooms. *Journal of mathematical biology* 46 (4), 333–346.
- Gillard, L. C., Hu, X., Myers, P. G., Bamber, J. L., 2016. Meltwater pathways from marine terminating glaciers of the greenland ice sheet. *Geophysical Research Letters* 43 (20).

- Gillett, N. P., Stone, D. A., Stott, P. A., Nozawa, T., Karpechko, A. Y., Hegerl, G. C., Wehner, M. F., Jones, P. D., 2008. Attribution of polar warming to human influence. *Nature Geoscience* 1 (11), 750.
- González Taboada, F., Anadón, R., 2014. Seasonality of north atlantic phytoplankton from space: Impact of environmental forcing on a changing phenology (1998–2012). *Global change biology* 20 (3), 698–712.
- Grenyer, R., Orme, C. D. L., Jackson, S. F., Thomas, G. H., Davies, R. G., Davies, T. J., Jones, K. E., Olson, V. A., Ridgely, R. S., Rasmussen, P. C., et al., 2006. Global distribution and conservation of rare and threatened vertebrates. *Nature* 444 (7115), 93.
- Groetsch, P. M., Simis, S. G., Eleveld, M. A., Peters, S. W., 2016. Spring blooms in the baltic sea have weakened but lengthened from 2000 to 2014. *Biogeosciences* 13 (17), 4959.
- Hanafin, J., Minnett, P., 2001. Cloud forcing of surface radiation in the north water polynya during now '98. *Atmosphere-Ocean* 39 (3), 239–255.
- Harrison, W. G., Børsheim, K. Y., Li, W. K., Maillet, G. L., Pepin, P., Sakshaug, E., Skogen, M. D., Yeats, P. A., 2013. Phytoplankton production and growth regulation in the subarctic north atlantic: A comparative study of the labrador sea-labrador/newfoundland shelves and barents/norwegian/greenland seas and shelves. *Progress in Oceanography* 114, 26–45.
- Hartigan, J. A., Wong, M. A., 1979. Algorithm as 136: A k-means clustering algorithm. *Journal of the Royal Statistical Society. Series C (Applied Statistics)* 28 (1), 100–108.
- Hátún, H., Olsen, B., Pacariz, S., 2017. The dynamics of the north atlantic subpolar gyre introduces predictability to the breeding success of kittiwakes. *Frontiers in Marine Science* 4, 123.
- Hátún, H., Payne, M., Beaugrand, G., Reid, P., Sandø, A., Drange, H., Hansen, B., Jacobsen, J., Bloch, D., 2009. Large bio-geographical shifts in the north-eastern atlantic ocean: From the subpolar gyre, via plankton, to blue whiting and pilot whales. *Progress in Oceanography* 80 (3-4), 149–162.
- Hazen, E. L., Suryan, R. M., Santora, J. A., Bograd, S. J., Watanuki, Y., Wilson, R. P., 2013. Scales and mechanisms of marine hotspot formation. *Marine Ecology Progress Series* 487, 177–183.
- Head, E., Harris, L., Campbell, R., 2000. Investigations on the ecology of calanus spp. in the labrador sea. i. relationship between the phytoplankton bloom and reproduction and development of calanus finmarchicus in spring. *Marine Ecology Progress Series* 193, 53–73.

- Heide-Jørgensen, M. P., Burt, L. M., Hansen, R. G., Nielsen, N. H., Rasmussen, M., Fossette, S., Stern, H., 2013. The significance of the north water polynya to arctic top predators. *Ambio* 42 (5), 596–610.
- Heller, N. E., Zavaleta, E. S., 2009. Biodiversity management in the face of climate change: a review of 22 years of recommendations. *Biological conservation* 142 (1), 14–32.
- Henson, S. A., Dunne, J. P., Sarmiento, J. L., 2009. Decadal variability in north atlantic phytoplankton blooms. *Journal of Geophysical Research: Oceans* 114 (C4).
- Henson, S. A., Robinson, I., Allen, J. T., Waniek, J. J., 2006. Effect of meteorological conditions on interannual variability in timing and magnitude of the spring bloom in the irvinger basin, north atlantic. *Deep Sea Research Part I: Oceanographic Research Papers* 53 (10), 1601–1615.
- Hernández-Stefanoni, J. L., Gallardo-Cruz, J. A., Meave, J. A., Rocchini, D., Bello-Pineda, J., López-Martínez, J. O., 2012. Modeling α -and β -diversity in a tropical forest from remotely sensed and spatial data. *International journal of applied earth observation and geoinformation* 19, 359–368.
- Hoekstra, J. M., Boucher, T. M., Ricketts, T. H., Roberts, C., 2005. Confronting a biome crisis: global disparities of habitat loss and protection. *Ecology letters* 8 (1), 23–29.
- Holdsworth, A. M., Myers, P. G., 2015. The influence of high-frequency atmospheric forcing on the circulation and deep convection of the labrador sea. *Journal of Climate* 28 (12), 4980–4996.
- Holte, J., Talley, L., 2009. A new algorithm for finding mixed layer depths with applications to argo data and subantarctic mode water formation. *Journal of Atmospheric and Oceanic Technology* 26 (9), 1920–1939.
- Holte, J., Talley, L. D., Gilson, J., Roemmich, D., 2017. An argo mixed layer climatology and database. *Geophysical Research Letters* 44 (11).
- Horvat, C., Jones, D. R., Iams, S., Schroeder, D., Flocco, D., Feltham, D., 2017. The frequency and extent of sub-ice phytoplankton blooms in the arctic ocean. *Science advances* 3 (3), e1601191.
- Hughes, T. P., Bellwood, D. R., Connolly, S. R., 2002. Biodiversity hotspots, centres of endemism, and the conservation of coral reefs. *Ecology Letters* 5 (6), 775–784.
- Huisman, J., Arrayás, M., Ebert, U., Sommeijer, B., 2002. How do sinking phytoplankton species manage to persist? *The American Naturalist* 159 (3), 245–254.

- Hunsicker, M. E., Kappel, C. V., Selkoe, K. A., Halpern, B. S., Scarborough, C., Mease, L., Amrhein, A., 2016. Characterizing driver–response relationships in marine pelagic ecosystems for improved ocean management. *Ecological applications* 26 (3), 651–663.
- Huot, Y., Babin, M., Bruyant, F., Grob, C., Twardowski, M., Claustre, H., 2007. Relationship between photosynthetic parameters and different proxies of phytoplankton biomass in the subtropical ocean. *Biogeosciences* 4 (5), 853–868.
- Hurrell, J. W., Deser, C., 2010. North atlantic climate variability: the role of the north atlantic oscillation. *Journal of Marine Systems* 79 (3-4), 231–244.
- Ingram, R. G., Bâcle, J., Barber, D. G., Gratton, Y., Melling, H., 2002. An overview of physical processes in the north water. *Deep Sea Research Part II: Topical Studies in Oceanography* 49 (22-23), 4893–4906.
- Jenkins, C. N., Pimm, S. L., Joppa, L. N., 2013. Global patterns of terrestrial vertebrate diversity and conservation. *Proceedings of the National Academy of Sciences* 110 (28), E2602–E2610.
- Jepson, P., Canney, S., 2001. Biodiversity hotspots: hot for what? *Global Ecology and Biogeography* 10 (3), 225–227.
- Ji, R., Edwards, M., Mackas, D. L., Runge, J. A., Thomas, A. C., 2010. Marine plankton phenology and life history in a changing climate: current research and future directions. *Journal of plankton research* 32 (10), 1355–1368.
- Ji, R., Jin, M., Varpe, Ø., 2013. Sea ice phenology and timing of primary production pulses in the arctic ocean. *Global change biology* 19 (3), 734–741.
- Jones, D. O., Yool, A., Wei, C.-L., Henson, S. A., Ruhl, H. A., Watson, R. A., Gehlen, M., 2014. Global reductions in seafloor biomass in response to climate change. *Global change biology* 20 (6), 1861–1872.
- Kachelriess, D., Wegmann, M., Gollock, M., Pettorelli, N., 2014. The application of remote sensing for marine protected area management. *Ecological Indicators* 36, 169–177.
- Kahru, M., Brotas, V., Manzano-Sarabia, M., Mitchell, B., 2011. Are phytoplankton blooms occurring earlier in the arctic? *Global Change Biology* 17 (4), 1733–1739.
- Kareiva, P., Marvier, M., 2003. Conserving biodiversity coldspots: Recent calls to direct conservation funding to the world’s biodiversity hotspots may be bad investment advice. *American Scientist* 91 (4), 344–351.
- Karnovsky, N. J., Hunt Jr, G. L., 2002. Estimation of carbon flux to dovekeys (alle alle) in the north water. *Deep Sea Research Part II: Topical Studies in Oceanography* 49 (22-23), 5117–5130.

- Keith, D. A., Mahony, M., Hines, H., Elith, J., Regan, T. J., Baumgartner, J. B., Hunter, D., Heard, G. W., Mitchell, N. J., Parris, K. M., et al., 2014. Detecting extinction risk from climate change by iucn red list criteria. *Conservation Biology* 28 (3), 810–819.
- Kieke, D., Yashayaev, I., 2015. Studies of labrador sea water formation and variability in the subpolar north atlantic in the light of international partnership and collaboration. *Progress in Oceanography* 132, 220–232.
- Klein, B., LeBlanc, B., Mei, Z.-P., Beret, R., Michaud, J., Mundy, C.-J., von Quillfeldt, C. H., Garneau, M.-È., Roy, S., Gratton, Y., et al., 2002. Phytoplankton biomass, production and potential export in the north water. *Deep Sea Research Part II: Topical Studies in Oceanography* 49 (22-23), 4983–5002.
- Kohlbach, D., Graeve, M., A Lange, B., David, C., Peeken, I., Flores, H., 2016. The importance of ice algae-produced carbon in the central arctic ocean ecosystem: Food web relationships revealed by lipid and stable isotope analyses. *Limnology and Oceanography* 61 (6), 2027–2044.
- Kopec, B. G., Feng, X., Michel, F. A., Posmentier, E. S., 2016. Influence of sea ice on arctic precipitation. *Proceedings of the National Academy of Sciences* 113 (1), 46–51.
- Körtzinger, A., Send, U., Wallace, D. W., Karstensen, J., DeGrandpre, M., 2008. Seasonal cycle of o₂ and pco₂ in the central labrador sea: Atmospheric, biological, and physical implications. *Global Biogeochemical Cycles* 22 (1).
- Kostadinov, T. S., Cabré, A., Vedantham, H., Marinov, I., Bracher, A., Brewin, R. J., Bricaud, A., Hirata, T., Hirawake, T., Hardman-Mountford, N. J., et al., 2017. Inter-comparison of phytoplankton functional type phenology metrics derived from ocean color algorithms and earth system models. *Remote Sensing of Environment* 190, 162–177.
- Kwok, R., Toudal Pedersen, L., Gudmandsen, P., Pang, S., 2010. Large sea ice outflow into the nares strait in 2007. *Geophysical Research Letters* 37 (3).
- Lab Sea Group, T. L. S., 1998. The labrador sea deep convection experiment. *Bulletin of the American Meteorological Society* 79 (10), 2033–2058.
- Lacour, L., Ardyna, M., Stec, K., Claustre, H., Prieur, L., Poteau, A., D’Alcala, M. R., Iudicone, D., 2017. Unexpected winter phytoplankton blooms in the north atlantic subpolar gyre. *Nature Geoscience* 10 (11), 836.
- Lacour, L., Claustre, H., Prieur, L., D’Ortenzio, F., 2015. Phytoplankton biomass cycles in the north atlantic subpolar gyre: A similar mechanism for two different blooms in the labrador sea. *Geophysical Research Letters* 42 (13), 5403–5410.

- Laidre, K. L., Stern, H., Kovacs, K. M., Lowry, L., Moore, S. E., Regehr, E. V., Ferguson, S. H., Wiig, Ø., Boveng, P., Angliss, R. P., et al., 2015. Arctic marine mammal population status, sea ice habitat loss, and conservation recommendations for the 21st century. *Conservation Biology* 29 (3), 724–737.
- Lamoreux, J. F., Morrison, J. C., Ricketts, T. H., Olson, D. M., Dinerstein, E., McKnight, M. W., Shugart, H. H., 2006. Global tests of biodiversity concordance and the importance of endemism. *Nature* 440 (7081), 212.
- Land, P. E., Shutler, J. D., Platt, T., Racault, M., 2014. A novel method to retrieve oceanic phytoplankton phenology from satellite data in the presence of data gaps. *Ecological indicators* 37, 67–80.
- Large, W. G., Yeager, S. G., 2004. Diurnal to decadal global forcing for ocean and sea-ice models: the data sets and flux climatologies. NCAR Technical Note: NCAR/TN-460+STR. CGD Division of the National Center for Atmospheric Research.
- Lee, Y. J., Matrai, P. A., Friedrichs, M. A., Saba, V. S., Antoine, D., Ardyna, M., Asanuma, I., Babin, M., Bélanger, S., Benoit-Gagné, M., et al., 2015. An assessment of phytoplankton primary productivity in the arctic ocean from satellite ocean color/in situ chlorophyll-a based models. *Journal of Geophysical Research: Oceans* 120 (9), 6508–6541.
- Lewandowska, A. M., Boyce, D. G., Hofmann, M., Matthiessen, B., Sommer, U., Worm, B., 2014. Effects of sea surface warming on marine plankton. *Ecology letters* 17 (5), 614–623.
- Lewandowska, A. M., Striebel, M., Feudel, U., Hillebrand, H., Sommer, U., 2015. The importance of phytoplankton trait variability in spring bloom formation. *ICES Journal of Marine Science* 72 (6), 1908–1915.
- Li, W. K., McLaughlin, F. A., Lovejoy, C., Carmack, E. C., 2009. Smallest algae thrive as the arctic ocean freshens. *Science* 326 (5952), 539–539.
- Li, Y., Ji, R., Jenouvrier, S., Jin, M., Stroeve, J., 2016. Synchronicity between ice retreat and phytoplankton bloom in circum-antarctic polynyas. *Geophysical Research Letters* 43 (5), 2086–2093.
- Lilly, J. M., Rhines, P. B., Schott, F., Lavender, K., Lazier, J., Send, U., D’Asaro, E., 2003. Observations of the labrador sea eddy field. *Progress in Oceanography* 59 (1), 75–176.
- Lindemann, C., Backhaus, J. O., St John, M. A., 2015. Physiological constraints on sverdrup’s critical-depth-hypothesis: the influences of dark respiration and sinking. *ICES Journal of Marine Science* 72 (6), 1942–1951.

- Lindemann, C., St John, M. A., 2014. A seasonal diary of phytoplankton in the north atlantic. *Frontiers in Marine Science* 1, 37.
- Link, H., Piepenburg, D., Archambault, P., 2013. Are hotspots always hotspots? the relationship between diversity, resource and ecosystem functions in the arctic. *PLoS One* 8 (9), e74077.
- Luo, H., Bracco, A., Di Lorenzo, E., 2011. The interannual variability of the surface eddy kinetic energy in the labrador sea. *Progress in oceanography* 91 (3), 295–311.
- Luo, H., Castelao, R. M., Rennermalm, A. K., Tedesco, M., Bracco, A., Yager, P. L., Mote, T. L., 2016. Oceanic transport of surface meltwater from the southern greenland ice sheet. *Nature Geoscience* 9 (7), 528.
- Mace, G. M., Balmford, A., Boitani, L., Cowlshaw, G., Dobson, A., Faith, D., Gaston, K. J., Humphries, C., Vane-Wright, R., Williams, P., et al., 2000. It's time to work together and stop duplicating conservation efforts.... *Nature* 405 (6785), 393.
- Madec, G., 2008. Nemo ocean engine, note du pole de modélisation. institut pierre-simon laplace (ipsl), tech. Tech. rep., Note 27, 219 pp.
- Mahadevan, A., D'Asaro, E., Lee, C., Perry, M. J., 2012. Eddy-driven stratification initiates north atlantic spring phytoplankton blooms. *Science* 337 (6090), 54–58.
- Malick, M. J., Cox, S. P., Mueter, F. J., Peterman, R. M., 2015. Linking phytoplankton phenology to salmon productivity along a north–south gradient in the northeast pacific ocean. *Canadian Journal of Fisheries and Aquatic Sciences* 72 (5), 697–708.
- Marchese, C., 2015. Biodiversity hotspots: A shortcut for a more complicated concept. *Global Ecology and Conservation* 3, 297–309.
- Marchese, C., Albouy, C., Tremblay, J.-É., Dumont, D., D'Ortenzio, F., Vissault, S., Bélanger, S., 2017. Changes in phytoplankton bloom phenology over the north water (now) polynya: a response to changing environmental conditions. *Polar Biology* 40 (9), 1721–1737.
- Maritorena, S., d'Andon, O. H. F., Mangin, A., Siegel, D. A., 2010. Merged satellite ocean color data products using a bio-optical model: Characteristics, benefits and issues. *Remote Sensing of Environment* 114 (8), 1791–1804.
- Maritorena, S., Siegel, D. A., Peterson, A. R., 2002. Optimization of a semianalytical ocean color model for global-scale applications. *Applied optics* 41 (15), 2705–2714.
- Maslanik, J., Stroeve, J., Fowler, C., Emery, W., 2011. Distribution and trends in arctic sea ice age through spring 2011. *Geophysical Research Letters* 38 (13).

- Matrai, P., Olson, E., Suttles, S., Hill, V., Codispoti, L., Light, B., Steele, M., 2013. Synthesis of primary production in the arctic ocean: I. surface waters, 1954–2007. *Progress in Oceanography* 110, 93–106.
- Matsuoka, A., Hill, V., Huot, Y., Babin, M., Bricaud, A., 2011. Seasonal variability in the light absorption properties of western arctic waters: parameterization of the individual components of absorption for ocean color applications. *Journal of Geophysical Research: Oceans* 116 (2).
- Mauri, E., Poulain, P.-M., Južnič-Zonta, Ž., 2007. Modis chlorophyll variability in the northern adriatic sea and relationship with forcing parameters. *Journal of Geophysical Research: Oceans* 112 (C3).
- Maury, O., Miller, K., Campling, L., Arrizabalaga, H., Aumont, O., Bodin, Ö., Guillotreau, P., Hobday, A., Marsac, F., Suzuki, Z., et al., 2013. A global science–policy partnership for progress toward sustainability of oceanic ecosystems and fisheries. *Current Opinion in Environmental Sustainability* 5 (3-4), 314–319.
- Mazel, F., Guilhaumon, F., Mouquet, N., Devictor, V., Gravel, D., Renaud, J., Cianciaruso, M. V., Loyola, R., Diniz-Filho, J. A. F., Mouillot, D., et al., 2014. Multifaceted diversity–area relationships reveal global hotspots of mammalian species, trait and lineage diversity. *Global ecology and biogeography* 23 (8), 836–847.
- Mazor, T., Levin, N., Possingham, H. P., Levy, Y., Rocchini, D., Richardson, A. J., Kark, S., 2013. Can satellite-based night lights be used for conservation? the case of nesting sea turtles in the mediterranean. *Biological Conservation* 159, 63–72.
- McDougall, T. J., 1987. Neutral surfaces. *Journal of Physical Oceanography* 17 (11), 1950–1964.
- McLaughlin, F. A., Carmack, E. C., 2010. Deepening of the nutricline and chlorophyll maximum in the canada basin interior, 2003–2009. *Geophysical Research Letters* 37 (24).
- Mei, Z.-P., Legendre, L., Gratton, Y., Tremblay, J.-E., LeBlanc, B., Mundy, C., Klein, B., Gosselin, M., Larouche, P., Papakyriakou, T., et al., 2002. Physical control of spring–summer phytoplankton dynamics in the north water, april–july 1998. *Deep Sea Research Part II: Topical Studies in Oceanography* 49 (22-23), 4959–4982.
- Meier, W., Fetterer, F., Savoie, M., Mallory, S., Duerr, R., Stroeve, J., 2013. Noaa/nsidc climate data record of passive microwave sea ice concentration, version 2. National Snow and Ice Data Center, Boulder, CO.[Available online at http://nsidc.org/data/docs/noaa/g02202_ice_conc_cdr/].
- Melling, H., Gratton, Y., Ingram, G., 2001. Ocean circulation within the north water polynya of baffin bay. *Atmosphere-Ocean* 39 (3), 301–325.

- Meyer, K. S., Soltwedel, T., Bergmann, M., 2014. High biodiversity on a deep-water reef in the eastern fram strait. *PloS one* 9 (8), e105424.
- Michel, C., Gosselin, M., Nozais, C., 2002. Preferential sinking export of biogenic silica during the spring and summer in the north water polynya (northern baffin bay): Temperature or biological control? *Journal of Geophysical Research: Oceans* 107 (C7).
- Mignot, A., Ferrari, R., Claustre, H., 2018. Floats with bio-optical sensors reveal what processes trigger the north atlantic bloom. *Nature communications* 9 (1), 190.
- Mittermeier, R. A., Myers, N., Mittermeier, C. G., Robles, G., et al., 1999. Hotspots: Earth's biologically richest and most endangered terrestrial ecoregions. CEMEX, SA, Agrupación Sierra Madre, SC.
- Mittermeier, R. A., Turner, W. R., Larsen, F. W., Brooks, T. M., Gascon, C., 2011. Global biodiversity conservation: the critical role of hotspots. In: *Biodiversity hotspots*. Springer, pp. 3–22.
- Mittermeier, R., Gil, P., Hoffman, M., Pilgrim, J., Brooks, T., Mittermeier, C., Lamoreux, J., Da Fonseca, G., 2005. Hotspots revisited: earth's biologically richest and most endangered terrestrial ecoregions. CEMEX, Mexico City.
- Moore, S. E., Huntington, H. P., 2008. Arctic marine mammals and climate change: Impacts and resilience. *Ecological Applications* 18 (2), S157–S165.
- Morato, T., Hoyle, S. D., Allain, V., Nicol, S. J., 2010. Seamounts are hotspots of pelagic biodiversity in the open ocean. *Proceedings of the National Academy of Sciences* 107 (21), 9707–9711.
- Mouillot, D., Bellwood, D. R., Baraloto, C., Chave, J., Galzin, R., Harmelin-Vivien, M., Kulbicki, M., Lavergne, S., Lavorel, S., Mouquet, N., et al., 2013. Rare species support vulnerable functions in high-diversity ecosystems. *PLoS biology* 11 (5), e1001569.
- Mouw, C. B., Hardman-Mountford, N. J., Alvain, S., Bracher, A., Brewin, R. J., Bricaud, A., Ciotti, A. M., Devred, E., Fujiwara, A., Hirata, T., et al., 2017. A consumer's guide to satellite remote sensing of multiple phytoplankton groups in the global ocean. *Frontiers in Marine Science* 4, 41.
- Myers, N., 1988. Threatened biotas:"hot-spots" in tropical forests. *Environmentalist* 8 (3), 187–208.
- Myers, N., 1990. The biodiversity challenge: expanded hot-spots analysis. *Environmentalist* 10 (4), 243–256.
- Myers, N., 2003. Biodiversity hotspots revisited. *BioScience* 53 (10), 916–917.

- Myers, N., Mittermeier, R. A., Mittermeier, C. G., Da Fonseca, G. A., Kent, J., 2000. Biodiversity hotspots for conservation priorities. *Nature* 403 (6772), 853.
- Nagendra, H., Lucas, R., Honrado, J. P., Jongman, R. H., Tarantino, C., Adamo, M., Mairota, P., 2013. Remote sensing for conservation monitoring: Assessing protected areas, habitat extent, habitat condition, species diversity, and threats. *Ecological Indicators* 33, 45–59.
- Odate, T., Hirawake, T., Kudoh, S., Klein, B., LeBlanc, B., Fukuchi, M., 2002. Temporal and spatial patterns in the surface-water biomass of phytoplankton in the north water. *Deep Sea Research Part II: Topical Studies in Oceanography* 49 (22-23), 4947–4958.
- O'Donnell, J., Gallagher, R. V., Wilson, P. D., Downey, P. O., Hughes, L., Leishman, M. R., 2012. Invasion hotspots for non-native plants in australia under current and future climates. *Global Change Biology* 18 (2), 617–629.
- Ólafsson, J., 2003. Winter mixed layer nutrients in the irminger and iceland seas. In: *ICES Marine Science Symposia*. Vol. 219. pp. 329–332.
- Orme, C. D. L., Davies, R. G., Burgess, M., Eigenbrod, F., Pickup, N., Olson, V. A., Webster, A. J., Ding, T.-S., Rasmussen, P. C., Ridgely, R. S., et al., 2005. Global hotspots of species richness are not congruent with endemism or threat. *Nature* 436 (7053), 1016.
- Oziel, L., Neukermans, G., Ardyna, M., Lancelot, C., Tison, J.-L., Wassmann, P., Sirven, J., Ruiz-Pino, D., Gascard, J.-C., 2017. Role for atlantic inflows and sea ice loss on shifting phytoplankton blooms in the barents sea. *Journal of Geophysical Research (Oceans)* 122, 5121–5139.
- O'Reilly, J. E., Maritorena, S., O'Brien, M. C., Siegel, D. A., Toole, D., Menzies, D., Smith, R. C., Mueller, J. L., Mitchell, B. G., Kahru, M., et al., 2000. Seawifs postlaunch calibration and validation analyses, part 3. NASA tech. memo 206892 (11), 3–8.
- Pabi, S., van Dijken, G. L., Arrigo, K. R., 2008. Primary production in the arctic ocean, 1998–2006. *Journal of Geophysical Research: Oceans* 113 (C8).
- Palacios, D. M., Bograd, S. J., Foley, D. G., Schwing, F. B., 2006. Oceanographic characteristics of biological hot spots in the north pacific: a remote sensing perspective. *Deep Sea Research Part II: Topical Studies in Oceanography* 53 (3-4), 250–269.
- Palmer, M. A., Saenz, B. T., Arrigo, K. R., 2014. Impacts of sea ice retreat, thinning, and melt-pond proliferation on the summer phytoplankton bloom in the chukchi sea, arctic ocean. *Deep Sea Research Part II: Topical Studies in Oceanography* 105, 85–104.

- Park, K.-A., Kang, C.-K., Kim, K.-R., Park, J.-E., 2014. Role of sea ice on satellite-observed chlorophyll-a concentration variations during spring bloom in the east/japan sea. *Deep Sea Research Part I: Oceanographic Research Papers* 83, 34–44.
- Parkinson, C. L., Comiso, J. C., 2013. On the 2012 record low arctic sea ice cover: Combined impact of preconditioning and an august storm. *Geophysical Research Letters* 40 (7), 1356–1361.
- Parravicini, V., Villéger, S., McClanahan, T. R., Arias-González, J. E., Bellwood, D. R., Belmaker, J., Chabanet, P., Floeter, S. R., Friedlander, A. M., Guilhaumon, F., et al., 2014. Global mismatch between species richness and vulnerability of reef fish assemblages. *Ecology letters* 17 (9), 1101–1110.
- Pereira, H. M., Ferrier, S., Walters, M., Geller, G. N., Jongman, R., Scholes, R. J., Bruford, M. W., Brummitt, N., Butchart, S., Cardoso, A., et al., 2013. Essential biodiversity variables. *Science* 339 (6117), 277–278.
- Perrette, M., Yool, A., Quartly, G., Popova, E., 2011. Near-ubiquity of ice-edge blooms in the arctic. *Biogeosciences* 8 (2), 515–524.
- Peters, H., O’leary, B. C., Hawkins, J. P., Roberts, C. M., 2015. Identifying species at extinction risk using global models of anthropogenic impact. *Global change biology* 21 (2), 618–628.
- Petrenko, D., Pozdnyakov, D., Johannessen, J., Counillon, F., Sychov, V., 2013. Satellite-derived multi-year trend in primary production in the arctic ocean. *International Journal of Remote Sensing* 34 (11), 3903–3937.
- Pettorelli, N., Laurance, W. F., O’Brien, T. G., Wegmann, M., Nagendra, H., Turner, W., 2014. Satellite remote sensing for applied ecologists: opportunities and challenges. *Journal of Applied Ecology* 51 (4), 839–848.
- Piatt, J. F., Wetzel, J., Bell, K., DeGange, A. R., Balogh, G. R., Drew, G. S., Geernaert, T., Ladd, C., Byrd, G. V., 2006. Predictable hotspots and foraging habitat of the endangered short-tailed albatross (*phoebastria albatrus*) in the north pacific: Implications for conservation. *Deep Sea Research Part II: Topical Studies in Oceanography* 53 (3-4), 387–398.
- Piepenburg, D., Archambault, P., Ambrose, W. G., Blanchard, A. L., Bluhm, B. A., Carroll, M. L., Conlan, K. E., Cusson, M., Feder, H. M., Grebmeier, J. M., et al., 2011. Towards a pan-arctic inventory of the species diversity of the macro-and megabenthic fauna of the arctic shelf seas. *Marine Biodiversity* 41 (1), 51–70.
- Pimm, S. L., Jenkins, C. N., Abell, R., Brooks, T. M., Gittleman, J. L., Joppa, L. N., Raven, P. H., Roberts, C. M., Sexton, J. O., 2014. The biodiversity of species and their rates of extinction, distribution, and protection. *Science* 344 (6187), 1246752.

- Piron, A., Thierry, V., Mercier, H., Caniaux, G., 2017. Gyre-scale deep convection in the subpolar north atlantic ocean during winter 2014–2015. *Geophysical Research Letters* 44 (3), 1439–1447.
- Platt, T., Sathyendranath, S., 2008. Ecological indicators for the pelagic zone of the ocean from remote sensing. *Remote Sensing of Environment* 112 (8), 3426–3436.
- Platt, T., White III, G. N., Zhai, L., Sathyendranath, S., Roy, S., 2009. The phenology of phytoplankton blooms: Ecosystem indicators from remote sensing. *Ecological Modelling* 220 (21), 3057–3069.
- Pohl, C., Hadorn, G. H., 2008. Methodological challenges of transdisciplinary research. *Natures Sciences Sociétés* 16 (2), 111–121.
- Possingham, H. P., Wilson, K. A., 2005. Biodiversity: Turning up the heat on hotspots. *Nature* 436 (7053), 919.
- Potts, T., Burdon, D., Jackson, E., Atkins, J., Saunders, J., Hastings, E., Langmead, O., 2014. Do marine protected areas deliver flows of ecosystem services to support human welfare? *Marine Policy* 44, 139–148.
- Pressey, R., 2004. Conservation planning and biodiversity: assembling the best data for the job. *Conservation biology* 18 (6), 1677–1681.
- Price, A. R., 2002. Simultaneous ‘hotspots’ and ‘coldspots’ of marine biodiversity and implications for global conservation. *Marine Ecology Progress Series* 241, 23–27.
- R Team, R. C., 2016. R: A language and environment for statistical computing. *r foundation for statistical computing, vienna, austria*. 2014.
- Racault, M.-F., Le Quéré, C., Buitenhuis, E., Sathyendranath, S., Platt, T., 2012. Phytoplankton phenology in the global ocean. *Ecological Indicators* 14 (1), 152–163.
- Racault, M.-F., Platt, T., Sathyendranath, S., Ağirbağ, E., Martinez Vicente, V., Brewin, R., 2014a. Plankton indicators and ocean observing systems: support to the marine ecosystem state assessment. *Journal of Plankton Research* 36 (3), 621–629.
- Racault, M.-F., Sathyendranath, S., Platt, T., 2014b. Impact of missing data on the estimation of ecological indicators from satellite ocean-colour time-series. *Remote sensing of environment* 152, 15–28.
- Rainville, L., Lee, C. M., Woodgate, R. A., 2011. Impact of wind-driven mixing in the arctic ocean. *Oceanography* 24 (3), 136–145.
- Ramirez-Llodra, E., Brandt, A., Danovaro, R., De Mol, B., Escobar, E., German, C. R., Levin, L. A., Martinez Arbizu, P., Menot, L., Buhl-Mortensen, P., et al., 2010. Deep, diverse and definitely different: unique attributes of the world’s largest ecosystem. *Biogeosciences* 7 (9), 2851–2899.

- Rasmussen, T. A., Kliem, N., Kaas, E., 2011. The effect of climate change on the sea ice and hydrography in nares strait. *Atmosphere-Ocean* 49 (3), 245–258.
- Renner, A. H., Gerland, S., Haas, C., Spreen, G., Beckers, J. F., Hansen, E., Nicolaus, M., Goodwin, H., 2014. Evidence of arctic sea ice thinning from direct observations. *Geophysical Research Letters* 41 (14), 5029–5036.
- Reyers, B., Polasky, S., Tallis, H., Mooney, H. A., Larigauderie, A., 2012. Finding common ground for biodiversity and ecosystem services. *BioScience* 62 (5), 503–507.
- Reynolds, R. W., Smith, T. M., Liu, C., Chelton, D. B., Casey, K. S., Schlax, M. G., 2007. Daily high-resolution-blended analyses for sea surface temperature. *Journal of Climate* 20 (22), 5473–5496.
- Ricker, R., Hendricks, S., Girard-Ardhuin, F., Kaleschke, L., Lique, C., Tian-Kunze, X., Nicolaus, M., Krumpen, T., 2017. Satellite-observed drop of arctic sea ice growth in winter 2015–2016. *Geophysical Research Letters* 44 (7), 3236–3245.
- Riordan, E. C., Rundel, P. W., 2014. Land use compounds habitat losses under projected climate change in a threatened california ecosystem. *PloS one* 9 (1), e86487.
- Rivers, M. C., Brummitt, N. A., Lughadha, E. N., Meagher, T. R., 2014. Do species conservation assessments capture genetic diversity? *Global Ecology and Conservation* 2, 81–87.
- Roberts, C. M., McClean, C. J., Veron, J. E., Hawkins, J. P., Allen, G. R., McAllister, D. E., Mittermeier, C. G., Schueler, F. W., Spalding, M., Wells, F., et al., 2002. Marine biodiversity hotspots and conservation priorities for tropical reefs. *Science* 295 (5558), 1280–1284.
- Roquet, C., Thuiller, W., Lavergne, S., 2013. Building megaphylogenies for macroecology: taking up the challenge. *Ecography* 36 (1), 13–26.
- Rosauer, D., Laffan, S. W., Crisp, M. D., Donnellan, S. C., Cook, L. G., 2009. Phylogenetic endemism: a new approach for identifying geographical concentrations of evolutionary history. *Molecular Ecology* 18 (19), 4061–4072.
- Rosauer, D. F., Mooers, A. O., 2013. Nurturing the use of evolutionary diversity in nature conservation. *Trends in Ecology & Evolution* 28 (6), 322.
- Rumyantseva, A., Lucas, N., Rippeth, T., Martin, A., Painter, S. C., Boyd, T. J., Henson, S., 2015. Ocean nutrient pathways associated with the passage of a storm. *Global Biogeochemical Cycles* 29 (8), 1179–1189.
- Sanders, R., Henson, S. A., Koski, M., Christina, L., Painter, S. C., Poulton, A. J., Riley, J., Salihoglu, B., Visser, A., Yool, A., et al., 2014. The biological carbon pump in the north atlantic. *Progress in Oceanography* 129, 200–218.

- Santora, J. A., Veit, R. R., 2013. Spatio-temporal persistence of top predator hotspots near the antarctic peninsula. *Marine Ecology Progress Series* 487, 287–304.
- Sapiano, M., Brown, C., Schollaert Uz, S., Vargas, M., 2012. Establishing a global climatology of marine phytoplankton phenological characteristics. *Journal of Geophysical Research: Oceans* 117 (C8).
- Sasaoka, K., Chiba, S., Saino, T., 2011. Climatic forcing and phytoplankton phenology over the subarctic north pacific from 1998 to 2006, as observed from ocean color data. *Geophysical Research Letters* 38 (15).
- Schmitt, C. B., 2011. A tough choice: approaches towards the setting of global conservation priorities. In: *Biodiversity Hotspots*. Springer, pp. 23–42.
- Schoemann, V., Becquevort, S., Stefels, J., Rousseau, V., Lancelot, C., 2005. Phaeocystis blooms in the global ocean and their controlling mechanisms: a review. *Journal of Sea Research* 53 (1-2), 43–66.
- Schröter, M., Zanden, E. H., Oudenhoven, A. P., Remme, R. P., Serna-Chavez, H. M., Groot, R. S., Opdam, P., 2014. Ecosystem services as a contested concept: a synthesis of critique and counter-arguments. *Conservation Letters* 7 (6), 514–523.
- Selig, E. R., Turner, W. R., Troëng, S., Wallace, B. P., Halpern, B. S., Kaschner, K., Lascelles, B. G., Carpenter, K. E., Mittermeier, R. A., 2014. Global priorities for marine biodiversity conservation. *PloS one* 9 (1), e82898.
- Serreze, M., Maslanik, J., Scambos, T., Fetterer, F., Stroeve, J., Knowles, K., Fowler, C., Drobot, S., Barry, R., Haran, T., 2003. A record minimum arctic sea ice extent and area in 2002. *Geophysical Research Letters* 30 (3).
- Severin, T., Conan, P., de Madron, X. D., Houpert, L., Oliver, M., Oriol, L., Caparros, J., Ghiglione, J., Pujó-Pay, M., 2014. Impact of open-ocean convection on nutrients, phytoplankton biomass and activity. *Deep Sea Research Part I: Oceanographic Research Papers* 94, 62–71.
- Siegel, D., Doney, S., Yoder, J., 2002. The north atlantic spring phytoplankton bloom and sverdrup's critical depth hypothesis. *science* 296 (5568), 730–733.
- Sigler, M. F., Kuletz, K. J., Ressler, P. H., Friday, N. A., Wilson, C. D., Zerbini, A. N., 2012. Marine predators and persistent prey in the southeast bering sea. *Deep Sea Research Part II: Topical Studies in Oceanography* 65, 292–303.
- Sirjacobs, D., Alvera-Azcárate, A., Barth, A., Lacroix, G., Park, Y., Nechad, B., Ruddick, K., Beckers, J.-M., 2011. Cloud filling of ocean colour and sea surface temperature remote sensing products over the southern north sea by the data interpolating empirical orthogonal functions methodology. *Journal of Sea Research* 65 (1), 114–130.

- Slagstad, D., Wassmann, P. F., Ellingsen, I., 2015. Physical constraints and productivity in the future arctic ocean. *Frontiers in Marine Science* 2, 85.
- Sloan, S., Jenkins, C. N., Joppa, L. N., Gaveau, D. L., Laurance, W. F., 2014. Remaining natural vegetation in the global biodiversity hotspots. *Biological Conservation* 177, 12–24.
- Smith, C. R., De Leo, F. C., Bernardino, A. F., Sweetman, A. K., Arbizu, P. M., 2008. Abyssal food limitation, ecosystem structure and climate change. *Trends in Ecology & Evolution* 23 (9), 518–528.
- Smith, G. C., Roy, F., Mann, P., Dupont, F., Brasnett, B., Lemieux, J.-F., Laroche, S., Bélair, S., 2014. A new atmospheric dataset for forcing ice–ocean models: Evaluation of reforecasts using the canadian global deterministic prediction system. *Quarterly Journal of the Royal Meteorological Society* 140 (680), 881–894.
- Smith, K. L., Ruhl, H. A., Kahru, M., Huffard, C. L., Sherman, A. D., 2013. Deep ocean communities impacted by changing climate over 24 y in the abyssal northeast pacific ocean. *Proceedings of the National Academy of Sciences* 110 (49), 19838–19841.
- Smith, T. B., Kark, S., Schneider, C. J., Wayne, R. K., Moritz, C., 2001. Biodiversity hotspots and beyond: the need for preserving environmental transitions. *Trends in Ecology & Evolution* 16 (8), 431.
- Smith Jr, K., Sherman, A., Huffard, C., McGill, P., Henthorn, R., Von Thun, S., Ruhl, H., Kahru, M., Ohman, M., 2014. Large salp bloom export from the upper ocean and benthic community response in the abyssal northeast pacific: day to week resolution. *Limnology and Oceanography* 59 (3), 745–757.
- Smith Jr, W., Barber, D., 2007. *Polynyas and climate change: a view to the future*. Elsevier Oceanography Series 74, 411–419.
- Søreide, J. E., Leu, E., Berge, J., Graeve, M., Falk-Petersen, S., 2010. Timing of blooms, algal food quality and calanus glacialis reproduction and growth in a changing arctic. *Global change biology* 16 (11), 3154–3163.
- Sørensen, H. L., Thamdrup, B., Jeppesen, E., Rysgaard, S., Glud, R. N., 2017. Nutrient availability limits biological production in arctic sea ice melt ponds. *Polar Biology* 40 (8), 1593–1606.
- Stocks, K. I., Hart, P. J., 2007. *Biogeography and biodiversity of seamounts. Seamounts: ecology, fisheries, and conservation*. Blackwell Fisheries and Aquatic Resources Series 12, 255–81.
- Stork, N. E., Habel, J. C., 2014. Can biodiversity hotspots protect more than tropical forest plants and vertebrates? *Journal of Biogeography* 41 (3), 421–428.

- Stroeve, J., Markus, T., Boisvert, L., Miller, J., Barrett, A., 2014. Changes in arctic melt season and implications for sea ice loss. *Geophysical Research Letters* 41 (4), 1216–1225.
- Stroeve, J. C., Serreze, M. C., Holland, M. M., Kay, J. E., Malanik, J., Barrett, A. P., 2012. The arctic's rapidly shrinking sea ice cover: a research synthesis. *Climatic Change* 110 (3-4), 1005–1027.
- Stuart-Smith, R. D., Bates, A. E., Lefcheck, J. S., Duffy, J. E., Baker, S. C., Thomson, R. J., Stuart-Smith, J. F., Hill, N. A., Kininmonth, S. J., Airoidi, L., et al., 2013. Integrating abundance and functional traits reveals new global hotspots of fish diversity. *Nature* 501 (7468), 539.
- Sunday, J. M., Calosi, P., Dupont, S., Munday, P. L., Stillman, J. H., Reusch, T. B., 2014. Evolution in an acidifying ocean. *Trends in Ecology & Evolution* 29 (2), 117–125.
- Suryan, R. M., Santora, J. A., Sydeman, W. J., 2012. New approach for using remotely sensed chlorophyll a to identify seabird hotspots. *Marine Ecology Progress Series* 451, 213–225.
- Sverdrup, H., 1953. On conditions for the vernal blooming of phytoplankton. *J. Cons. Int. Explor. Mer* 18 (3), 287–295.
- Sydeman, W. J., Brodeur, R. D., Grimes, C. B., Bychkov, A. S., McKinnell, S., 2006. Marine habitat “hotspots” and their use by migratory species and top predators in the north pacific ocean: Introduction. *Deep Sea Research Part II: Topical Studies in Oceanography* 53, 247–249.
- Taylor, J. R., Ferrari, R., 2011. Shutdown of turbulent convection as a new criterion for the onset of spring phytoplankton blooms. *Limnology and Oceanography* 56 (6), 2293–2307.
- Taylor, M., 2016. *sinkr*: collection of functions with emphasis in multivariate data analysis. r package version 0.4.
- Taylor, M. H., Losch, M., Wenzel, M., Schröter, J., 2013. On the sensitivity of field reconstruction and prediction using empirical orthogonal functions derived from gappy data. *Journal of Climate* 26 (22), 9194–9205.
- Torres, M. E., Zima, D., Falkner, K. K., Macdonald, R. W., O'BRIEN, M., Schöne, B. R., Siferd, T., 2011. Hydrographic changes in nares strait (canadian arctic archipelago) in recent decades based on $\delta^{18}\text{O}$ profiles of bivalve shells. *Arctic* 64, 45–58.
- Tovar-Sánchez, A., Duarte, C. M., Alonso, J. C., Lacorte, S., Tauler, R., Galbán-Malagón, C., 2010. Impacts of metals and nutrients released from melting multiyear arctic sea ice. *Journal of Geophysical Research: Oceans* 115 (C7).

- Townsend, D. W., Cammen, L. M., Holligan, P. M., Campbell, D. E., Pettigrew, N. R., 1994. Causes and consequences of variability in the timing of spring phytoplankton blooms. *Deep Sea Research Part I: Oceanographic Research Papers* 41 (5-6), 747–765.
- Tremblay, J.-É., Anderson, L. G., Matrai, P., Coupel, P., Bélanger, S., Michel, C., Reigstad, M., 2015. Global and regional drivers of nutrient supply, primary production and co₂ drawdown in the changing arctic ocean. *Progress in Oceanography* 139, 171–196.
- Tremblay, J.-É., Bélanger, S., Barber, D., Asplin, M., Martin, J., Darnis, G., Fortier, L., Gratton, Y., Link, H., Archambault, P., et al., 2011. Climate forcing multiplies biological productivity in the coastal arctic ocean. *Geophysical Research Letters* 38 (18).
- Tremblay, J.-É., Gratton, Y., Carmack, E. C., Payne, C. D., Price, N. M., 2002a. Impact of the large-scale arctic circulation and the north water polynya on nutrient inventories in baffin bay. *Journal of Geophysical Research: Oceans* 107 (C8).
- Tremblay, J.-É., Gratton, Y., Fauchot, J., Price, N. M., 2002b. Climatic and oceanic forcing of new, net, and diatom production in the north water. *Deep Sea Research Part II: Topical Studies in Oceanography* 49 (22-23), 4927–4946.
- Tremblay, J.-É., Hattori, H., Michel, C., Ringuette, M., Mei, Z.-P., Lovejoy, C., Fortier, L., Hobson, K. A., Amiel, D., Cochran, K., 2006a. Trophic structure and pathways of biogenic carbon flow in the eastern north water polynya. *Progress in Oceanography* 71 (2-4), 402–425.
- Tremblay, J.-É., Michel, C., Hobson, K. A., Gosselin, M., Price, N. M., 2006b. Bloom dynamics in early opening waters of the arctic ocean. *Limnology and Oceanography* 51 (2), 900–912.
- Tremblay, J.-É., Smith Jr, W., 2007. Primary production and nutrient dynamics in polynyas. *Elsevier Oceanography Series* 74, 239–269.
- Tucker, C. M., Cadotte, M. W., Davies, T. J., Rebelo, T. G., 2012. Incorporating geographical and evolutionary rarity into conservation prioritization. *Conservation Biology* 26 (4), 593–601.
- Turner, W. R., Brandon, K., Brooks, T. M., Costanza, R., Da Fonseca, G. A., Portela, R., 2007. Global conservation of biodiversity and ecosystem services. *AIBS Bulletin* 57 (10), 868–873.
- Våge, K., Pickart, R. S., Thierry, V., Reverdin, G., Lee, C. M., Petrie, B., Agnew, T. A., Wong, A., Ribergaard, M. H., 2009. Surprising return of deep convection to the subpolar north atlantic ocean in winter 2007–2008. *Nature Geoscience* 2 (1), 67.

- Vancoppenolle, M., Meiners, K. M., Michel, C., Bopp, L., Brabant, F., Carnat, G., Delille, B., Lannuzel, D., Madec, G., Moreau, S., et al., 2013. Role of sea ice in global biogeochemical cycles: emerging views and challenges. *Quaternary science reviews* 79, 207–230.
- Venter, O., Fuller, R. A., Segan, D. B., Carwardine, J., Brooks, T., Butchart, S. H., Di Marco, M., Iwamura, T., Joseph, L., O'Grady, D., et al., 2014. Targeting global protected area expansion for imperiled biodiversity. *PLoS Biology* 12 (6), e1001891.
- Vidussi, F., Roy, S., Lovejoy, C., Gammelgaard, M., Thomsen, H. A., Booth, B., Tremblay, J.-E., Mostajir, B., 2004. Spatial and temporal variability of the phytoplankton community structure in the north water polynya, investigated using pigment biomarkers. *Canadian Journal of Fisheries and Aquatic Sciences* 61 (11), 2038–2052.
- Vincent, R., 2013. The 2009 north water anomaly. *Remote sensing letters* 4 (11), 1057–1066.
- Waldron, A., Mooers, A. O., Miller, D. C., Nibbelink, N., Redding, D., Kuhn, T. S., Roberts, J. T., Gittleman, J. L., 2013. Targeting global conservation funding to limit immediate biodiversity declines. *Proceedings of the National Academy of Sciences* 110 (29), 12144–12148.
- Walter, B., Peters, J., Van Beusekom, J., St. John, M., 2014. Interactive effects of temperature and light during deep convection: a case study on growth and condition of the diatom *thalassiosira weissflogii*. *ICES Journal of Marine Science* 72 (6), 2061–2071.
- Wang, Y., Liu, D., 2014. Reconstruction of satellite chlorophyll-a data using a modified dineof method: a case study in the bohai and yellow seas, china. *International journal of remote sensing* 35 (1), 204–217.
- Waniek, J. J., 2003. The role of physical forcing in initiation of spring blooms in the northeast atlantic. *Journal of Marine Systems* 39 (1-2), 57–82.
- Wassmann, P., Duarte, C. M., Agusti, S., Sejr, M. K., 2011. Footprints of climate change in the arctic marine ecosystem. *Global change biology* 17 (2), 1235–1249.
- Wassmann, P., Reigstad, M., 2011. Future arctic ocean seasonal ice zones and implications for pelagic-benthic coupling. *Oceanography* 24 (3), 220–231.
- Watson, J. E., Rao, M., Ai-Li, K., Yan, X., 2012. Climate change adaptation planning for biodiversity conservation: A review. *Advances in Climate Change Research* 3 (1), 1–11.
- Weaver, P. P., Billett, D. S., Boetius, A., Danovaro, R., Freiwald, A., Sibuet, M., 2004. Hotspot ecosystem research on europe's deep-ocean margins. *Oceanography* 17 (4), 132–143.

- Williams, K. J., Ford, A., Rosauer, D. F., De Silva, N., Mittermeier, R., Bruce, C., Larsen, F. W., Margules, C., 2011. Forests of east australia: the 35th biodiversity hotspot. In: Biodiversity hotspots. Springer, pp. 295–310.
- Winder, M., Sommer, U., 2012. Phytoplankton response to a changing climate. *Hydrobiologia* 698 (1), 5–16.
- Wingfield, D. K., Peckham, S. H., Foley, D. G., Palacios, D. M., Lavaniegos, B. E., Durazo, R., Nichols, W. J., Croll, D. A., Bograd, S. J., 2011. The making of a productivity hotspot in the coastal ocean. *PLoS one* 6 (11), e27874.
- Winter, M., Devictor, V., Schweiger, O., 2013. Phylogenetic diversity and nature conservation: where are we? *Trends in Ecology & Evolution* 28 (4), 199–204.
- Worm, B., Barbier, E. B., Beaumont, N., Duffy, J. E., Folke, C., Halpern, B. S., Jackson, J. B., Lotze, H. K., Micheli, F., Palumbi, S. R., et al., 2006. Impacts of biodiversity loss on ocean ecosystem services. *science* 314 (5800), 787–790.
- Worm, B., Lotze, H. K., Myers, R. A., 2003. Predator diversity hotspots in the blue ocean. *Proceedings of the National Academy of Sciences* 100 (17), 9884–9888.
- Wu, Y., Platt, T., Tang, C. C., Sathyendranath, S., 2008a. Regional differences in the timing of the spring bloom in the labrador sea. *Marine Ecology Progress Series* 355, 9–20.
- Wu, Y., Platt, T., Tang, C. C., Sathyendranath, S., Devred, E., Gu, S., 2008b. A summer phytoplankton bloom triggered by high wind events in the labrador sea, july 2006. *Geophysical Research Letters* 35 (10).
- Yamamoto-Kawai, M., McLaughlin, F., Carmack, E., Nishino, S., Shimada, K., Kurita, N., 2009. Surface freshening of the canada basin, 2003–2007: River runoff versus sea ice meltwater. *Journal of Geophysical Research: Oceans* 114 (C1).
- Yang, Q., Dixon, T. H., Myers, P. G., Bonin, J., Chambers, D., Van Den Broeke, M., Ribergaard, M. H., Mortensen, J., 2016. Recent increases in arctic freshwater flux affects labrador sea convection and atlantic overturning circulation. *Nature communications* 7, ncomms10525.
- Yashayaev, I., Loder, J. W., 2009. Enhanced production of labrador sea water in 2008. *Geophysical Research Letters* 36 (1).
- Yashayaev, I., Loder, J. W., 2016. Recurrent replenishment of labrador sea water and associated decadal-scale variability. *Journal of Geophysical Research: Oceans* 121 (11), 8095–8114.
- Yashayaev, I., Loder, J. W., 2017. Further intensification of deep convection in the labrador sea in 2016. *Geophysical Research Letters* 44 (3), 1429–1438.

- Yashayaev, I., Seidov, D., Demirov, E., 2015. A new collective view of oceanography of the arctic and north atlantic basins.
- Yun, M., Whitley, T., Stockwell, D., Son, S., Lee, J., Park, J., Lee, D., Park, J., Lee, S., 2016. Primary production in the chukchi sea with potential effects of freshwater content. *Biogeosciences* 13 (3), 737.
- Zhai, L., Gudmundsson, K., Miller, P., Peng, W., Guðfinnsson, H., Debes, H., Hátún, H., White III, G. N., Walls, R. H., Sathyendranath, S., et al., 2012. Phytoplankton phenology and production around iceland and faroes. *Continental Shelf Research* 37, 15–25.
- Zhai, L., Platt, T., Tang, C., Sathyendranath, S., Walne, A., 2013. The response of phytoplankton to climate variability associated with the north atlantic oscillation. *Deep Sea Research Part II: Topical Studies in Oceanography* 93, 159–168.
- Zhang, H.-M., Bates, J. J., Reynolds, R. W., 2006. Assessment of composite global sampling: Sea surface wind speed. *Geophysical Research Letters* 33 (17).
- Zhang, J., Spitz, Y. H., Steele, M., Ashjian, C., Campbell, R., Berline, L., Matrai, P., 2010. Modeling the impact of declining sea ice on the arctic marine planktonic ecosystem. *Journal of Geophysical Research: Oceans* 115 (C10).
- Zhang, W., Yan, X.-H., 2018. Variability of the labrador sea surface eddy kinetic energy observed by altimeter from 1993 to 2012. *Journal of Geophysical Research: Oceans* 123 (1), 601–612.
- Zupan, L., Cabeza, M., Maiorano, L., Roquet, C., Devictor, V., Lavergne, S., Mouillot, D., Mouquet, N., Renaud, J., Thuiller, W., 2014. Spatial mismatch of phylogenetic diversity across three vertebrate groups and protected areas in europe. *Diversity and Distributions* 20 (6), 674–685.